Techno-economic feasibility study of a photovoltaic-equipped plug-in electric vehicle public parking lot with coordinated charging

by

Alyona Ivanova
B.Eng, University of Victoria, 2016

A Thesis Submitted in Partial Fulfillment of the
Requirements for the Degree of

MASTER OF APPLIED SCIENCE

in the Department of Mechanical Engineering

Techno-economic feasibility study of a photovoltaic-equipped plug-in electric vehicle public parking lot with coordinated charging

by

Alyona Ivanova
B.Eng, University of Victoria, 2016

Supervisory Committee

Dr. N. Djilali, Supervisor
(Department of Mechanical Engineering)

Dr. C. Crawford, Supervisor
(Department of Mechanical Engineering)

Supervisory Committee

Dr. N. Djilali, Supervisor
(Department of Mechanical Engineering)

Dr. C. Crawford, Supervisor
(Department of Mechanical Engineering)

ABSTRACT

In the effort to reduce the release of harmful gases associated with the transportation sector, Plug-in Electric Vehicles (PEV) have been deployed on the account of zero-tail pipe emissions. With electrification of transport it is imperative to address the electrical grid emissions during vehicle charging by motivating the use of distributed generation. This thesis employs optimal charging strategies based on solar availability and electrical grid tariffs to minimize the cost of retrofitting an existing parking lot with photovoltaic (PV) and PEV infrastructure. The optimization is cast as a unit-commitment problem using the CPLEX optimization tool to determine the optimal charge scheduling. The model determines the optimal capacity of system components and assesses the techno-economic feasibility of PV infrastructure in the microgrid by minimizing the net present cost (NPC) in two case studies: Victoria, BC and Los Angeles, CA. It was determined that due to a relatively low grid tariff and scarcity of solar irradiation, it is not economically feasible to install solar panels and coordination of charging reduces the operating cost by 11% in Victoria. Alternatively, with a high grid tariff and abundance of solar radiation, it shown that Los Angeles is a promising candidate for PV installations. With the implementation of a charging coordination scheme in this region, NPC savings of 8-16% are simulated with the current prices of solar infrastructure. Additionally, coordinated charging was assessed in conjunction with various commercial buildings posing as a base load and it was determined that the effects of coordination were more prominent with smaller base loads.

Contents

List of Tables

List of Figures

List of Acronyms and Symbols

Abbreviations

AC	Alternating Current
BNEF	Bloomberg New Energy Finance
CPV	Concentrating Photovoltaic
DC	Direct Current
EVSE	Electric Vehicle Supply Equipment
EVSPL	Electric Vehicle Solar Parking Lots
FIT	Feed-in Tariff
GAMS	General Algebraic Modeling System
GHG	Greenhouse Gas
GHI	Global Horizontal Irradiation
HDKR	Hay, Davies, Klutcher, Reindl
HOMER	Hybrid Optimization Model for Multiple Energy Resources
LP	Linear Programming
MATLAB	Matrix Laboratory
MILP	Mixed Integer Linear Programming
MPPT	Maximum Power Point Tracking
NPC	Net Present Cost

NREL	National Renewable Energy Laboratory	
PEV	Plug-in Electric Vehicle	
PG&E	Pacific Gas and Electric	
PV	Photovoltaic	
RFID	Radio Frequency Identification	
S2V	Solar to Vehicle	
TMY3	Typical Meteorological Year 3	
TOU	Time of Use	
V2G	Vehicle to Grid	
V2V	Vehicle to Vehicle	

Symbols

β	Tilt of the photovoltaic panel	^{o}
ΔT	Time step	min
δ	Solar declination	^{o}
δ_{thresh}	Power threshold beyond which a demand charge is applied	kW
$\eta_{charger}$	Charging station efficiency	
$\eta_{inverter}$	DC/AC inverter efficiency	
γ	Azimuth	^{o}
λ	Wavelength of a photon	m
λ_L	Longitude of the photovoltaic panel's location	^{o}
$\overline{G}$	Global horizontal irradiation on Earth's surface averages over a time step	kW/m^2
$\overline{G}_o$	Average extraterrestrial horizontal radiation	kW/m^2

$\overline{G}_{STC}$	Incident radiation under standard test conditions	$1kW/m^2$
$\overline{G}_T$	Solar radiation incident on the photovoltaic array in the current timestep	kW/m^2
ϕ	Latitude of the photovoltaic panel's location	^{o}
ρ	Ground reflectance or albedo	
θ	Angle of incidence	^{o}
θ_Z	Zenith angle	^{o}
A_i	Anisotropy index	
c	Speed of light	m/s
C_{demand}	Demand charge	$\$/kW$
C_{NPC}	Total cost to the owner	$\$$
$C_{salvage}$	Salvage value of the equipment at end of life	$\$$
CAP	Total capital investment cost	$\$$
CAP_{conn}	Capital investment cost of grid connectivity	$\$$
CAP_{PV}	Photovoltaic carport capital investment cost	$\$$
CAP_{st}	Capital investment cost of charging stations	$\$$
CRF	Capital Recovery Factor	
D	Project lifetime	$years$
d	Day of year	
E	Equation of time	hr
$E^n_{consumed}$	Energy consumed by the vehicle per charge cycle	kWh
E_{ph}	Energy of a photon	J/m
f	Horizon brightening factor	

f_{PV}	Derating factor	
G_b	Beam radiation	kW/m^2
G_d	Diffuse radiation	kW/m^2
G_{on}	Extraterrestrial normal radiation	kW/m^2
G_{sc}	Solar constant	$1.367kW/m^2$
h	Plank's constant	$6.626 * 10^{-34}\ m/s$
i	Real discount rate	
i'	Nominal discount rate	
i_f	Expected inflation rate	
k_T	Clearness index	
L_t	Load at time t	kW
N	Total number of cars served by the parking lot on day d	
n	Vehicle number	
OC_d	Operating cost on day, d	\$
P_{ch}	nominal charging rate of the charging stations	kW
P_{PV}	Power output from a photovoltaic array	kW
R_b	Ratio of beam radiation on tilted surface to beam radiation on horizontal surface	
$S^{+}_{demand,t}$	Amount of power that exceeds the demand charge threshold at time t	kW
$S^{-}_{demand,t}$	Negative component of the difference between required power and the threshold beyond which a demand charge is applied	kW
$s_{n,t}$	binary state matrix for each vehicle	
$S^{+}_{net,t}$	Solar surplus sold to the grid for each time step	kW

$S^{-}_{net,t}$	Net power used by the load from grid and/or photovoltaic installation at time t	kW
T	Total number of time steps during the day	
t_c	Civil time	hr
t_s	Solar time	hr
$t_{arr,n}$	Time of arrival for car n	min
$t_{dep,n}$	Time of departure for car n	min
w	Hour angle	^{o}
w_1	Hour angle at the beginning of the time step	^{o}
w_2	Hour angle at the end of the time step	^{o}
Y_{PV}	Rated capacity of a photovoltaic array	kW
Z_c	Time zone east of GMT	

ACKNOWLEDGEMENTS

I would like to thank Dr. Ned Djilali for giving me the opportunity of pursuing my passion as a graduate student under his mentorship that taught me lifelong and invaluable skills. He was always available for discussions and counsel even during the times of struggle, challenges and tight deadlines, which I treasure immensely.

My sincerest appreciation goes out to Dr. Curran Crawford for support and guidance with his experience and insights in the field over the duration of my graduate work.

A special thank you to Dr. David Chassin for sparking my interest in a research career and presenting the opportunity for a strong collaboration with Stanford National Accelerator Laboratory.

I am grateful for Dr. Julian Alberto Fernandez's day to day assistance with ongoing projects and ideas.

This research was part of the Transportation initiative in the Big Five projects from the Pacific Institute for Climate Solutions and I am deeply grateful for their financial support and collaboration.

I am grateful to my parents, Sergiy Ivanov and Nataliya Ivanova, for the love and encouragement to pursue my educational goals. My gratitude goes to my boyfriend, Reed Teyber, for his strength, immense support and his master skills in word-smithing. As well as his family, Kathy Pezdek and Edward Teyber, for their moral support and optimism.

I would also like to acknowledge the IESVIC community and friends for making graduate school such an enjoyable and positive experience.

Chapter 1

Introduction

1.1 Motivation

It is known that plug-in electric vehicles (PEV) have an advantage over internal combustion engines in terms of their potential to reduce fossil fuel dependence, eliminate tailpipe emissions and improve energy efficiency [5, 6]. However, the amount of pollution from powering a PEV is dependent on the source of electrical generation or the fuel mix of the region. Bloomberg New Energy Finance (BNEF) estimates a 54% increase in electric light-duty vehicles sales by 2040 globally, which would reduce transport fuel consumption by 8 million barrels per day and increases global electricity consumption by 5% [7]. In the US, BNEF projected that 58% of total vehicle sales will be electric, despite low oil prices [7].

Currently, California has the highest PEV adoption rate [8], however upwards of 40% of the fuel mix in California is dependent on fossil fuels and increased penetration of PEVs in this market would result in additional grid-side emissions [9]. California's geographical location favours the implementation of solar technology, which can offset greenhouse gas (GHG) emissions from additional PEV electrical demand. Nevertheless, National Renewable Energy Laboratory (NREL) projected that too much solar can lead to an over-generation risk during peak solar times resulting in curtailment and problems coping with the rapid generation ramping required to meet the high demand peak between 6 pm and 10 pm when solar energy is no longer available as shown in Fig. 1.1. The ramping problem is further aggravated by increased penetration of PEVs in the market due to the residential PEV charging load. Methods such as demand response and coordinated scheduling have been studied to level out and shift the additional demand to off-peak hours [10, 11, 12]. Two notable pilot projects that have been implemented to support and validate the research are (1) Olympic peninsula demonstration project [13, 14], and (2) American electric power gridSMART demonstration [15]. Even with demand response, PEVs choosing to charge overnight at home present a new load on the existing primary and secondary distribution networks, in turn limiting the opportunity for equipment to ramp down at night and cause premature equipment failure [16].

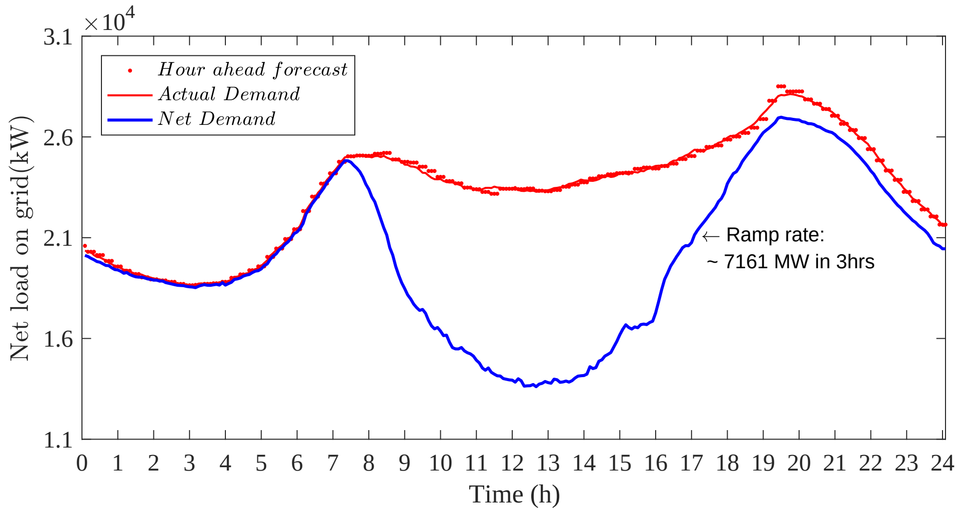

Figure 1.1: Net Demand (demand minus solar and wind) on March 12, 2018 from CAISO. [3]

Home charging is potentially available to 42% of US households equipped with Electric Vehicle Supply Equipment (EVSE) [17] and, is arguably the most convenient option for powering a PEV. Alternatively, workplace day-time charging: (a) does not require the home owner to retrofit their house with a charging facility and (b) presents an opportunity for customers living in multi-unit residential buildings who face challenges charging while street parking. Regardless, day-time charging creates an additional load, which could lead to load shedding and disruption of grid stability. A synergistic opportunity is to integrate renewable energy with the charging infrastructure to shave the load peaks [18]. A case study at University of California, Los Angeles has shown the successful performance of a two-tier energy management system for smart PEV charging [19]. Studies have also shown that photovoltaic (PV) powered work place charging has favourable economic and environmental impacts [20].

In major US cities a third of the surface area is dedicated to parking and roughly 3 non-residential parking spaces are available for each car comprising a total area larger than Puerto Rico [21]. Statistically, most private vehicles remain parked for 95% of the time and follow a schedule conducive to solar charging during the time the vehicle is parked [22].

There are a number of benefits from coupling PEV charging with PV solar generation and placing them in publicly available areas called electric vehicle solar parking lots (EVSPL). The PEV can be directly supplied with clean energy and avoid the majority of transmission losses. The addition of chargers in public locations is predicted to stimulate the local economy through promotion of PEV uptake which is limited by customer range anxiety. In addition, the US department of energy advises that hot weather decreases vehicle efficiencies by upwards of 25% due to increased air conditioning loads when the car is turned on [23, 24]. A viable solution is a PV equipped parking lot which provides sun shade and additional protection from other elements for the vehicles charging underneath them. Since existing parking lots can be retrofitted with solar panels and charging equipment, there is no competition for land or high capital investment costs.

Moreover, deployment of PEVs requires a highly capable distribution grid infrastructure [25, 26]. Approaches such as centralized control and transactive power control, where the peak load is reduced by posing PEV agents as bidders in a real-time market have been explored [10]. Other approaches take advantage of solar to reduce the grid-side emissions by implementing the concept of smart parking lots through matching PEV demand to solar production. Smart EVSPLs may be equipped with a control system that can act as a PEV aggregator to optimally allocate energy with minimal cost to the parking lot owner [27].

1.2 Description of System Components

1.2.1 Configuration of EVSPL

A typical solar equipped parking lot consists of two sets of rows of 12-16 m^2 parking spaces separated by charging equipment as seen in Fig.1.2. These sets are built parallel to each other with a separation for driveways and vehicle access. Solar panels are placed overhead in three common configurations: fixed angle, multiple fixed angles or equipped with tracking. Alternatively, a less common and more costly configuration is a solar tree where 4-6 vehicles park around a common tracking PV system in an island arrangement. Some parking structures maximize the solar yield by covering the entire lot with PV arrays, which is favoured in areas that connect to adjacent buildings or employ storage to consume the excess energy left over from primary load.

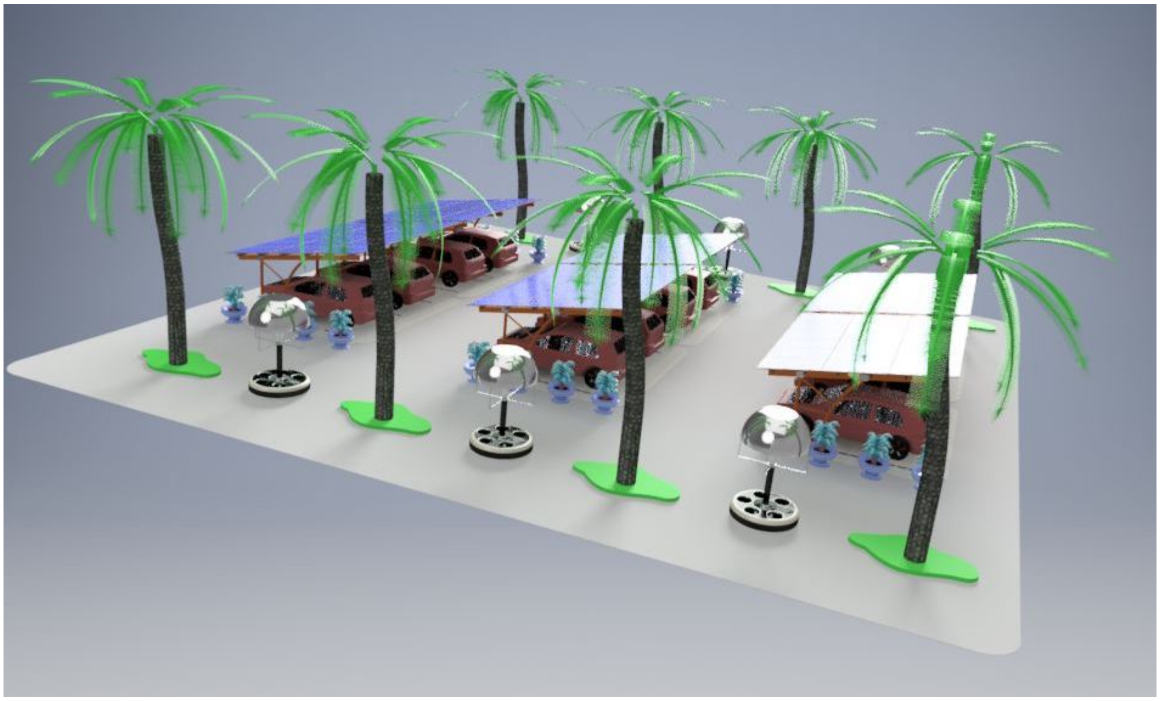

Figure 1.2: A typical solar equipped parking lot configuration. [4]

1.2.2 Photovoltaic Technology

To convert sunlight into electricity a PV cell is used, which is essentially an adaptation of an electrical semiconductor. The cells convert the light photons to electrons that are then channeled into an external circuit. To perform the conversion process, the cell must have a specific molecular structure that is lined with semiconductors at the edge of the cell. Roughly 20-50 PV cells connect together into a PV panel, which forms an electrical circuit as shown in Fig.1.3, connecting to an external electrical load at a single point. To meet the needs of a load at a specific voltage, an array of panels is integrated into a system that delivers energy to the demand.

The photoelectric effect is the phenomenon whereby sunlight striking a particular material generates electrical current which is the fundamental principle behind PV technology. The manufacturing of PV cells is subdivided into two methods:

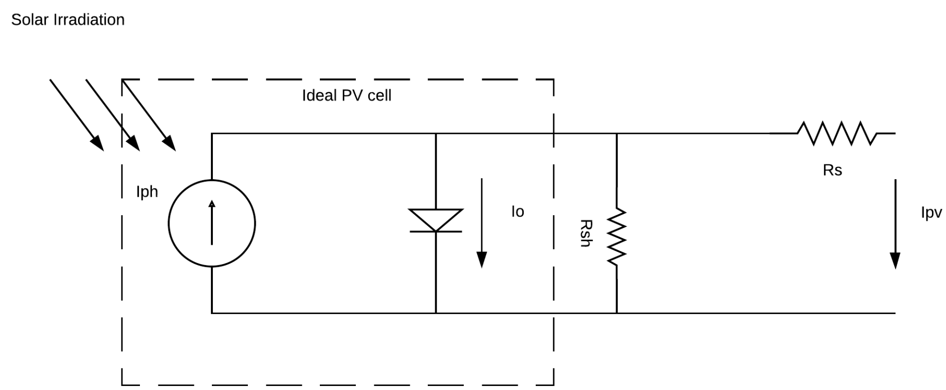

Figure 1.3: Electrical circuit representing a PV cell.

crystalline and thin-film. In the process of creating crystalline cells a silicon wafer is designed to harnesses the photovoltaic effect. Cells manufactured from a single crystal are called monocrystalline and manufacturing from multiple crystals refers to multicrystalline solar cells. These crystals are grown and sliced into thin pieces for panel production. Monocrystalline technology is more efficient at converting sunlight into usable electricity compared to multicrystalline cells, however they are costly.

Thin-film panels are manufactured by laying down a thin film of photovoltaic effect material (amorphous, silicon or nonsilicon combination of metals) on a backing material. Mass manufacturing capability and cost efficient scalability of thin-film panels facilitate the economic superiority of the technology, however this comes with compromised efficiency in contrast to crystalline type cells.

PV cell Performance

To stimulate the conversion of sunlight (photons) to electrical energy (electrons) using the photovoltaic effect, layers of silicon are modified to produce either loose electrons or holes in the molecular matrix for electron reattachment. In a common PV cell design, the silicon atom (4 valence electrons) is doped with phosphorus (5 valence electrons) to create n-type layer, or doped with boron (3 valence electrons) to create p-type layer, together forming a p-n junction. The transfer of free electrons to holes is the essence of the permanent electrical field, which creates a path for the electrons to and from the external circuit and load.

An illustration of the design is presented in Fig.1.4 where the upper layer is an n-type silicon doped with phosphorus (with excess electrons) and the lower layer is a p-type silicon doped with boron (with extra holes). The rightmost photon breaks an electron loose in the n-type layer projecting the electron into the collector comb and the electron hole is gathered by the conductive backing which contributes to the current flow to the load. The collectors are generally laid out in a comb pattern since they block the entrance of the photons into the PV cell. However, there has to be sufficient area to collect as many electrons as possible posing a design trade-off between collector area and open PV cell area.

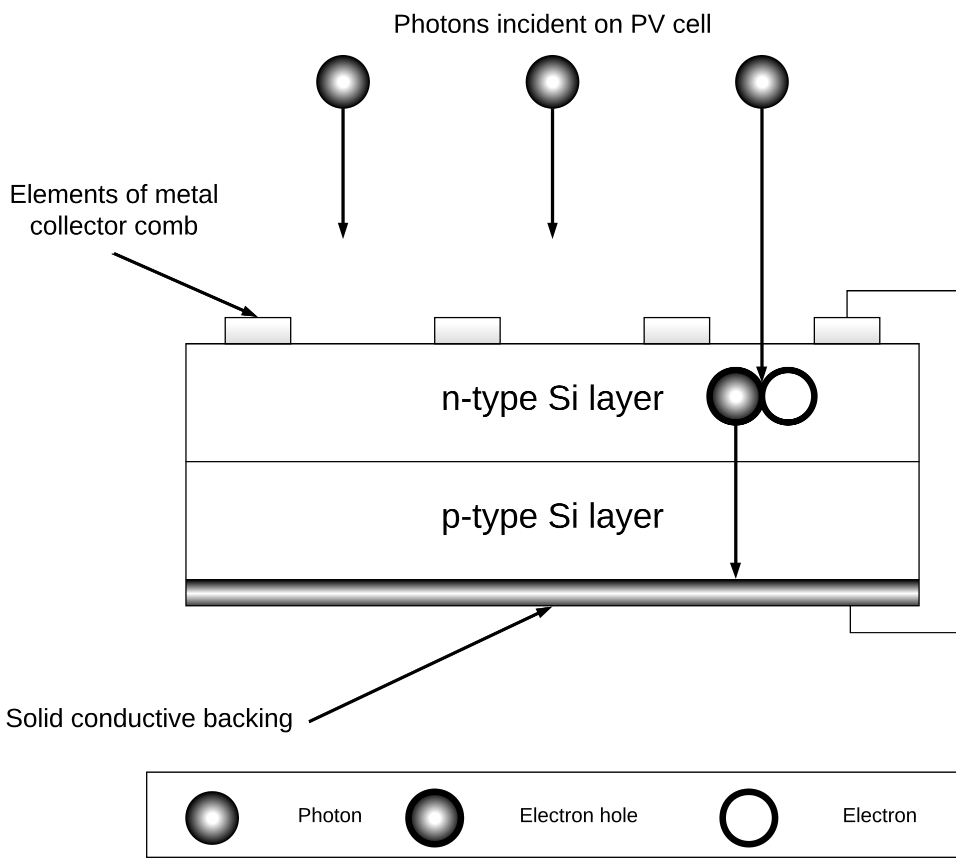

Figure 1.4: A cross section of a PV cell.

Only the photons with energy greater than the bandgap energy [1] are able to break the bond between the electron-hole pair in the PV cell. Eq.1.1 shows that energy is inversely proportional to the wavelength (λ) of the photon.

$$E_{ph} = \frac{hc}{\lambda} \tag{1.1}$$

[1]Bandgap energy is the energy range where no electron states can exist between the top of the valence band and the bottom of the conduction band

where h is Plank's constant, and c is the speed of light, meaning that photons with wavelengths greater than the bandgap wavelength do not possess enough energy to convert to an electron.

At 100% efficiency a PV cell could convert all the incoming light into electrical current and the magnitude of this current would be equivalent to the energy available in the light per unit surface area. Outside of Earth's atmosphere that value is equivalent to 1.37 kW/m^2, at the Earth's surface the value reduces to 1 kW/m^2 due to refraction and absorption in the atmosphere. Additional losses pertain to the solar cell itself as follows:

1. **Quantum losses** are due to the cell's inability to gather the energy from the photons that have insufficient energy for the photoelectric effect, in turn losing the opportunity for conversion of photons to electrons.

2. **Reflection losses** are due to fractional reflection loss at the surface of the PV cell which is proportional to the energy of the photon. To minimize these losses, PV cells are covered with antireflective coating.

3. **Transmission losses** are due to the anomaly when the photon passes through the structure and avoids the collision with an atom in the structure. The magnitude of the transmission losses is a function of cell width and the energy of the photon.

4. **Collection losses** are due to certain electrons getting permanently absorbed by the collector before they are able to leave the cell. These losses are more prominent for photons with very high energy.

A number of other factors affect the performance of a PV cell such as temperature, concentration, resistance in series or in parallel with other PV cells in a panel, and age of the device.

The leading PV panel manufacturers aim to either increase efficiency or reduce the cost of manufacturing. Most notable efforts are: (1) Concentrating PV (CPV), (2) Multi-junction PV, and (3) Nanotechnology. CPV uses the fundamentals of a conventional PV cell and retrofits it with a light concentrating system to increase the efficiency of the cell. The additional cost due to the concentrating technology is offset by the higher rated output of the cell. To take full advantage of the CPV, the panel must be equipped with tracking capability in order to follow the sun throughout the day. Another method, multi-junction technology, combines multiple single-junctions (traditionally used) into one panel with the top layer responsible for conversion of the highest energy photons and layers underneath target the lower energy photons for conversion to maximize efficiency. The cost of manufacturing these cells is so high that they can only be viable in applications that prioritize efficiency such as space flight. Alternatively, nanotechnology involves manipulating components in a cell on a nanometer scale, focusing on thin-films technology to maximize the efficiency of the PV cell and reduce cost per Watt. At this level the cell can be designed with the desired structural qualities that maximize photon to electron conversion while minimizing losses.

1.2.3 Microgrid Inverters

PV solar panels inherently use Direct Current (DC), while the electrical grid uses Alternative Current (AC). To inject the excess energy generated by the PV panels to the grid a converter must be deployed. A converter, or solar inverter, adapts variable DC output of a PV panel into a utility frequency AC employed by the electrical grid as shown in Fig.1.5. Additional features can be included in the inverter design such as maximum power point tracking (MPPT) and anti-islanding protection.

Solar inverters equipped with MPPT can increase amount of energy from the PV array [28]. Due to solar cells having a complicated relationship between solar irradiation, temperature and total resistance, the efficiency of the cells is non-linear and characterized by current-voltage, or I-V, curves. The MPPT system is able to sample the output of the cells to match the load to receive the maximum power regardless of the environmental conditions.

Islanding occurs when a distributed generator, such as PV panel array, continues to provide power to the load even though electrical grid power is unavailable which becomes dangerous to the utility workers, who are unaware of the powered circuit, and leads to lack of frequency control responsible for the frequency balance between load and generation. Inverters with anti-islanding protection immediately disconnect the circuit when islanding is detected to preserve safety and frequency control.

1.2.4 Charger types

There are several charger connection types due to lack of consensus between PEV manufacturers as in Fig.1.6a. The connector types correlate to the types of chargers installed and in the US, charger types are categorized into 3 levels. Level 1, the

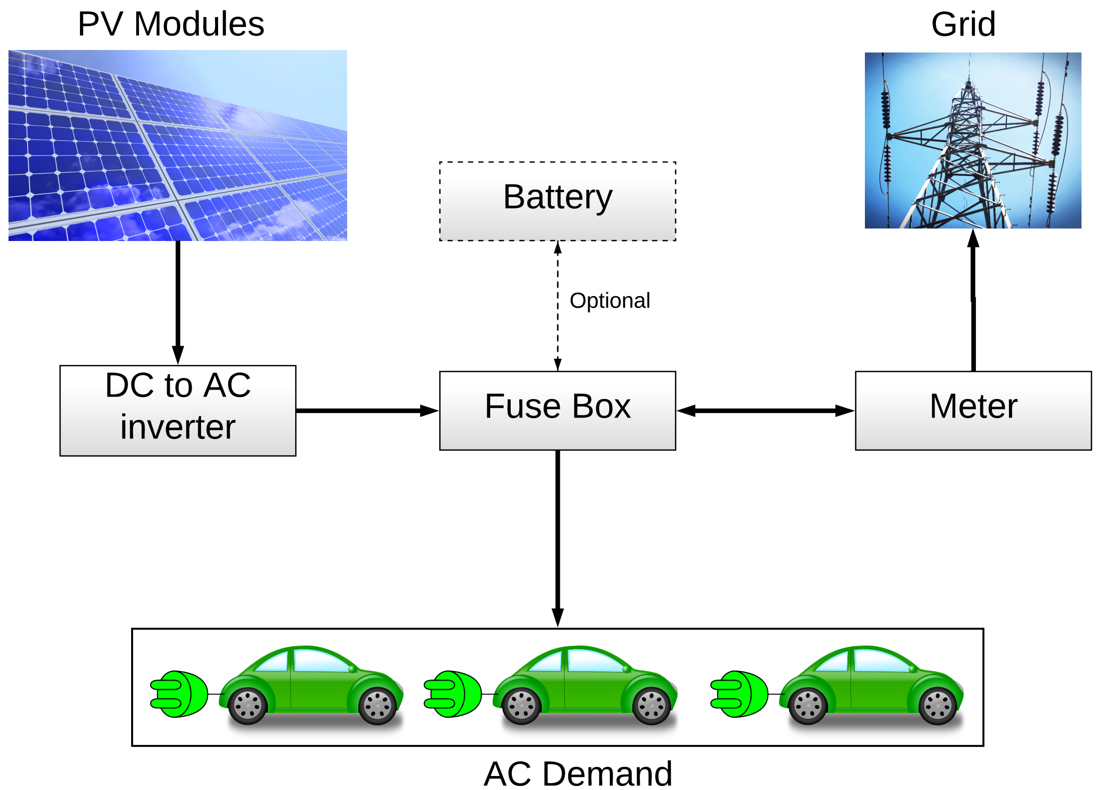

Figure 1.5: A simplified schematic of a grid connected PV-equipped parking lot power system.

slowest rate of charging congruent with the standard household outlet, supplies 15-20 A current through 120 V AC plug connected to the vehicle through SAE J1772 (Fig.1.6b) port providing 1.8-2.4 kW of power (2-5 miles per hour) to the vehicle. Level 2 uses the same connector type as Level 1 and provides power at 30 A and at voltage of either 220 V or 240 V; adding 10-25 miles of range per hour of charging. This type of charger can be used at home or in public areas since they are relatively inexpensive compared to Level 3 chargers. DC fast chargers or Level 3 chargers are capable of rapid recharging of vehicles appropriate for near freeway installations. Unlike Level 1 and Level 2, Level 3 chargers employ DC at 50-62.5 kW of power. There is no standard connector type for a DC fast charger. Tesla uses a proprietary Supercharger network (Fig.1.6c), where Nissan, Toyota and Mitsubishi connects via CHAdeMO, and SAE Combo connector is used by BMW and Chevrolet (Fig.1.6a).

(a) Charging stations for different vehicle brands. [29]

(b) SAE J1772 connector. [30]

(c) Tesla Supercharger station. [31]

Figure 1.6: Examples of various types of chargers.

1.3 Demonstration Projects

The first EVSPL was piloted in California with 7 parking spots and a 2.1 kWp PV array in 1996 [32]. This was followed by several other case studies that explore the benefits and challenges of implementing an EVSPL. The most current and significant results are mentioned below.

The Solar-to-Vehicle (S2V) concept was first introduced by arguing that two thirds of the commuters in the US reside within 25 km of their workplace which benefits the idea of installing solar panels in parkings lots where they can be optimally placed contrast to a residential building [33]. This was extended to a vehicle-solar roof concept and it was determined that two charging resources must be coordinated to take advantage of the solar resource [34].

British Columbia Institute of Technology has implemented a pilot project that integrates PV renewable energy and a Li-Ion energy storage system with a Level 3 electric vehicle charge station in a microgrid scenario [35]. This study employs controls that mitigate power transfer, however only a single costly charging station was present that can power one vehicle at a time.

A case study in Tehran [36] considers a movie theatre parking lot with a capacity of 1000 vehicles equipped with PV, wind turbines and a diesel generator. The study demonstrates a methodology for determining the optimal site location, battery charging rate, sizing of renewable energy infrastructure and hybrid system capacity for a worst case solar and wind scenario. With an optimal system of 190 kWp PV, 30 kW wind and a 520 kW diesel generator, power quality improvements and lower power losses were observed while charging at a higher rate during off-peak hours and lower rate during peak hours. Full charge, however was not guaranteed to the vehicles.

A smart city in Malaga, Spain was demonstrated as the largest vehicle to grid (V2G) pilot project called Zem2All. It featured 23 CHAdeMO DC fast charging stations with 6 bidirectional chargers capable of V2G functionality, 229 charging points around the city and 200 PEVs (Nissan Leafs and Mitsubishi iMiEVs) capable of DC fast charging [37]. PEVs support the integration of intermittent renewable energy sources by transferring excess power to the grid through V2G.

1.4 Optimization Studies

To charge a fleet of vehicles in an EVSPL, smart or coordinated charging strategies are being investigated to prevent overloading of the electrical network or posing additional investment cost to the power distribution system [38, 39, 40]. Unlike the uncontrolled method, smart charging can delay the supply of power until certain technical or economical objectives are met. Two main approaches to formulate a controlled charging scheme are identified: (1) grid impact minimization and (2) cost minimization.

The grid impact minimization formulation avoids unnecessary stress on the grid by minimizing system losses, charging costs or GHG emissions. To maximize the economic benefit for the distribution system, an optimization scheme was formulated using a genetic algorithm to determine the parking lot capacity and location in the distribution network [41]. In this scenario the investment costs and power losses were minimized to enhance energy reliability. Since V2G is employed, the utility provides free energy for driving and reimburses the costs incurred by the owner of the vehicle through PEV battery degradation. A 9 bus distribution system and 15 kWp PV panel for each PEV was considered and it was determined that vehicle availability below 35% has negative benefits and smaller optimal sizing leads to smaller total benefits but the reliability increases. Another study aims to minimize power losses and improve voltage profiles through a controlled load charging of a PEV fleet [42]. The methodology was tested on a modified IEEE 23kV distribution system connected to a number of low voltage residential buildings with PEVs. This approach was able to reduce the generation costs by incorporating time-varying market energy prices and PEV owner preferred charging time zones. The study demonstrates that with uncontrolled charging and high or low PEV penetration, the system's voltage profile is subject to high deviations of up to 0.07 p.u. below an acceptable margin. In addition, the uncontrolled charging scheme results in high power losses and high generation fees. Alternatively, controlled charging improves the voltage profile to meet standards and losses are reduced.

A real-time smart energy management algorithm is developed in Ref.[43] to minimize the PEV charging costs and grid impacts in a 350 car parking lot with a 75 kWp PV installation. It was shown that the grid impacts were reduced by 0.20 p.u. through scheduling the charging of the vehicles. Another real-time smart energy management algorithm was explored in Ref.[44] with 1500 cars and a 1500 kWp PV installation connected to a IEEE 69-radial distribution system. Using a dynamic charging rate, V2G or Vehicle-to-vehicle (V2V) and scheduling, the authors were able to minimize power losses and achieve 12-16% charging cost reduction.

In contrast to the minimization of the grid impact approach, cost minimization formulation focusses on modelling the electrical supply and demand through valley-filling type schemes for PEV charging. Day ahead methodology for scheduling energy resources for a smart grid was developed by considering distributed energy resources (DERs) and V2G through a particle swarm optimization approach [45]. Additionally, the PEVs participate in demand response programs. As a result, the intelligent charging methodology was proved effective in a smart grid environment by demonstrating a reduction in operating costs. Another study explored cost minimization in relation to charging PEVs and V2G operation with implementation of Radio Frequency Identification (RFID) tag technology to acquire information and obtain control over PEV charging [46]. The methodology was able to achieve 10% cost savings for drivers with flexible charging needs, 7% cost savings for enterprise commuters and a 56% demand power peak reduction.

In Ref.[47], a parking lot with and without PV was considered for two types of PEV models with stochastic modelling of demand, supply, time of arrival and time of departure. The study concludes that V2G concept can bring economic benefits to the parking lot owner and improve grid stability by diminishing stress on the grid.

In Ref.[48], the grid autonomy potential of a parking lot with three Nissan Leafs (10 kWh battery capacity) in Netherlands was studied by implementing a 10 kWp PV with optimal orientation and inclination of modules. PV modules with tracking were considered an economically inviable option. The study explores eight dynamic scheduling profiles of three types: (1) four Gaussian, (2) two fixed and (3) two rectangular and determines that Gaussian charge distribution is most favourable. Additionally, it was found that even a small amount of storage dedicated solely to PEV charging significantly improves grid independence and at larger capacities returns start to diminish.

The energy economics and emissions of a PV equipped workplace charging station are analyzed with both uncoordinated and coordinated charging in Ref.[20]. The coordinated charging algorithm employs a stochastic systems dynamic programming algorithm for real-time charge scheduling. The study advises on the preferred cost of parking, and solar dependent optimal parking locations. In conclusion, a 55% reduction in emissions is recorded with a PV powered workplace charger compared to a residential charger. Notably, the study only accounts for two types of vehicles, neglects charging power losses, employs a coarse 1 hour time step and uses a computationally expensive algorithm to predict economic feasibility.

The objective of this thesis is to reduce range anxiety and provide publicly available, low cost charging solutions for PEVs. To accomplish this, a lifetime cost minimization methodology is employed to demonstrate the techno-economic feasibility of EVSPLs with the intention that the cost savings acquired by the EVSPL owner will be passed on to the PEV owners through free or affordable charging. A modified unit-commitment strategy developed by Ref.[20] is applied with real-world driving patterns and solar irradiation data for system optimization and cost minimization on a 15 minute time scale using mixed-integer linear programming (MILP).

1.5 Software Overview

To implement the system and cost optimization model using real-world data for an EVSPL, a number of software packages were explored before a bespoke numerical model was developed. Hybrid Optimization Model for Multiple Energy Resources (HOMER) is a micropower optimization package developed by NREL and distributed by HOMER Energy. HOMER simulates electric and thermal demand by implementing the energy balance equations for each hour in a year and determines the flows of energy in and out of each microgrid component. HOMER, then determines whether the given configuration of components is feasible by calculating the electrical demand requirements. An estimate of the overall optimized lifetime system costs is calculated by considering costs such as capital, replacement, operation, maintenance, fuel and interest while meeting the energy demand. This work seeks to reduce the operating costs, therefore the required software must be able to exert control over the electrical load. HOMER is constrained by manual user entry of demand profiles for the system feasibility study, which can not be controlled using the user interface provided. This characteristic deems HOMER unsuitable for the work in this thesis due lack of access to the internal components, which prevents the user from implementing demand response and control strategies required for smart charging. In addition, the time step is limited to 1 hour intervals resulting in significant inaccuracies in the final system cost estimate. This is discussed further in section 2.6, where HOMER is used as a validation tool for simplified components and an invariable demand profile formulated by uncontrolled charging to determine the reliability of the developed method using in-house code.

Since the existing models are not well-suited for this specific application, development environments were explored that allow for full control of the model. General Algebraic Modeling System (GAMS) is capable of high-level system modeling for mathematical optimization. It is capable of solving linear, nonlinear, and mixed-integer optimization problems. The development environment is capable of integrating with third-party optimization solvers such as IBM ILOG CPLEX Optimization studio for problems with high complexity. The downfall is that GAMS is a costly software package, therefore an alternative is explored.

Matrix Laboratory (MATLAB) is a multi-paradigm numerical computing environment for matrix manipulation, implementation of algorithms and creation of user interfaces. MATLAB has an in-house optimization package, however it was deemed unfit for MILP problem with binary decision variables due to the computational complexity of the internal algorithm used. MATLAB allows for seamless integration with CPLEX that implements optimized methods for handling binary and continuous MILP problems. The software combination creates full control of the model components and allows for a reduced time step to reflect realistic conditions. It is capable of handling parallel processes and has unrestricted database access. Similarly to GAMS, MATLAB is not an open-source software, however the University of Victoria provides a number of licenses for educational purposes, therefore the in-house model of the cost components of an EVSPL was built in MATLAB with a third-party optimization tool to handle MILP with binary and continuous decision variables.

GridLAB-D is an open-source power distribution system simulation and analysis tool for a wide array of components from the distribution system to end-use applications. Unfortunately, the PEV charger object within the software is designed for residential applications and does not support large fleet aggregation for optimal control schemes in a commercial scenario. However, GridLAB-D is a valuable tool for further exploration of this topic beyond the scope of this thesis, since it can provide insights into the power quality of the EVSPL and optimal size and location of the EVSPLs on the distribution network.

1.6 Scope and Contributions

The literature explores various avenues of PEV integration into the grid, however there is a lack of investigations of real-world scenarios and driving patterns based on recorded data. In addition, the effect of demand charges is not fully analysed. This thesis uses real-world charging data coupled with grid tariffs that contain high demand charges to determine the techno-economic feasibility of solar infrastructure in conjunction with a coordinated charging scheme. In this work the main contributions are as follows:

1. Formulation of a cost minimization scheme of the Net Present Cost (NPC) based on the electricity price, demand charge, solar availability and a base load.

2. Application of real world charging data and solar data to accurately predict the grid purchases required by the EVSPL.

3. Investigation of coordinated charging compared to the uncoordinated charging.

4. Parametric study of system costs on the cost feasibility of the EVSPL.

1.7 Overview

The thesis outline is as follows:

Chapter 1 describes the background information pertaining to EVSPLs and motivation for the research. In addition, overview of the technology referred to the thesis is mentioned.

Chapter 2 outlines the modelling techniques used to determine the feasibility of the EVSPL. A verification of the model is illustrated in this section.

Chapter 3 presents the results and discusses insights developed in this work.

Chapter 4 summarizes the main findings and conclusions based on the results obtained and presents an outlook for future work.

Chapter 2

Model Definition

The model defined in this work employs a unit-commitment strategy to minimize the cost of installing an EVSPL by minimizing the NPC through optimal allocation of charging profiles for a PEV fleet. The coordination is performed by considering the grid tariff, solar profiles and system constraints at each time step. This work considers two types of charging strategies: uncoordinated and coordinated. The two methods are contrasted through an in-depth cost analysis of both strategies. The portion of the methodology pertaining to operating cost minimization was published in IEEE ISGT Europe 2017 conference proceedings [49].

2.1 Cost Minimization Formulation

In the effort to reduce the cost to both the consumer and the parking lot owner the problem was formulated as a cost minimization of NPC. The total NPC is the difference between the present value of all costs the system incurs over the lifetime and the present value all the revenue generated by the business. Eq.2.1 breaks down the components of the total cost of owning the parking lot equipped with charging stations.

$$C_{NPC} = (OC + CAP - C_{salvage}) \tag{2.1}$$

where OC is the operating cost over the lifetime of the project, $C_{salvage}$ is the salvage value and CAP is the capital investment cost of the charger equipped parking structure as defined below:

$$CAP = CAP_{PV} + CAP_{conn} + CAP_{st} \tag{2.2}$$

where CAP_{PV} is the cost of solar panels and the mechanical shelter structure, DC/AC inverter , CAP_{conn} is the cost for grid connectivity and CAP_{st} is the total cost of charging stations. The total NPC is calculated by summing the total discounted cash flows for each year over the duration of the project's lifetime through time value of money. The real discount rate is calculated as follows:

$$i = \frac{i' - i_f}{1 + i_f} \tag{2.3}$$

where i is the real discount rate, i' is nominal discount rate or the rate at which the money is borrowed and i_f is the expected inflation rate. The real discount rate is then used in calculating the capital recovery factor (CRF) to determine the present value of an annuity as below:

$$CRF(i, D) = \frac{i(1 + i)^D}{(1 + i)^D - 1} \tag{2.4}$$

where D is project lifetime.

2.2 Optimization

To maximize the benefit of an EVSPL this study explores the impact of coordinated charging by minimizing the operating cost through MILP. In this work MILP is performed using MATLAB 2016b coupled with IBM ILOG CPLEX Optimizer Single User Edition 12.7 with 32GB RAM and AMD eight-core processor.

The fundamental concept of linear programming (LP) assumes the objective function and the constraints are linear. This type of programming has four basic components: (1) decision variables or the elements the optimizer determines, (2) an objective function with certain related quantities targeted to either minimize or maximize the value of the function, (3) the decision variables that are limited through a set of constraints which determine their distribution, and (4) additional data that can be included to quantify the relationship built in the objective function and constraints. The particular deviation of linear programming is restricted to mixed integer programming, which allows for both discrete and continuous decisions. Since the charging station can either provide electricity or remain on stand-by, the decision variables associated with the state of the chargers must be not only integers but also binary variables. MILP is a fairly complex problem to solve compared to a linear problem, therefore a more sophisticated tool, such as CPLEX, is required to implement techniques that systematically search over many possible combinations of discrete decision variables using linear or quadratic programming relaxations to compute bounds on the value of the optimal solution. In addition, the linear components are solved using LP to eliminate solutions that violate the constraints. CPLEX Single User Edition is capable of handling 1000 decision variables and 1000 of constraints with superior performance by using the Branch and Bound methods of optimization. [50]

Branch and Bound optimization relies on two subroutines that compute upper and lower bounds on the optimal value over a given region by partitioning the feasible set into convex sets. Global upper and lower bounds are then found. If the result is not within the region of optimality, the problem is refined and repeated until the solution is within the error bound. Generally, the upper bound is found by choosing a point in the region or by a local optimization method, where the lower bound is found through convex relaxation, duality or Lipschitz bounds.

2.3 PV Array Power Output

For the optimization to be able to minimize the cost of charging, the solar array output must be known given the global horizontal irradiation (GHI) data at each time step. The power output of PV array is calculated as follows:

$$P_{PV} = Y_{PV} f_{PV} \left(\frac{\overline{G}_t}{\overline{G}_{STC}} \right) \tag{2.5}$$

where Y_{PV} is the rated capacity of the PV array, f_{PV} is the PV derating factor, $\overline{G}_{STC}$ is the incident radiation under standard test conditions (1 kW/m^2) and $\overline{G}_T$ is the solar radiation incident on the PV array in the current time step, t, (kW/m^2) as shown in the next section. The derating factor is a scaling factor that accounts for reduced output in real-world operating conditions compared to the conditions which the PV panel was rated. Note, that in this work the effect of temperature on the array is neglected.

2.3.1 Incident Radiation

To calculate the power output from a PV array, incident radiation must be determined. Using the typical GHI in a region, which is the total amount of radiation striking the Earth's surface at a specific location for each time step, geographical location and PV panel orientation, the total amount of solar radiation incident on a surface can be calculated based on the methods described in Ref.[51]. A PV panel's

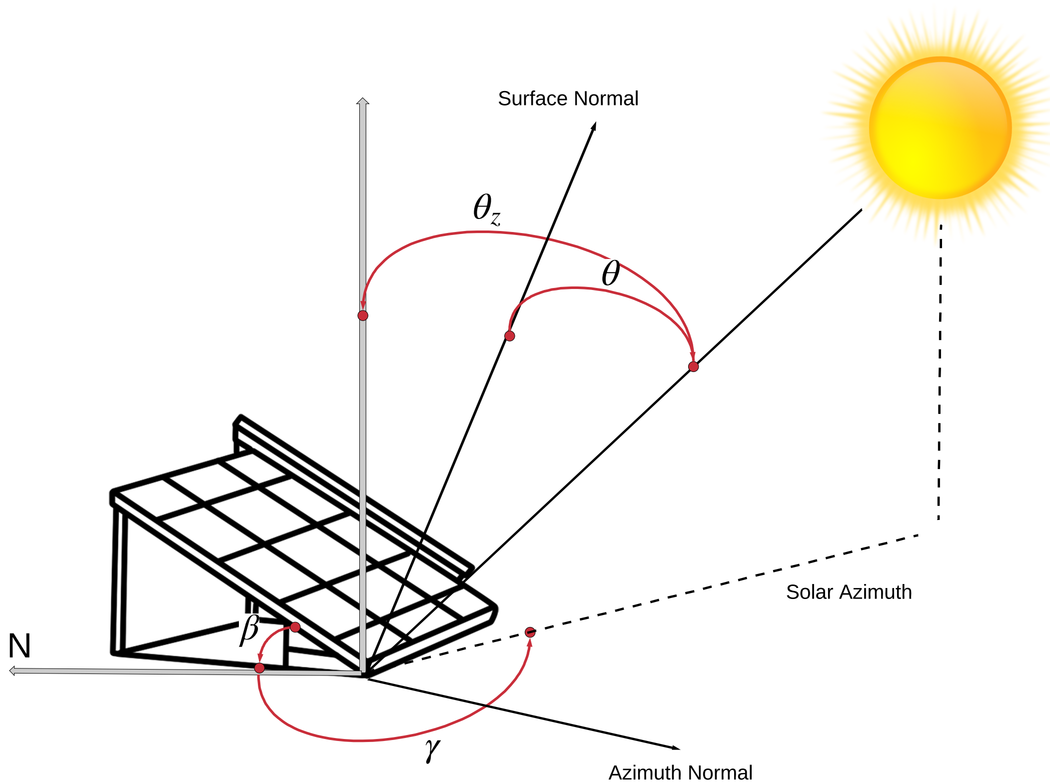

Figure 2.1: Solar panel with terrain and solar angles.

orientation is a function of two parameters: slope, β, and azimuth γ. The slope is the angle between the panel and the horizontal surface, where the azimuth is the direction the panel faces with respect to the North. These values are optimized based on the geographical region for optimal PV power output. First, solar declination is calculated for each day of the year, d, as in the equation below:

$$\delta = 23.45^o sin\left(360^o \frac{284 + d}{365}\right) \tag{2.6}$$

Next, the hour angle, w, is determined which describes the location of the sun in the sky throughout the day assuming the sun moves across the sky in 15^o per hour increments.

$$w = (t_s - 12hr)15^o/hr \tag{2.7}$$

where t_s is the solar time in (hr). To convert from civil time, in which data is usually presented, to solar time equation below is used:

$$t_s = t_c + \frac{\lambda_L}{15^o/hr} - Z_c + E \tag{2.8}$$

where t_c is the civil time corresponding to the midpoint of the time step (hr), λ_L is the longitude $(^o)$, Z_c is the time zone in hours east of GMT (hr) and E is the equation of time. The equation of time as shown in Fig.2.2 accounts for the tilt of the Earth's axis of rotation relative to the place of the ecliptic and eccentricity of the Earth's orbit as follows:

$$\begin{aligned} E = 3.82\Big(&0.000075 + 0.001868cosB - 0.032077sinB \\ &- 0.014615cos2B - 0.04089sin2B\Big) \end{aligned} \tag{2.9}$$

where

$$B = 360^o\frac{d-1}{365} \tag{2.10}$$

Next, the angle of incidence, θ, the angle the sun's beam radiation makes with the

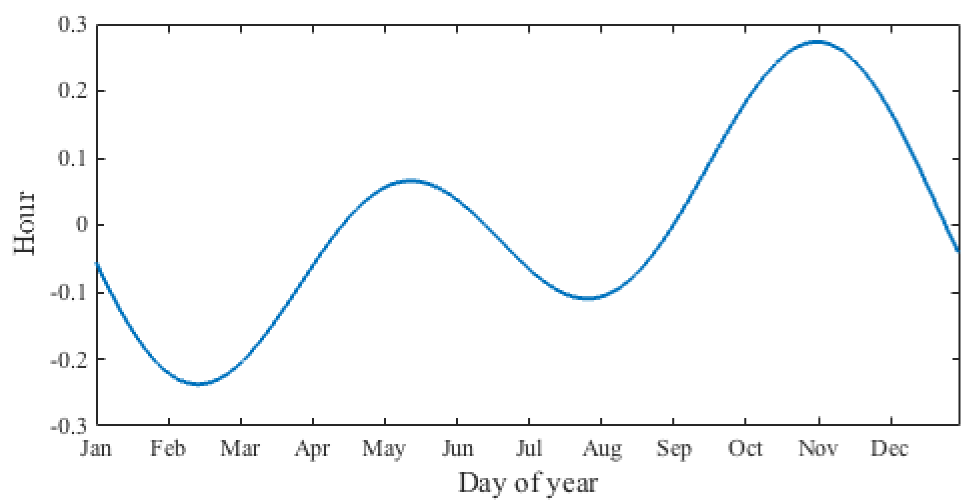

Figure 2.2: Equation of time.

normal of the surface, is defined based on the angles calculated above as shown in Fig.2.1.

$$\begin{aligned} cos(\theta) = {} & sin(\delta)sin(\phi)cos(\beta) \\ & - sin(\delta)cos(\phi)sin(\beta)cos(\gamma) \\ & + cos(\delta)cos(\phi)cos(\beta)cos(w) \\ & + cos(\delta)sin(\phi)sin(\beta)cos(\gamma)cos(w) \\ & + cos(\delta)sin(\beta)sin(\gamma)sin(w) \end{aligned} \tag{2.11}$$

where ϕ is the latitude of the panel's location. The zenith angle, θ_z, is the incidence angle that describes the angle between the vertical line and the line to the sun as in Fig.2.1. The equation for the zenith angle is derived from Eq.2.11 by setting $\beta = 0$, since zenith angle is 0^o when the sun is directly overhead and 90^o when the sun is at the horizon, yielding:

$$cos(\theta_z) = cos\phi cos(\delta)cos(w) + sin(\phi)sin(\delta) \tag{2.12}$$

Calculating the extraterrestrial normal radiation or the amount of solar radiation striking the surface perpendicular to the sun's rays at the top of Earth's atmosphere, G_{on}, in (kW/m^2), using the equation below:

$$G_{on} = G_{sc}\left(1 + 0.033cos\frac{360d}{365}\right) \tag{2.13}$$

where G_{sc} is the solar constant (1.367 kW/m^2). The extraterrestrial horizontal radiation or the amount of solar radiation striking a horizontal surface at the top of the atmosphere, G_o, in (kW/m^2) is as follows:

$$G_o = G_{on}cos(\theta_z) \tag{2.14}$$

The average extraterrestrial horizontal radiation over a time step is obtained by integrating:

$$\overline{G}_o = \frac{12}{\pi}G_{on}[cos(\phi)cos(\delta)(sin(w_2) - sin(w1)) + \frac{\pi(w_2 - w_1)}{180^o}sin(\phi)sin(\delta)] \tag{2.15}$$

where w_1 is the hour angle at the beginning of the time step (^{o}) and w_2 is the hour angle at the end of the time step (^{o}). Next, the clearness index is determined, which is the ratio of the surface radiation to the extraterrestrial radiation.

$$k_T = \frac{\overline{G}}{\overline{G}_o} \tag{2.16}$$

where $\overline{G}$ is the GHI on Earth's surface averaged over the time step (kW/m^2). Once the extraterrestrial radiation penetrates Earth's atmosphere it is broken down into components due to photon scattering and absorption out of the beam into random paths in the atmosphere as shown in Fig.2.3. Photons whose direction has been changed by Earth's atmosphere become scattered in turn forming the diffuse sky radiation, $\overline{G}_d$, which comes from all parts of the sky and can not cast a shadow. The unabsorbed and unscattered photons (nearly collimated) that cast a shadow are defined as direct beam radiation, $\overline{G}_b$. Both diffuse and direct beam radiation combine together to form GHI. Note, the ground reflected radiation component is added later to the total global radiation, $\overline{G}_T$.

In the cases where beam and diffuse radiation are not given by component, the clearness index is used to determine the diffuse fraction as below.

$$\frac{\overline{G}_d}{\overline{G}} = \begin{cases} 1.0 - 0.09k_T, & \text{for } k_T \leq 0.22 \\ 0.9511 - 0.1604k_T + 4.388k_T^2 - 16.638k_T^3 + 12.336k_T^4, & \text{for } 0.22 < k_T \leq 0.80 \\ 0.165, & \text{for } k_T > 0.80 \end{cases}$$

Then, the beam radiation is calculated as follows,

$$\overline{G}_b = \overline{G} - \overline{G}_d \tag{2.17}$$

The total global radiation on a PV surface is calculated using the Hay, Davies, Klucher, Reindl (HDKR) model [51] which involves three distinct components: (1) isotropic component from all parts of the sky, (2) circumsolar component related to the direction of the sun, and (3) horizon brightening component from the horizon. These components are dependent on three factors: ratio of beam radiation on tilted surface to beam radiation on the horizontal surface, R_b, anisotropy index, A_i, and the horizon brightening factor, f as described in the following equations Eq.2.18-2.20. The anisotropy index is the measure of atmospheric transmittance of beam radiation,

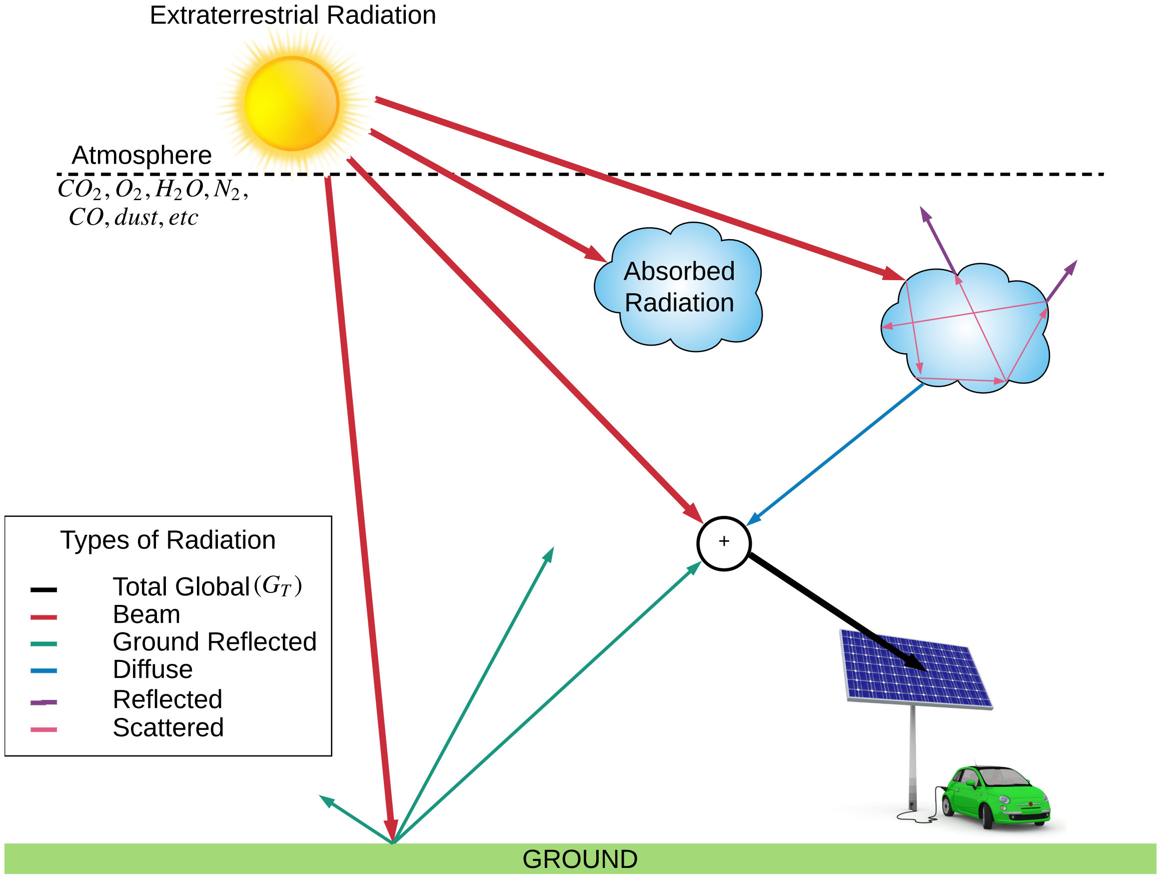

Figure 2.3: Solar radiation components.

which is used to calculate the amount of circumsolar or scattered radiation. The horizon brightening factor accounts for the fact that more diffuse radiation comes from the horizon than from the rest of the sky, which is related to cloudiness as below.

$$R_b = \frac{cos\theta}{cos\theta_z} \tag{2.18}$$

$$A_i = \frac{\overline{G}_b}{\overline{G}_o} \tag{2.19}$$

$$f = \sqrt{\frac{\overline{G}_b}{\overline{G}}} \tag{2.20}$$

The HDKR model combines the above mentioned components to determine the solar radiation incident on a PV array as follows:

$$\overline{G}_T = (\overline{G}_b+\overline{G}_d A_i)R_b+\overline{G}_d(1-A_i)\left(\frac{1+cos(\beta)}{2}\right)\left[1+f sin^3\left(\frac{\beta}{2}\right)\right]+\overline{G}\rho_g\left(\frac{1-cos(\beta)}{2}\right) \tag{2.21}$$

where ρ_g is the ground reflectance, or the albedo (%).

2.4 Uncoordinated Charging

Uncoordinated charging or charging upon request is the simplest form of charging that is widely used today. As the vehicle arrives at the charging station the power is provided immediately until the station receives a full capacity signal or the vehicle is unplugged from the charging station. This strategy does not involve any control and does not match the installed renewable energy generation. Any renewable energy generated either contributes to charging if requested or is injected directly into the grid.

2.5 Coordinated Charging

Coordinated charging implements unit-commitment strategies to determine the optimal load profile, while ensuring full charge at minimal cost to both the customer and parking lot owner.

2.5.1 Objective Function

The optimization problem is formulated using MILP with the target of minimizing the OC as defined per day, d, in Eqn. 2.22. The decision vector contains: solar surplus sold to the grid for each time step, t ($S^{+}_{net,t}$), net power used by the load from grid and/or PV installation at time t ($S^{-}_{net,t}$), load at time t (L_t), a binary state matrix (1-charging or 0-stand-by) for each vehicle entered, n, at time t ($s_{n,t}$) and amount of power that exceeds the demand charge threshold at time t (S^{+}_{demand}).

$$OC_d = \sum_{t=1}^{T}(C_{in,t}S^{-}_{net,t} - C_{out,t}S^{+}_{net,t}) + C_{demand}S^{+}_{demand,t} \tag{2.22}$$

where $C_{in,t}$ and $C_{out,t}$ are the cost of purchasing the deficit electricity at time t and the profit earning surplus electricity back to the grid at time t, respectively. C_{demand}

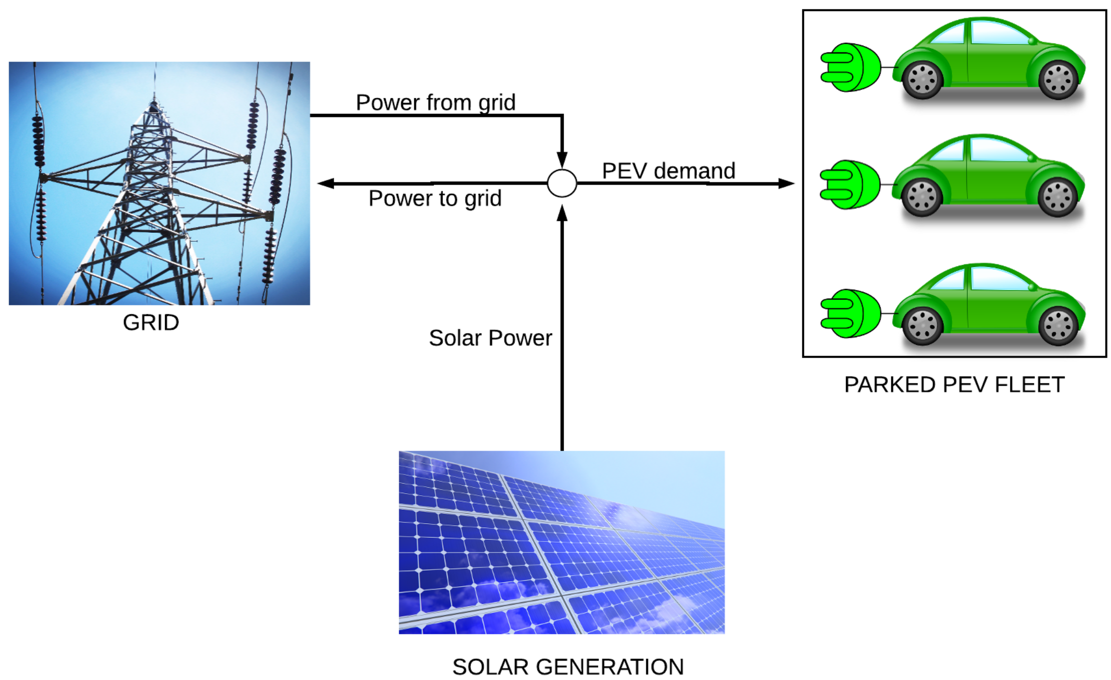

Figure 2.4: The system power allocation.

is the demand charge for penalizing the objective function when the maximum peak is high and $S^{+}_{demand,t}$ is the positive semidefinite matrix of electricity surpassing the threshold beyond which the demand charge is penalizes the objective function. Fig. 2.4 illustrates the power balance flow as defined below:

$$S_{gen,t} - L_t = \eta_{inverter} S^{+}_{net,t} - \frac{S^{-}_{net,t}}{\eta_{inverter}} \tag{2.23}$$

where $\eta_{inverter}$ is the efficiency of the AC/DC inverter.

Note, that $S^{+}_{net,t}$ is a positive semidefinite variable and $S^{-}_{net,t}$ is a negative semidefinite variable. The load is defined as follows:

$$L_t = \eta_{charger} P_{ch} \sum_{n=1}^{N_d} s_{n,t} \tag{2.24}$$

where P_{ch} is the nominal charging rate of the charging stations limited by the on-board PEV charger, N_d is the number of cars that enter during the day and $\eta_{charger}$ is the PEV charger efficiency.

2.5.2 Operational Constraints

In addition to Eqn. 2.1 - 2.24, the MILP is programmed given a number of constraints to ensure proper operation of the load scheduling algorithm. The algorithm must ensure that at the time of departure, each car is charged up to an acceptable State of Charge (percentage), SOC_n^{max}, as shown below,

$$\frac{P_{ch}}{CAP_n^b}\Delta T\sum_{t=1}^{T} s_{n,t} \leq SOC_n^{arr} - SOC_n^{max} \tag{2.25}$$

where CAP_n^b is the capacity of the battery for each vehicle n, ΔT is the time step, and SOC_n^{arr} is the SOC of vehicle n at the time of arrival, $t_{arr,n}$. Note, that if the battery capacity and SOC information is unavailable and only the energy consumed is provided the Eq.2.25 is reduced to

$$-P_{ch}\sum_{t=1}^{T} s_{n,t} \leq -E_{consumed}^n \tag{2.26}$$

where $E_{consumed}^n$ is the amount of energy consumed by vehicle n.

The lower and upper boundary constraints are defined to create a capacity limit on the feeders. L_{max} is a limiting constant of the amount of power transferred to the load ($S_{net,t}^-$), and S_{max} limits the amount of solar power sold to the grid ($S_{net,t}^+$). To account for the charging only during the period when the car is present, $s_{n,t}$ is bounded as shown below:

$$0 \leq s_{n,t} \leq \begin{cases} 1, & t_{arr,n} \leq t \leq t_{dep,n} \\ 0, & otherwise \end{cases} \tag{2.27}$$

where $t_{dep,n}$ is the vehicle's departure time. For the case study in Victoria, BC additional logic is added to cope with the demand charge structure. The region abides by a tiered system of demand charges. There are no demand charges if the peak power usage is under a certain threshold, therefore an additional constraint as shown in Eq.2.28 is added to ensure global minimum when determining the operation charges.

$$S_{net,t}^- + S_{demand,t}^+ - S_{demand,t}^- = \delta_{thresh} \tag{2.28}$$

where δ_{thresh} is the power threshold determined by the electric utility above which a demand charge is applied, S_d^- and S_d^+ is the negative and positive component of the power difference between the required power and δ_{thresh} that ensures feasibility of the problem while penalizing the solution that surpasses the threshold as seen in Eqn.2.22.

2.6 Model Verification

Due to lack of infrastructure available to test the methodology in a real world scenario, the model was compared to an existing validated model available in HOMER Legacy v2.68. HOMER is a powerful tool, however it has limitations in this application. The software uses a graphical user interface where the inputs are entered manually, and the internal components of the program are protected, hence the electrical demand control can not be implemented within HOMER. Additionally, HOMER uses a 1 hr time step for all of the component simulations, while the service provider in California, Pacific Gas and Electric (PG&E), uses a fine 15 min time step for demand charge recording. A simplified system with a coarse 1 hr time scale is used in this thesis as shown in Fig.2.5.

To test the methodology demand profiles built based on the vehicles arriving at the parking lot were used as input into the HOMER model. Additional variables such as electricity tariff, capital costs and specification of the equipment were matched between the two models. For verification purposes a net-metered grid tariff of 0.34$/kWh and a demand charge of 19.743 $/kW with geographical specifications for Los Angeles, CA were defined. Fig.2.6a shows the difference in NPC between the HOMER model and the in-house MATLAB model for a range of PV carport prices (3.6-7.2$/kW). The most costly NPC curve correlating to the highest cost of the PV carport. Similarly, in Fig.2.6b analogous results were obtained for NPC with peak demand recorded every 15 min with the in-house MATLAB model and every 1 hr with HOMER. The averaging error leading to cost under-estimation using the HOMER result is emphasized in this scenario.

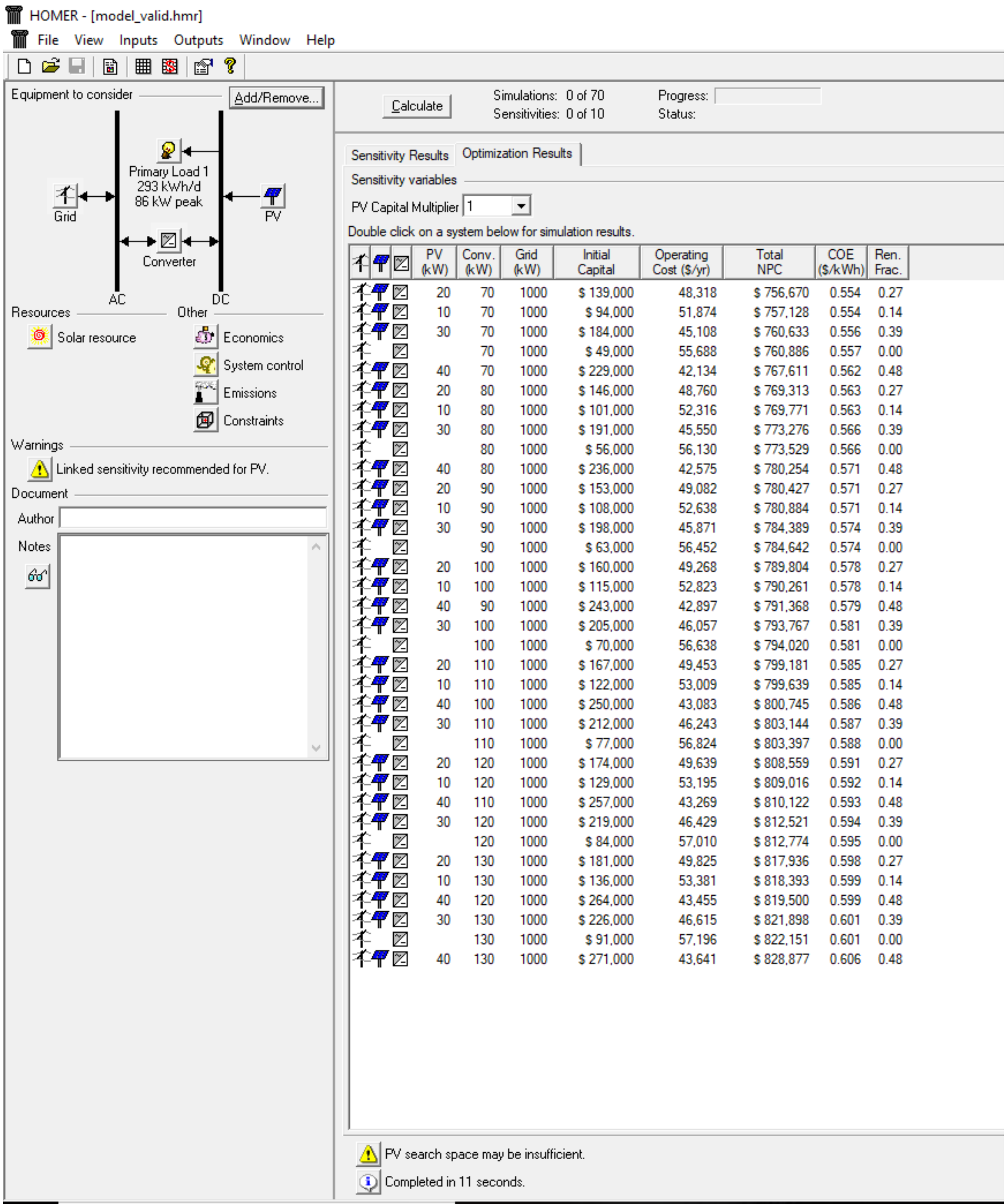

Figure 2.5: Sample model output using HOMER Legacy v2.68.

Even though HOMER is a well-tested and validated software it has shortcomings in this application. The effect of this is especially obvious in Fig.2.6b. In addition, the PG&E grid tariff implements a 30 minute interval time of use pricing, increasing the error differences between the HOMER model and the realistic scenario. Finally, HOMER lacks input/output interface and access to internal system components, which poses an issue when implementing control schemes and demand optimization strategies necessary for coordinated charging. Hence, the coordinated charging techniques described in Sec.2.5 were designed in MATLAB.

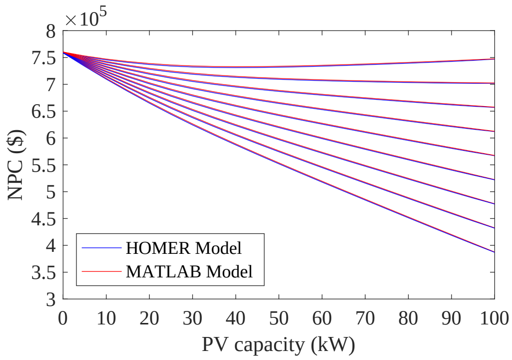

(a) NPC comparison with demand charges recorded at 1hr interval.

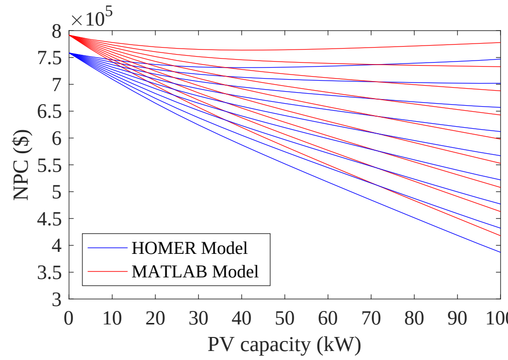

(b) NPC comparison with demand charges recorded at 15min interval.

Figure 2.6: Comparison of NPC formulated by HOMER model and by MATLAB model. Each curve represents a different capital investment cost for PV carport; increasing from 3.6$/W (top curve) to 7.2 $/kW (bottom curve).

Chapter 3

Results

Using the methodology described in Chapter 2, two case studies, exploring EVSPLs with widely different electricity tariff structures and geographic characteristics, are compared: Victoria, BC and Los Angeles, CA. In this chapter the results for techno-economical feasibility of an EVSPL are presented based on real-world parameters for driving patterns, solar resource, grid tariffs and typical base loads pertained to the two cities. Additionally, the effects of coordinated charging are quantified and component optimization is conducted. Lastly, a parametric study is carried out to determine the limits of economic feasibility.

3.1 Parameter Definitions

3.1.1 Driving Patterns Parameters

To test the methodology, a dataset was collected from individual EVSE in various zip codes in Southern California in 2013 from ChargePoint [52]. Each charging station provides information regarding time of arrival and departure, average power, maximum power on 15 minute time interval, charging port type, zip code and non-residential building category.

The distribution of arrival and departure times is shown in Figs. 3.1a and 3.1b, respectively. Note, that the majority of cars arrive in the morning between 7 am and 9 am with another peak in the afternoon between 12 pm and 1 pm. The amount of energy each car requires to complete full charge is shown in Fig. 3.2. It is evident that a majority of the cars that park in this area do not require more than 20 kWh of charge to reach full capacity.

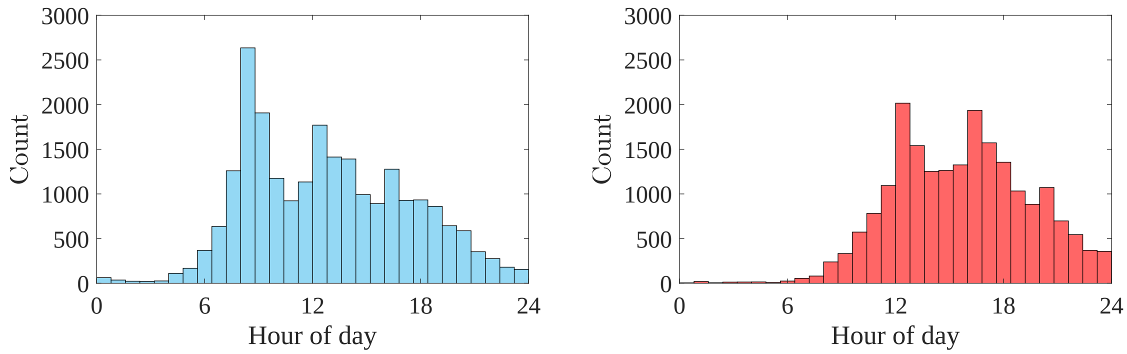

(a) Distribution of arrival time

(b) Distribution of departure time

Figure 3.1: Arrival and departure time characteristics

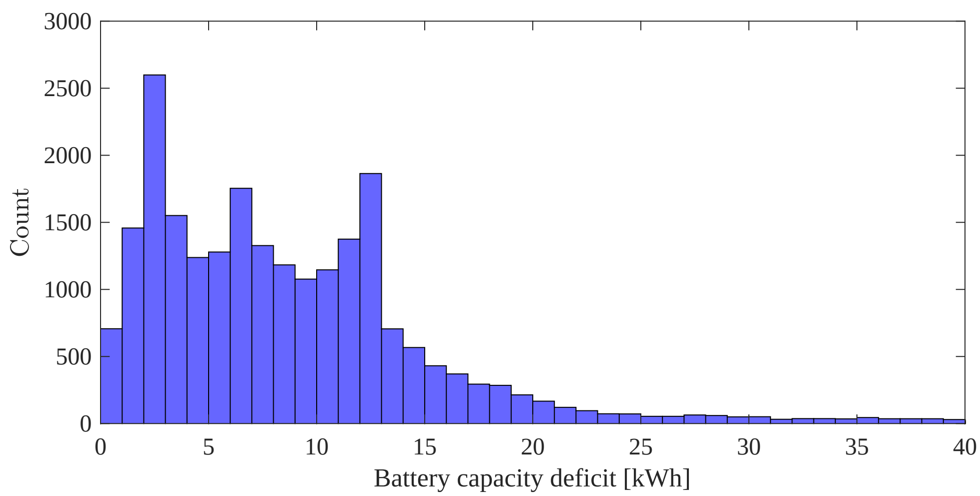

Figure 3.2: Distribution of energy required to reach full charge by each car.

3.1.2 Charger Specifications

As suggested in Ref.[53], Level 2 and DC chargers are most suitable for the EVSPL scenario since Level 1 chargers can not provide sufficient current to charge PEVs quickly. The ChargePoint data presented in the previous section shows that 17% of vehicles do not reach full charge at the time of the departure with Level 2 charging however the majority of the vehicles leave with over 75% capacity as seen in Fig.3.3. In contrast DC chargers can ensure all vehicles are at full battery capacity upon departure; however the cost of installation and equipment of a DC charger is much higher than a Level 2 charger as shown in Table.3.1. In this work it is assumed that each station is able to provide power when plugged in and a plug is available for each vehicle parked in the lot. In other words, the vehicles remain connected regardless of the state of charge of the battery, hence the same amount of charging stations is required regardless of the charging level.

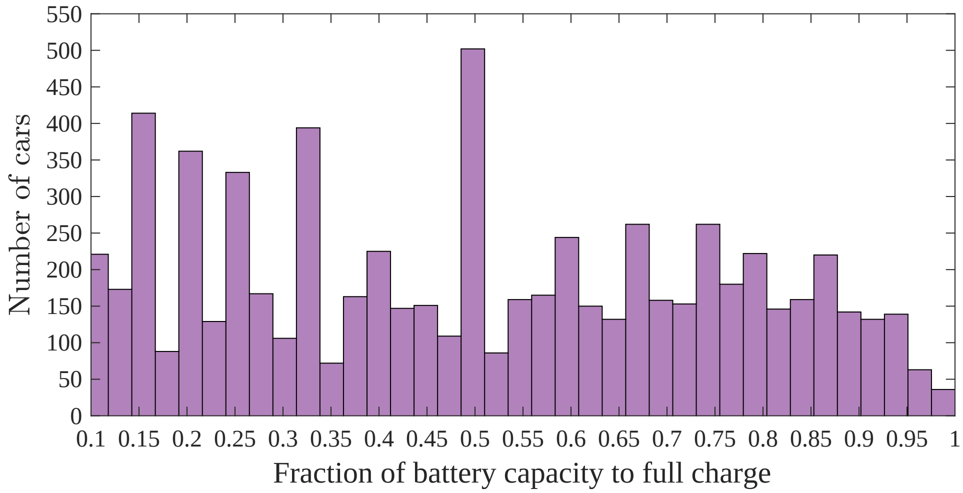

Figure 3.3: Distribution of vehicles that leave the parking lot with incomplete charge in a parking lot with Level 2 chargers.

Table 3.1: Cost break down of charging stations.

	Level 2	DC Charger
Station Cost	\$500-700	\$10,000
Parts & Labour	\$1200-2000	\$40,000-50,000
Total	\$1700-2700	\$50,000-60,000

The ChargePoint data is subject to a vehicle queueing algorithm that determines the minimum number of charging stations required to ensure an acceptable level of customer satisfaction. To illustrate the relationship between number of charging stations and customer acceptance, Fig.3.4 depicts 100 vehicles of one realization of normally distributed time of arrival, departure, state of charge and 5 kW on-board peak charging charging power. In this configuration coordinated charging scheme mandates a 60 kW feeder to abide by feasibility limits of the problem resulting in a maximum of 12 vehicles capable of charging in one time slot. However, as shown in

Fig.3.4, 12 charging stations are associated with 31% refusal rate and 45% of vehicles with incomplete charge. This outcome is due to the time restrictions of each vehicle and the assumption that vehicle power connectors remain plugged-in until the time of departure. Even though only 12 charging stations are powered at once, 30 charging stations are required to accommodate all the parking lot customers. Since the number of vehicles and their specifications vary daily, the algorithm to assess the number of stations is applied to each day to find the minimum amount of stations required each day of the year. Then, using the largest value of the array, the queueing algorithm reorders the vehicles according to the final number of stations required to ensure maximum customer satisfaction.

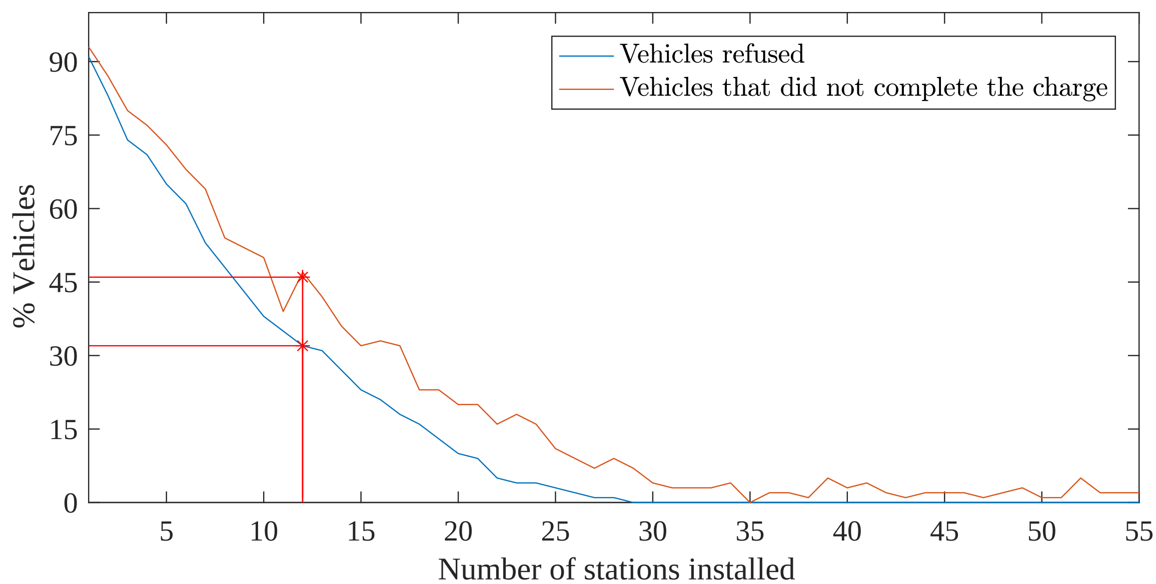

Figure 3.4: Percent of vehicles refused and those not fully charged versus number of charging stations.

3.1.3 Solar Parameters

Solar Irradiation

Time-varying solar irradiation data was obtained for Southern Los Angeles, CA for a typical meteorological year (TMY3) from NREL as shown in Fig. 3.5a [54]. For comparison, a Northern location was chosen in Victoria, BC to demonstrate the geographical dependence of time-varying solar irradiation as shown in Fig.3.5b. This data was provided on a minute scale by a School-Based Weather Network for 2014 [55].

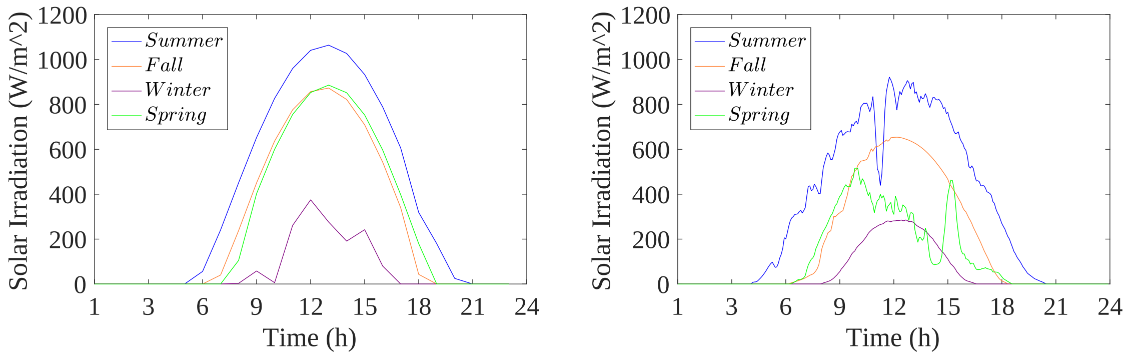

(a) Typical seasonal solar profiles in Southern Los Angeles, CA

(b) Typical seasonal solar profiles in Victoria, BC

Figure 3.5: Typical solar profiles comparison in Southern Los Angeles, CA and Victoria, BC

Due to the southern geographic positioning, Los Angeles receives more solar irradiation compared to Victoria. In addition, Victoria is subjected to more intermittency due to cloud coverage as shown in the summer and spring months in Fig. 3.5b.

PV specifications

In this study, state of the art Sunpower X-series PV panels we analysed. Their specifications are shown in Table. 3.2.

Table 3.2: PV Panel Specifications

Panel Specification	**Value**
Panel name	SunPower X-series
Efficiency	22.2%
Area of Panel	1.6 m^2
Tilt in Los Angeles	28.81 deg
Tilt in Victoria	39.9 deg
Warranty	25 years
Cost of shelter	4.5$/W-6.0$/W

3.1.4 Electricity Tariffs

In Victoria, BC Hydro is the main service provider with the tariff for commercial applications as shown in Table.3.5 [1]. The electricity tariffs included in this study for Los Angeles are obtained from PG&E rate structure E-19 for solar customers as depicted in Table.3.3. In addition, California customers are subject to a Time of Use (TOU) demand charge as in Table. 3.4. Note, the summer rates apply starting May 1st until October 31st.

Table 3.3: E-19 electricity tariff structure in Los Angeles, CA.[1]

Energy Charges	**$/kWh**	**Time Period**
Peak Summer	0.34020	12:00 PM-6:00 PM
Part-Peak Summer	0.15997	8:30 AM-12:00 PM 6:00 PM-9:30 PM
Off-Peak Summer	0.08512	9:30 PM-8:30 AM
Part-Peak Winter	0.10689	8:30 AM-9:30 PM
Off-peak Winter	0.09178	9:30 PM-8:30 AM

Table 3.4: E-19 electricity demand charges structure in Los Angeles, CA.[1]

Demand Charges	**$/kW**	**Time Period**
Max. Peak Demand Summer	17.71253	12:00 PM-6:00 PM
Max. Part-Peak Summer	0.51	8:30 AM-12:00 PM 6:00 PM-9:30 PM
Max. Demand Summer	19.71253	Any time
Max. Part-Peak Demand Winter	0.03	8:30 AM-9:30 PM
Max. Demand Winter	19.71253	Any time

Table 3.5: BC Hydro Commercial Electricity Rates. [2]

Max. Demand	**Electricity Tariff ($/kWh)**	**Base Demand Charge ($/kW)**	**Demand Charge ($/kW)**
Under 35 kW	0.1139	0.3312	0
Between 35kW-150kW	0.088	0.2429	4.92
Above 150kW	0.055	0.2429	11.21

[1] The Canadian Dollar is assumed to be on par with the US Dollar.

3.1.5 Base Load

To explore the effects of coordination, five types of base loads are identified: no base load, small office load, large office load, strip mall and a full-service restaurant. The data was obtained from NREL repository for Los Angeles, CA and Seattle, WA as shown in Fig.3.6. Note, that NREL does not gather such information in Canada, therefore data from Seattle, WA was used to represent a similar economic and climactic environment to Victoria, BC [2]. The office buildings vary in load seasonally with higher demand depending on the region. In the summer, Los Angeles has increased electrical consumption due to the HVAC demand, where Seattle has increased electrical consumption in the winter due to heating. The low demand days are attributed to weekends and holidays in the office buildings. Alternatively, restaurants and strip malls maintain the same level of demand throughout the year with slight seasonal variation.

[2] Seattle, WA and Victoria, BC have similar average yearly sunshine hours

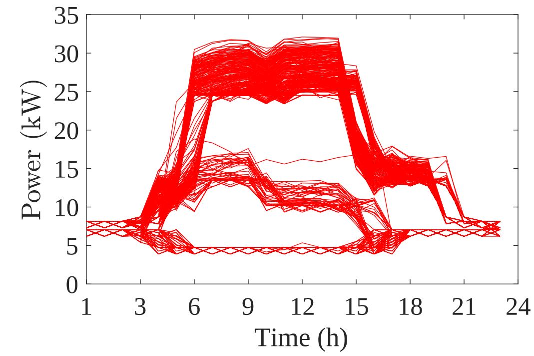

(a) Small office base load in Los Angeles, CA.

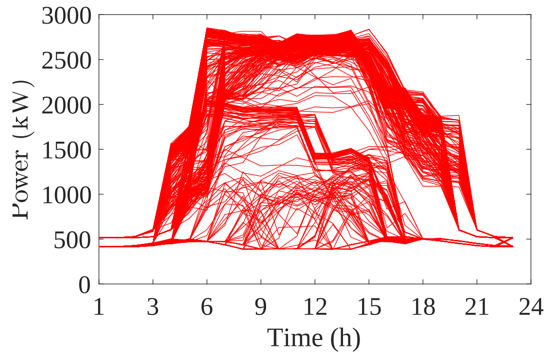

(b) Large office base load in Los Angeles, CA.

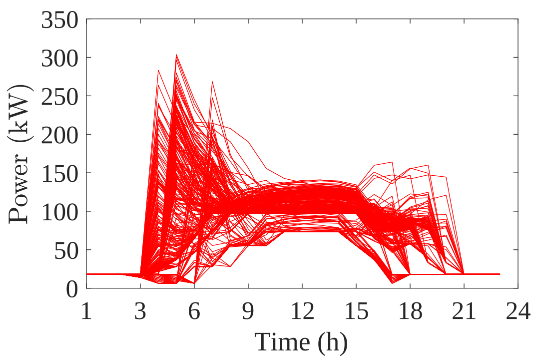

(c) Strip mall base load in Los Angeles, CA.

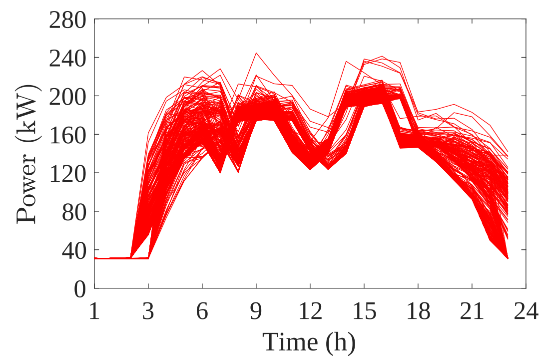

(d) Restaurant base load in Los Angeles, CA.

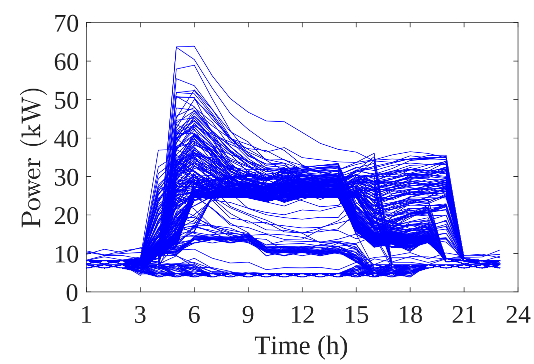

(e) Small office base load in Seattle, WA.

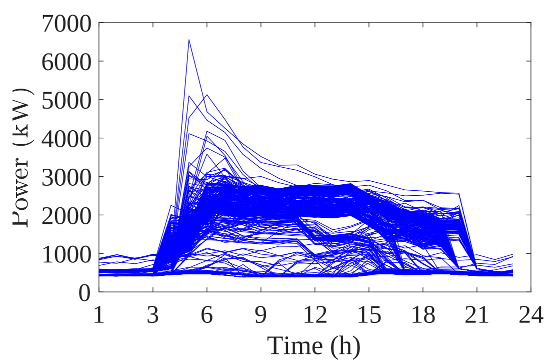

(f) Large office base load in Seattle, WA.

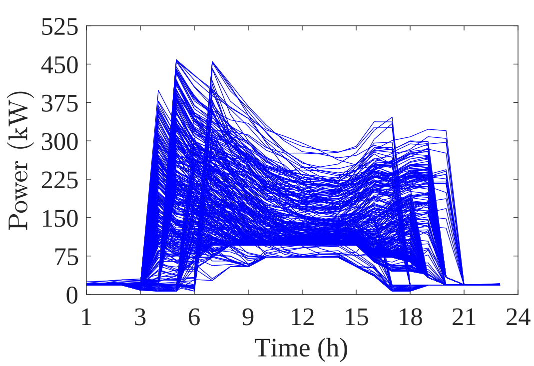

(g) Strip mall base load in Seattle, WA.

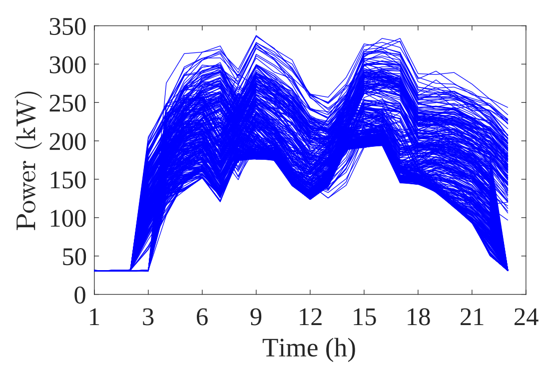

(h) Restaurant base load in Seattle, WA.

Figure 3.6: Types of base load profiles near large parking structures in Los Angeles, CA and Seattle, WA; each curve represents day of year.

3.2 Coordinated Charging

Using the parameters defined in Section 3.1 two techno-economic studies were conducted comparing the viability of installing solar equipped parking lots for charging electric vehicles in Victoria, BC and Los Angeles, CA.

3.2.1 Load on the grid

Applying the algorithm described in Section 2, for the case of TOU tariffs, reveals the impact on grid load of coordinated versus uncoordinated charging in Fig.3.7. Car 1 and Car 4 are parked in the lot for a short duration and require the full time slot to charge. In contrast, Car 2 is parked for a longer duration and remains plugged-in during peak and part peak tariff. To abide by the cost minimization scheme the second car begins to charge during the morning part peak, halts during peak hours and resumes in the evening part peak. Similarly to Car 2, Car 3 is parked during peak and part peak hours. However, since the vehicle requires more time to charge than the amount of time available in the part peak hours, it is forced to partially charge during peak hours to make up for the difference. Addition of solar further exemplifies the methodology in Fig.3.8 for uncoordinated charging and Fig.3.9 for coordinated charging. It is clear that with coordination the algorithm takes advantage of solar when available by shifting the demand while simultaneously reducing load peaks and cost of charging.

3.2.2 Operating Costs

The formulation of cost minimization is resolved on a 15 minute time scale for each day of year and integrated over the project lifetime of 25 years. The operating costs comprise of two components: electricity charges and demand charges as specified in section 3.1.4. These costs include losses due to energy conversion for both AC/DC and DC/AC conversion. Both case studies, Victoria and Los Angeles, implement a net-metering strategy; however, the billing structures for the two locations differ. Victoria breaks down the electricity price based on peak demand recorded each year in-turn, categorizing the business as small, medium or large. Once the business is classified, the same price of electricity is maintained until next year's evaluation of the business category. Since the electricity tariff abides by net-metering rules and remains the same regardless of TOU there is effectively no savings in cumulative

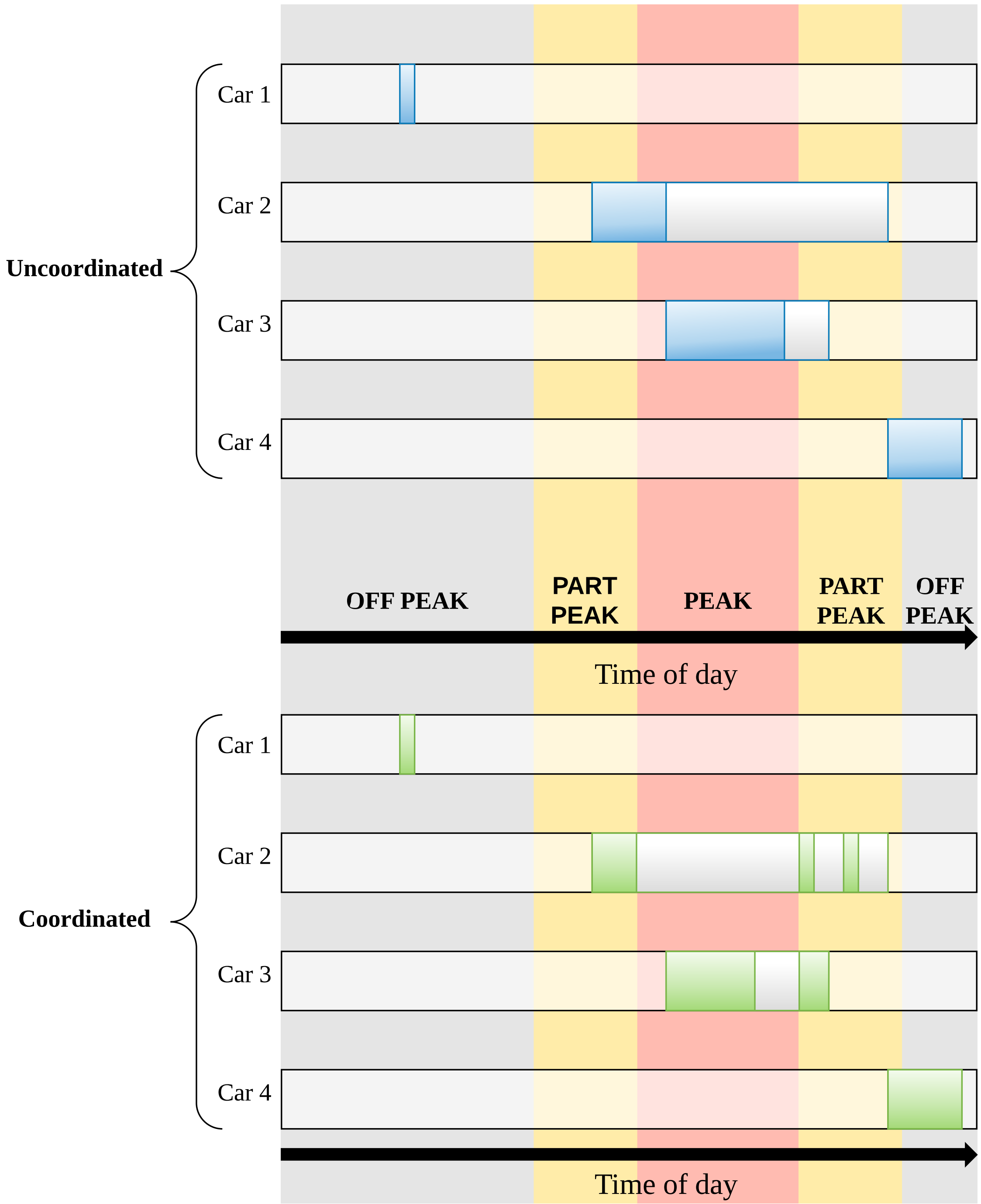

Figure 3.7: Comparison of uncoordinated charging to coordinated charging under TOU tariff.

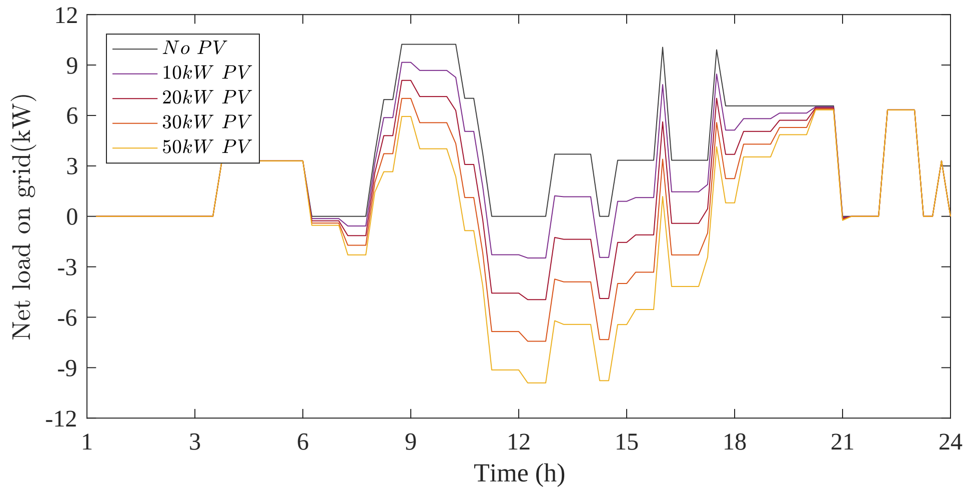

Figure 3.8: Power transfer ($S_{net}^{-} - S_{net}^{+}$) for uncoordinated charging with different PV penetrations.

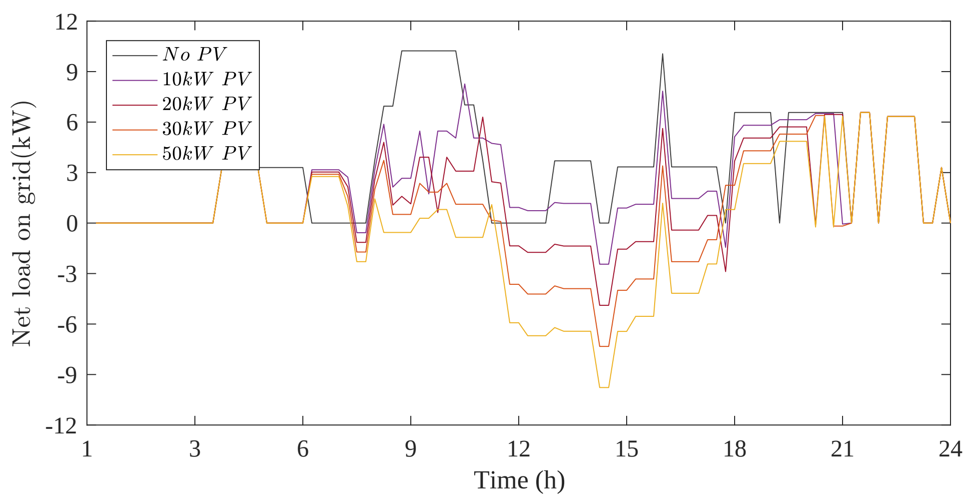

Figure 3.9: Power transfer ($S_{net}^{-} - S_{net}^{+}$) for coordinated charging with different PV penetrations.

electricity costs with coordination. However, with coordination the system is able to bypass a fraction of the demand charges as shown in Table.3.6. On the other hand, Los Angeles uses a TOU tariff structure, which gives the opportunity for coordinated charging to have a higher impact on both electricity charges and demand charges by shifting the load to a more cost favourable region as shown in Table.3.7. The savings accumulated by implementing coordination increase with higher PV capacities. This increase is expected since solar has zero marginal costs, which at higher capacities with more room for coordination can bring down the operating costs.

Table 3.6: Operating Costs in Victoria, BC

PV Capacity (kW)	Electricity Charges ($/yr)	Uncoordinated charging		Coordinated charging		Cost Savings (%)
		Demand Charges ($/yr)	Operating Costs ($/yr)	Demand Charges ($/yr)	Operating Costs ($/yr)	
0	10,539	6,600	17,139	4,622	15,161	11.5
5	9,966	6,537	16,503	4,560	14,526	12.0
10	9,397	6,486	15,883	4,500	13,897	12.5
15	8,835	6,444	15,279	4,399	13,234	13.4
20	8,282	6,404	14,686	4,385	12,667	13.7
25	7,741	6,369	14,110	4,491	12,232	13.3
30	7,209	6,334	13,543	4,417	11,626	14.2
35	6,688	6,300	12,988	4,429	11,117	14.4
40	6,174	6,270	12,444	4,377	10,551	15.2
45	5,668	6,250	11,918	4,348	10,016	16.0
50	5,167	6,234	11,401	4,411	9,578	16.0
55	4,670	6,221	10,891	4,395	9,065	16.8
60	4,177	6,210	10,387	4,308	8,485	18.3
65	3,688	6,199	9,887	4,339	8,027	18.8
70	3,200	6,187	9,387	4,323	7,523	19.9
75	2,714	6,176	8,890	4,335	7,049	20.7
80	2,231	6,165	8,396	4,355	6,586	21.6
85	1,748	6,153	7,901	4,324	6,072	23.1
90	1,267	6,142	7,409	4,287	5,554	25.0
95	787	6,132	6,919	4,274	5,061	26.9
100	308	6,122	6,430	4,298	4,606	28.4

Table 3.7: Operating Costs, Los Angles, CA

PV Capacity (kW)	Uncoordinated Charging			Coordinated Charging			Cost Savings (%)
	Electricity Charges ($/yr)	Demand Charges ($/yr)	Operating Costs ($/yr)	Electricity Charges ($/yr)	Demand Charges ($/yr)	Operating Costs ($/yr)	
0	19,604	42,534	62,138	16,168	40,479	56,647	8.8
5	17,508	41,990	59,498	14,288	39,810	54,098	9.1
10	15,436	41,523	56,959	12,424	39,602	52,025	8.7
15	13,410	41,149	54,559	10,618	39,158	49,776	8.8
20	11,441	40,869	52,310	8,823	38,129	46,952	10.2
25	9,532	40,633	50,164	6,978	37,206	44,184	11.9
30	7,670	40,397	48,066	5,107	36,885	41,992	12.6
35	5,845	40,191	46,035	3,239	36,504	39,743	13.7
40	4,045	40,004	44,049	1,380	36,438	37,817	14.1
45	2,265	39,837	42,102	-484	36,048	35,564	15.5
50	499	39,691	40,190	-2,350	35,569	33,219	17.3
55	-1,257	39,556	38,299	-4,217	35,476	31,259	18.4
60	-3,006	39,422	36,416	-6,086	35,235	29,149	20.0
65	-4,749	39,292	34,542	-7,959	35,142	27,183	21.3
70	-6,487	39,176	32,689	-9,837	34,481	24,645	24.6
75	-8,221	39,068	30,847	-11,720	34,045	22,325	27.6
80	-9,952	38,961	29,009	-13,603	34,071	20,468	29.4
85	-11,681	38,854	27,173	-15,485	33,450	17,965	33.9
90	-13,408	38,747	25,339	-17,362	33,160	15,798	37.7
95	-15,133	38,639	23,507	-19,246	32,990	13,743	41.5
100	-16,857	38,532	21,676	-21,130	33,387	12,257	43.5

3.3 Net Present Cost

To determine the NPC, all the costs are summarized and discounted to present value while accounting for inflation for a 25 year amortization period. The NPC for Victoria and Los Angeles without a base-load are shown in Fig.3.10 and Fig.3.11 assuming the parking lot is already retrofitted with Level 2 charging equipment. Evidently, Victoria does not receive enough sunlight to take full advantage of PV. In addition, with net-metering and uniform grid tariff in Victoria, coordination is not able significantly reduce the NPC.

Alternatively, Los Angeles typically has higher levels of GHI which makes PV arrays a feasible option. The TOU grid tariff allows for coordination to play a higher role in reducing the NPC by shifting the load to off-peak or part-peak hours. The irregularities in the trend when using coordination are related to TOU demand charge scheme. With uncoordinated charging the demand peak decreases linearly with increased PV, however with coordinated charging the peak may appear elsewhere causing a non-smooth transition in the trend.

Notably, the savings from coordination diminish as PV capacity increases. This is to be expected since PV resource is effectively free, therefore when capacity of solar power is not limited, coordination becomes ineffective because grid participation is no longer required.

3.4 Component Optimization

To ensure the lowest cost to the EVSPL owner each system component is optimized. Retrofitting an existing parking structure may require additional electrical capacity which is quantified by a distribution feeder size. Lack of infrastructure to support additional electrical load can be a costly improvement, therefore feeder requirements are explored in the next section to quantify the effect of coordination of the distribution feeder size. Determining the optimal PV size is also crucial for cost minimization of the overall system. The optimal size depends on the geographic location, cost of the panels, grid tariff and the demand profile. The determined PV panel sizes for Victoria and Los Angeles are explored in this section.

3.4.1 Distribution Feeder

As electrical power is delivered from the transmission system to the individual customer, in this case an EVSPL, through a distribution feeder. This electrical wiring circuit, or feeder, carries power from the transformer or switch gear to a distribution panel. The feeder size determines the maximum amount of power that can be transferred to the network, which is measured by the electrical company on 15 minute intervals. Size requirement for each system varies based on the load profile. An oversized feeder for the demand profile has economic implications, such as costly electrical

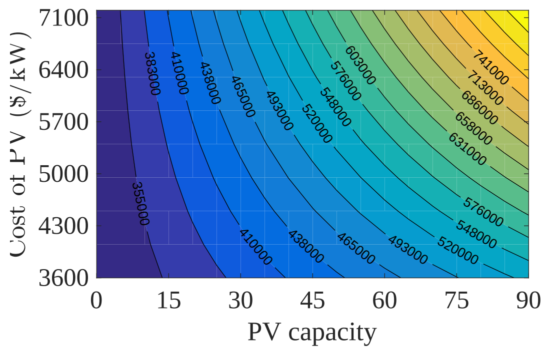

(a) NPC for uncoordinated charging for variable PV capacities and variable PV car port prices in Victoria, BC.

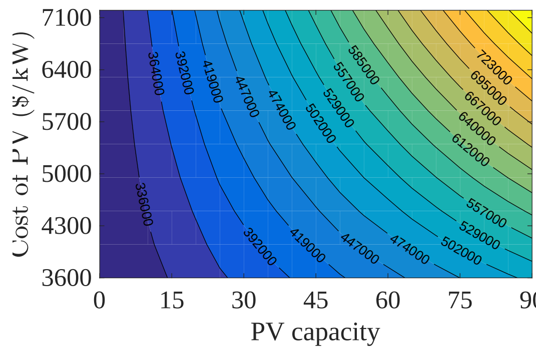

(b) NPC for coordinated charging for variable PV capacities and variable PV car port prices in Victoria, BC.

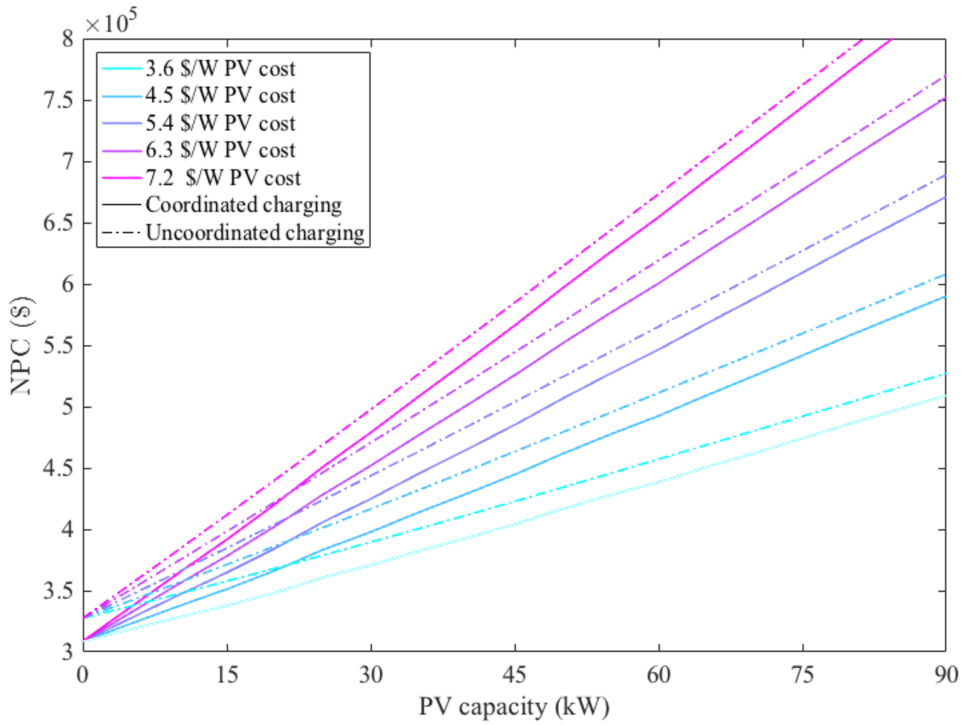

(c) NPC comparison of uncoordinated charging to coordinated charging for variable PV capacities and variable cost of PV car port in Victoria, BC.

Figure 3.10: NPC for a range of PV capacities and variable PV car port prices in Victoria, BC.

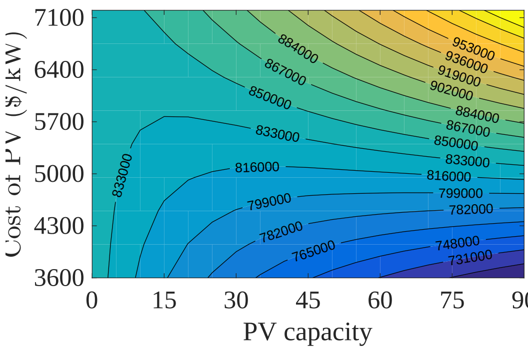

(a) NPC for uncoordinated charging for variable PV capacities and variable PV car port prices in Los Angeles, CA.

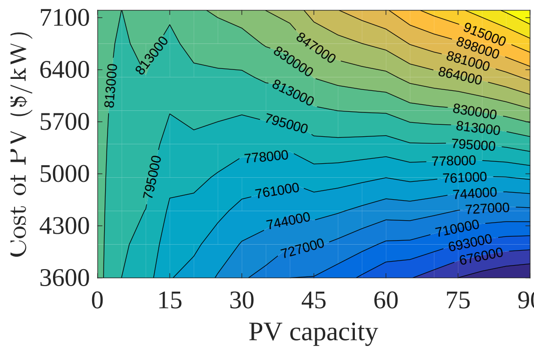

(b) NPC for coordinated charging for variable PV capacities and variable PV car port prices in Los Angeles, CA.

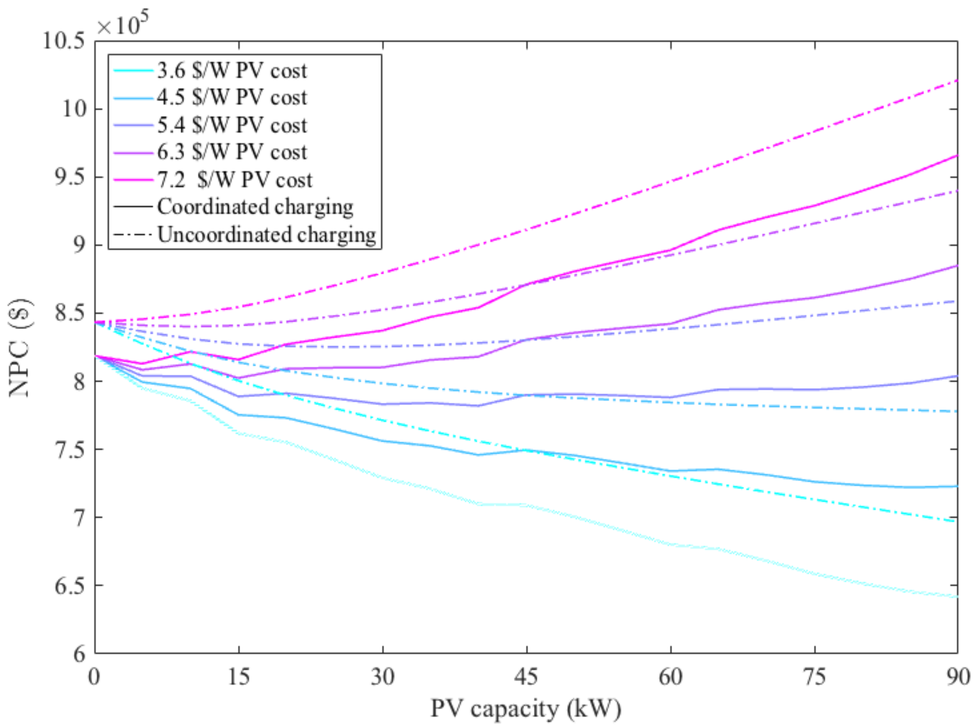

(c) NPC comparison of uncoordinated charging to coordinated charging for variable PV capacities and variable cost of PV car port in Los Angeles, CA.

Figure 3.11: NPC for a range of PV capacities and variable PV car port prices in Los Angeles, CA.

equipment upgrades and additional permits. Alternatively, feeders limit the potential of economic savings stemmed from the coordination algorithm in undersized configurations, since the algorithm can not take advantage of the off-peak or part-peak electricity tariff as effectively, which leads to an overall increased cost of operation. The feeder sizes required for this case study are shown in Table.3.8, and were determined based on feasibility of the system optimization. The values are determined without a PV installation to ensure reliable operation of the system despite lack of GHI. In Victoria, the feeder size can only be reduced through coordination with a small load. Alternatively, due to the TOU grid tariff in Los Angeles, coordination reduces the feeder size in all base load types but the biggest impact is with smaller loads since the algorithm has control over the entire demand profile rather than just a small portion, as in the case of the larger base loads.

Table 3.8: Feeder size requirements.

		No base load	Small Office	Large Office	Strip mall	Restaurant
Feeder size in Victoria (kW)	Uncoordinated	109	112	1639	150	150
	Coordinated	90	95	1639	150	150
	% Reduction	**17**	**15**	**0**	**0**	**0**
Feeder size in Los Angeles (kW)	Uncoordinated	110	113	770	126	144
	Coordinated	105	109	762	120	140
	% Reduction	**4.5**	**3.5**	**1.0**	**4.8**	**2.8**

3.4.2 PV Optimization

To minimize the cost of retrofitting an existing parking lot with PV array an optimization was performed to determine the cost sensitive solution. With small amount of solar irradiation in Victoria, PV arrays are not feasible with current capital cost of PV panels and relatively low electricity prices. Without PV arrays in Victoria, the NPC is determined to be \$327,496 with uncoordinated charging and \$308,780 with coordinated charging yielding 5.7% cost savings.

In Los Angeles, where solar irradiation is abundant and the prices of electricity are high, a PV array equipped parking lot is feasible. Table.3.9 presents the optimization results for a span of PV array prices. Due to computational complexity of the algorithm the optimization was bounded by 100 kW limit, therefore for a PV carport costing less than 3.60\$/W, EVSPL owners are profitable at any PV array capacity. The inverse is true for prices higher than 6.75\$/W. Above this price, PV arrays are no longer economically feasible. With coordination, the EVSPL is able to take advantage of higher PV array capacities without compromising the NPC. The cost savings range from 8-17% with addition of coordination. Note, that the current cost of PV carports is between 4.5-6.0\$/W and the extended range of values was investigated to determine the system's economic limits and the effect of PV car port costs on the size of the system.

Table 3.9: Optimal PV array sizes and the corresponding NPC for Los Angeles, CA.

PV Cost (\$/W)	Uncoordinated charging		Coordinated charging		
	Optimal PV array (kW)	NPC (\$)	Optimal PV array (kW)	NPC (\$)	Cost Savings (%)
3.60	100	686,088	100	565,692	17.5
4.05	100	731,088	95	609,437	16.6
4.50	100	776,088	95	652,187	16.0
4.95	45	809,956	95	694,937	14.2
5.40	25	825,268	90	736,948	10.7
5.85	15	834,195	25	760,074	8.9
6.30	10	840,127	25	771,324	8.2
6.75	0	843,329	0	773,139	8.3
7.20	0	843,329	0	773,139	8.3

Effect of a base load

This section explores the possibility of a parking lot sharing a common connection with a nearby business. Four types of base loads are employed with uncoordinated and coordinated schemes: small office building, large office building, full-service restaurant and a strip mall. In Victoria the optimal PV size is 0 kW regardless of the base load for cost of PV between 3.6 \$/W-7.2\$/W. The savings from coordination of charging are negligible in every base load scenario. In Los Angeles, PV car ports become an economically feasible option. With assistance of coordination, NPC is further reduced.

Table.3.11 shows the optimal PV capacity for an EVSPL merged with a large office. Note, the optimization for large office base load was bounded by 200 kW. At

PV car port cost between 3.6$/W-6.3$/W any PV capacity is feasible. In this price range there is a linear relationship between cost of PV car ports and NPC. With increasing PV capacity, the NPC decreases linearly, therefore it is advised to install the maximum PV capacity allowable. This behaviour is extended up to 6.75 $/W with coordinated charging. As PV car port prices increase beyond 6.3$/W without coordination and 6.75$/W with coordination the PV capacity optimization results dictate that smaller capacities are advantageous. However, since the base load is much higher than the PEV demand, the effects of coordination are minimal.

When considering a small office base load, the PV capacity optimization was bounded by 120 kW. Similarly, to large office scenario, the PV car ports are advantageous at prices between 3.6$/W-4.5$/W. At higher prices, smaller PV capacities are suggested as in Table.3.12. Since the baseload is comparable to the PEV demand, the savings from coordination are between 2%-7%, proportional to the price of PV carports.

Results achieved for a scenario with a full service restaurant serving as a base load, shown in Table.3.13, determine that coordination for this scheme achieved 0-1.6% NPC cost reduction. Note, the simulation was bound by 90 kW PV capacity. For PV carport prices up to 4.95$/W any PV capacity is economically feasible for both uncoordinated and coordinated charging scenarios. If charging is uncoordinated, at the highest PV carport price PV arrays are no longer feasible but with coordination a small 5 kW array has an economical advantage.

The optimal PV capacity for a strip mall EVSPL is summarized in Table.3.14. The simulation was bounded by 120 kW and the result indicates that any PV capacity is feasible for PV carport prices higher than 4.5$/W. If charging is uncoordinated, at the highest PV carport price, PV arrays are no longer feasible but with coordination a small 5 kW array has an economical advantage. In this scenario cost savings for coordination are between 2.25% and 4.8%.

Table 3.10: Optimal PV size and NPC with base load consideration for cost of PV car port between 3.6 $/W and 7.2 $/W in Victoria, BC.

	Optimal PV Size (kW)	**NPC ($)**		**Cost Savings (%)**
		Uncoordinated	**Coordinated**	
Large office	0	4,666,791	4,661,129	0.12
Small office	0	375,214	375,214	0
Strip mall	0	4,693,057	4,687,577	0.12
Restaurant	0	645,423	645,423	0

It is notable that the highest economical savings are without the base load scenario since the algorithm minimizes cost across the entire load. With a base load the cost minimization algorithm can only control a portion of the load rendering the effects of coordination less effective. With smaller base loads the coordination impacts are more prominent and as the base load increases the PEV demand becomes insignificant rendering coordination insignificant as well.

Table 3.11: Optimal PV size and NPC with a large office base load consideration for cost of PV car port between 3.6 $/W and 7.2 $/W in Los Angeles, BC.

PV cost ($/W)	**Uncoordinated**		**Coordinated**		**Cost savings (%)**
	PV size (kW)	**NPC ($)**	**PV size (kW)**	**NPC ($)**	
3.6	200	13,339,897	200	13,313,469	0.12
4.05	200	13,429,897	200	13,403,469	0.2
4.5	200	13,519,897	200	13,493,469	0.2
4.95	200	13,609,897	200	13,583,469	0.19
5.4	200	13,699,897	200	13,673,469	0.19
5.85	200	13,789,897	200	13,763,469	0.19
6.3	200	13,879,897	200	13,853,469	0.19
6.75	190	13,969,195	200	13,943,468	0.18
7.2	80	14,021,452	80	13,994,785	0.19

Table 3.12: Optimal PV size and NPC with a small office base load consideration for cost of PV car port between 3.6 $/W and 7.2 $/W in Los Angeles, BC.

PV cost ($/W)	**Uncoordinated**		**Coordinated**		**Cost savings (%)**
	PV size (kW)	**NPC ($)**	**PV size (kW)**	**NPC ($)**	
3.6	120	748,314	120	694,605	7.18
4.05	120	802,314	120	748,605	6.69
4.5	120	856,314	120	802,605	6.27
4.95	50	896,327	50	854,036	4.72
5.4	30	914,597	50	876,536	4.16
5.85	25	927,043	30	891,838	3.8
6.3	20	936,529	30	905,338	3.33
6.75	5	941,414	5	913,665	2.95
7.2	0	942,276	5	915,915	2.8

Table 3.13: Optimal PV size and NPC with a restaurant base load consideration for cost of PV car port between 3.6 \$/W and 7.2 \$/W in Los Angeles, BC.

PV cost (\$/W)	**Uncoordinated**		**Coordinated**		**Cost savings (%)**
	PV size (kW)	**NPC (\$)**	**PV size (kW)**	**NPC (\$)**	
3.6	90	1,614,657	90	1,589,377	1.57
4.05	90	1,655,157	90	1,629,877	1.53
4.5	90	1,695,657	90	1,670,377	1.49
4.95	90	1,736,157	90	1,710,877	1.46
5.4	70	1,773,482	85	1,750,770	1.28
5.85	50	1,800,137	50	1,785,249	0.83
6.3	20	1,818,136	50	1,807,749	0.57
6.75	10	1,823,972	20	1,822,915	0.06
7.2	0	1,830,479	5	1,829,040	0.08

Table 3.14: Optimal PV size and NPC with a strip mall base load consideration for cost of PV car port between 3.6 \$/W and 7.2 \$/W in Los Angeles, BC.

PV cost (\$/W)	**Uncoordinated**		**Coordinated**		**Cost savings (%)**
	PV size (kW)	**NPC (\$)**	**PV size (kW)**	**NPC (\$)**	
3.6	120	1,135,201	120	1,080,986	4.78
4.05	120	1,189,201	120	1,134,986	4.56
4.5	120	1,243,201	120	1,188,986	4.36
4.95	80	1,346,394	115	1,237,517	8.09
5.4	60	1,325,451	60	1,275,454	3.77
5.85	40	1,346,799	55	1,297,857	3.63
6.3	35	1,362,587	35	1,319,617	3.15
6.75	10	1,374,199	35	1,335,367	2.83
7.2	0	1,377,456	5	1,346,394	2.25

3.5 Parametric Study

3.5.1 Grid Tariff

From the NPC results it is clear that addition of solar to an EVSPL in Victoria, BC is not feasible, therefore a parametric study of the grid tariff on the total NPC was completed. Three tariff limits to assess solar feasibility are addressed for a boundary of PV car port costs: (1) Feed-in tariff (FIT), (2) Net-metering tariff, (3) Demand charge limits. With a FIT tariff the cost of purchasing electricity is higher than the sell price. To ensure economic feasibility the price of purchasing electricity has to be over three times higher than the current lowest price of PV carport and over four times higher for the current highest price of PV carport as shown in Table.3.15. Net-metering implies that the cost of purchasing electricity remains equivalent to sell price, therefore both values were scaled together for this parametric study. Net-metering tariff does not need to increase as much as the FIT tariff to ensure economic feasibility of the PV carports. Coordination has no effect in this scenario. Lastly, demand charges were explored to determine their effect on the feasibility of PV car ports. As a result demand charges have to increase upwards of 20 times to meet the economic feasibility requirements.

Table 3.15: Grid tariff sensitivity analysis for a EVSPL feasibility in Victoria, BC.

	Uncoordinated		**Coordinated**	
PV Cost	**4.5$/kW**	**6.0 $/kW**	**4.5 $/kW**	**6.0 $/kW**
Feasible electricity cost to current electricity cost (FIT)	3.1:1	4.1:1	3.1:1	4.1:1
Feasible electricity price with net-metering	3.0:1	4.0:1	3.0:1	4.0:1
Demand cost ratio	23:1	29:1	23:1	29:1

3.5.2 Cost of PV

The feasibility of the EVSPL is highly dependent on the capital cost of the PV car port. Given the grid tariff for Victoria, the addition of solar becomes feasible at prices lower than 3.0$/W for uncoordinated and coordinated charging as shown in Fig.3.12. Even though it is not currently advantageous to equip the parking lot with solar panels, government incentives can play a major role in the economic feasibility of such project if the capital cost reduction amounts to 33%. According to BNEF's projections the cost of solar is projected to drop 33% by 2020 [7], at which price the economic feasibility of PV will become viable in Victoria. At 3.0$/W the optimal PV size is 25 kW with uncoordinated charging and 30 kW with coordinated charging. With addition of optimally sized PV carports, a 2.2% NPC reduction using uncoordinated charging and 2.7% NPC reduction is achieved with coordinated charging. Overall, a 4.4% NPC reduction is achieved with coordination and optimally sized PV carports.

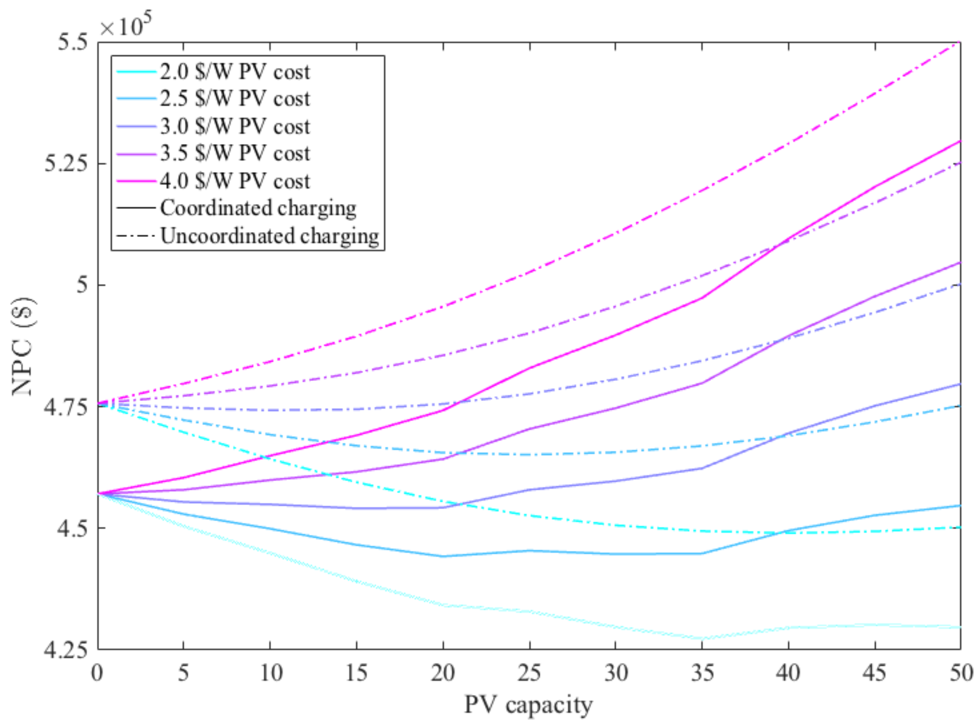

Figure 3.12: NPC comparison of uncoordinated charging to coordinated charging for variable PV capacities and variable cost of PV car port between 2.0-4.0$/W in Victoria, BC.

3.5.3 Impact of Solar Irradiation

The economic feasibility of PV equipped parking lots is highly dependent on the amount of power that can be generated by the PV panels, which is dependent on the amount of raw solar irradiation available in the region and the efficiency of the panels. Raw solar irradiation varies greatly according to the geographic location, local landscape and climatic conditions of the region studied. Cloud coverage or fog can cause intermittency of insolation seen by the solar panel in turn yielding irregular power profiles provided to the load. To assess the impact of solar irradiation on the economic feasibility of the EVSPL four insolation profiles: (1) Kelowna, BC and (2) Winnipeg, MB (3) Los Angeles, CA and (4) Death Valley, CA are considered while maintaining the remaining model parameters as in Victoria, BC. Kelowna is a sunnier interior location compared to Victoria, while Winnipeg demonstrates favourable clear sky conditions. Los Angeles solar irradiation and grid tariffs deemed the region to be economically feasible, therefore the insolation profiles for Los Angeles was tested with Victoria conditions to determine the impact of solar irradiation on the NPC. Lastly, Death Valley, an area that receives over 2000 $kWh/m^2/yr$ of incoming solar energy, was also compared. Conclusively, all four solar irradiation profiles yielded PV carports economically infeasible with both uncoordinated and coordinated charging schemes and upper limit of the derating factor. This result dictates that economic feasibility of PV carports in areas with relatively low grid tariffs is only marginally affected by the amount of irradiation in the region.

Chapter 4

Conclusion and Future Work

4.1 Key Findings

To reduce the impact of the transportation sector on climate change, plug-in electric vehicles have been widely deployed due to their characteristic of zero-emissions. Supplying the electric vehicles with clean power, however can only be done in regions with clean energy generation. Nonetheless, PEVs create a surplus demand which can create electrical grid inefficiencies and reliability problems. To deal with both of these issues, this thesis developed a methodology to determine the feasibility of retrofitting an existing parking lot with solar power and smart charging coordination schemes. The methodology was applied to two case studies in Victoria, BC and Los Angeles, CA. Both regions have widely different grid tariff structures and solar availability. It was determined that in Victoria, with business as usual, solar power is not cost optimal. However, the grid tariff and geographic positioning of Los Angeles allows costs to be reduced. Furthermore, with coordination, larger PV capacities can be installed with over 10% reduction in net present cost and an overall reduced impact on the electrical grid. These cost reductions can be extended over a large amount of parking lots resulting in significant cumulative savings to the district.

With the current prices of solar technology, Victoria is not yet economically positioned to take advantage of PV carports. The combination of relatively low electricity prices, high capital investment costs, deficiency in GHI, and insufficient panel efficiency prevents an EVSPL from becoming an economically feasible solution in Victoria. In addition, coordination did not make a significant impact on the overall cost of the system. Coordinated charging affects the operating costs only, and since Victoria has a uniform electricity price independent of time, there is lack of opportunity for coordination to make a significant impact on the electricity prices. However, by reducing the demand charges through coordination, the overall operating costs were reduced in excess of 11%. If the cost of solar panels was lower, the cutback of demand charges can grow significantly with solar implementation due to the tiered grid tariff. With sufficient solar irradiation, the peak demand is reduced, which can change the demand category of the microgrid (from medium business (35kW-150kW) to small business (<35 kW)). With this shift the demand charges are less than 50% of the cost, in turn reducing the operating costs even further. In Victoria, the effect of coordination with the presence of a base load is marginal. PV carports are not economically viable in this region, regardless of the base load based on the given PV array cost and grid tariff.

Alternatively, Los Angeles is an economically viable candidate for implementation of solar in a parking lot. With the current prices of solar technology, the cost savings of retrofitting a parking lot with PV panel is upwards of 4%. The negatively trending slope of levelized cost of electricity (LCOE) for solar indicates that installing large capacities of panels can be cost beneficial to the owner of the parking lot. With addition of control and coordination, larger PV capacities can be installed and lower NPC can be achieved. The savings start at 8% given the highest cost of the PV carports and 20% with the lowest cost of the PV carports. Coordination makes a more significant impact in Los Angeles due to the TOU electricity tariff. By shifting the load into off-peak or part-peak hours, cumulative cost of electricity and demand charges are largely reduced. In Los Angeles, the smaller the base load, the more prominent the effects of coordination. EVSPLs are feasible at maximum allowable capacity when the cost of the PV carport is at the lowest boundary. When considering the highest cost of PV carports with uncoordinated charging, PV infrastructure is no longer viable, where with coordination a small 5 kW PV carport is economically feasible.

The highest cost savings from coordination are achieved without a base load due to the coordination algorithm having full control of the load. As the base load or uncontrollable load increases, the PEV demand becomes increasingly insignificant rendering coordination insignificant as well.

4.2 Future Outlook

In the efforts to promote PEV uptake and reduce range anxiety, charging stations must become publicly available at low cost to the consumer and the owner. This thesis demonstrates that EVSPLs in locations combining large solar irradiation with relatively high electricity tariffs, such as Los Angeles, can integrate renewable energy with PEV charging with economical advantages.

To complement the presented work, it is suggested to shift this algorithm into a real-time scheduling scheme to be used in a physical application of the system with the optimized system components.

Additionally, large scale storage system solutions have not been fully explored in this work due to the high cost of batteries. To continue the research, it is suggested to enhance the optimization by considering battery storage and determining the boundaries of feasibility for the component. Other renewable sources such as wind, wave and geothermal were not considered in this work. The economic and physical feasibility of these sources should be explored further.

The research presented focuses on the advantages and disadvantages of an EVSPL on a microgrid scale, however understanding the higher scale impacts can be very valuable. It is suggested to integrate the current model with a distribution system modelling software such as GridLAB-D to study the effects of power quality on the distribution grid. Understanding effects of vehicle fleet scale coordination can lead to important insights to infrastructure design. In addition an optimization, facilitated by GridLAB-D, of the most favourable distribution grid locations of the EVSPLs would be a valuable tool for city planning studies.

Lastly, the sociological component should be considered before building an application of an EVSPL. It is important to understand how the public will respond to availability of such structures and whether the average person will find value in publicly available charging on a day-to-day basis.

Bibliography

[1] PG&E, "Pge Electric Schedule E-19," 2010. [Online]. Available: https://www.pge.com/tariffs/assets/pdf/tariffbook/ELEC{_}SCHEDS{_}E-19.pdf

[2] BC Hydro, "General Service Business Rates." [Online]. Available: https://www.bchydro.com/accounts-billing/rates-energy-use/electricity-rates/business-rates.html

[3] P. Denholm, M. O'Connell, G. Brinkman, and J. Jorgenson, "Overgeneration from Solar Energy in California. A Field Guide to the Duck Chart," no. November, 2015. [Online]. Available: http://www.osti.gov/servlets/purl/1226167/

[4] R. V. Singh, "Solar Car Parking," 2015. [Online]. Available: https://grabcad.com/library/solar-car-parking-1

[5] D. Turchetta, "The car of the future," *Issues Sci. Technol.*, vol. 18, no. 4, p. 5, 2002.

[6] DOE, "Electric and hybrid vehicle program," 1993.

[7] BNEF, "New Energy Outlook 2017," Blommberg New Energy Finance, Tech. Rep., 2017.

[8] E. Wood, C. Rames, M. Muratori, S. Raghavan, and M. Melaina, "National Plug-In Electric Vehicle Infrastructure Analysis," no. September, 2017. [Online]. Available: https://www.afdc.energy.gov/uploads/publication/national{_}pev{_}infrastructure.pdf

[9] M. Nyberg, "Total System Electric Generation," 2017. [Online]. Available: http://www.energy.ca.gov/almanac/electricity{_}data/total{_}system{_}power.html

[10] S. Behboodi, D. P. Chassin, C. Crawford, and N. Djilali, "Electric vehicle participation in transactive power systems using real-time retail prices," *Proc. Annu. Hawaii Int. Conf. Syst. Sci.*, vol. 2016-March, pp. 2400–2407, 2016.

[11] M. A. A. Pedrasa, T. D. Spooner, and I. F. MacGill, "Coordinated scheduling of residential distributed energy resources to optimize smart home energy services," *IEEE Trans. Smart Grid*, vol. 1, no. 2, pp. 134–143, 2010.

[12] Z. Liu, D. Wang, H. Jia, N. Djilali, and W. Zhang, "Aggregation and Bidirectional Charging Power Control of Plug-in Hybrid Electric Vehicles: Generation System Adequacy Analysis," *IEEE Trans. Sustain. Energy*, vol. 6, no. 2, pp. 325–335, 2015.

[13] D. P. Chassin, "Pacific Northwest GridWise Testbed Demonstration Projects Part II . Grid Friendly Appliance Project," *Appliance*, vol. 91, no. October, pp. 1–123, 2007.

[14] T. Broeer, J. Fuller, F. Tuffner, D. Chassin, and N. Djilali, "Modeling framework and validation of a smart grid and demand response system for wind power integration," *Appl. Energy*, vol. 113, pp. 199–207, 2014. [Online]. Available: http://dx.doi.org/10.1016/j.apenergy.2013.06.058

[15] AEP Ohio, "gridSMART Demonstration Project: A Community-Based Approach to Leading the Nation in Smart Energy Use," AEP Ohio, Tech. Rep., 2014.

[16] Q. Gong and S. Midlam-Mohler, "PEV charging impact on residential distribution transformer life," *Energytech*, vol. 43212, pp. 1–6, 2011.

[17] Consumer's Union, "Electric Vehicle Survey Methodology and Assumptions: American Driving Habits, Vehicle Needs, and Attitudes toward Electric Vehicles," Union of Concerned Scientists, Tech. Rep. December, 2013.

[18] F. Mwasilu, J. J. Justo, E. K. Kim, T. D. Do, and J. W. Jung, "Electric vehicles and smart grid interaction: A review on vehicle to grid and renewable energy sources integration," *Renew. Sustain. Energy Rev.*, vol. 34, pp. 501–516, 2014.

[19] T. Zhang, C.-c. Chu, and R. Gadh, "A Two-Tier Energy Management System for Smart Electric Vehicle Charging in UCLA : A Solar-To- Vehicle (S2V) Case Study," in *IEEE Innov. Smart Grid Technol. - Asia*, 2016, pp. 288–293.

[20] P. J. Tulpule, V. Marano, S. Yurkovich, and G. Rizzoni, "Economic and environmental impacts of a PV powered workplace parking garage charging station," *Appl. Energy*, vol. 108, pp. 323–332, 2013.

[21] E. Ben-Joseph, *ReThinking a Lot*, Cambridge, 2015.

[22] D. Shoup, *High cost of free parking.* New York: American Planning Association.

[23] S. Huff, B. West, and J. Thomas, "Effects of Air Conditioner Use on Real-World Fuel Economy," in *SAE Tech. Pap.* SAE International, 2013.

[24] H. Lohse-Busch, M. Duoba, E. Rask, K. Stutenberg, V. Gowri, L. Slezak, and D. Anderson, "Ambient Temperature (20F, 72F and 95F) Impact on Fuel and Energy Consumption for Several Conventional Vehicles, Hybrid and Plug-In Hybrid Electric Vehicles and Battery Electric Vehicle," in *SAE Tech. Pap.* opti: SAE International, 2013.

[25] R. C. Green, L. Wang, and M. Alam, "The impact of plug-in hybrid electric vehicles on distribution networks: A review and outlook," *Renew. Sustain. Energy Rev.*, vol. 15, no. 1, pp. 544–553, 2011.

[26] D. B. Richardson, "Electric vehicles and the electric grid: A review of modeling approaches, Impacts, and renewable energy integration," *Renew. Sustain. Energy Rev.*, vol. 19, pp. 247–254, 2013.

[27] I. Rahman, P. M. Vasant, B. S. M. Singh, M. Abdullah-Al-Wadud, and N. Adnan, "Review of recent trends in optimization techniques for plug-in hybrid, and electric vehicle charging infrastructures," *Renew. Sustain. Energy Rev.*, vol. 58, pp. 1039–1047, 2016.

[28] N. Belhaouas, M.-S. Ait Cheikh, P. Agathoklis, M.-R. Oularbi, B. Amrouche, K. Sedraoui, and N. Djilali, "PV array power output maximization under partial shading using new shifted PV array arrangements," *Appl. Energy*, vol. 187, pp. 326–337, 2017. [Online]. Available: http://dx.doi.org/10.1016/j.apenergy.2016.11.038

[29] H. Lee, "EVSE for Electric Vehicles," 2017. [Online]. Available: https://pixabay.com/en/charger-evse-electric-cars-2377021/

[30] GG, “ITT J1772,” 2017. [Online]. Available: https://grabcad.com/library/itt-j1772-1

[31] Blomst, “Tesla Supercharger.” [Online]. Available: https://pixabay.com/en/tesla-tesla-model-x-charging-1738969/

[32] J. Ingersoll and C. Perkins, “The 2.1 kW photovoltaic electric vehicle charging station in the\ncity of Santa Monica, California,” *Conf. Rec. Twenty Fifth IEEE Photovolt. Spec. Conf. - 1996*, pp. 1509–1512, 1996.

[33] D. P. Birnie, “Solar-to-vehicle (S2V) systems for powering commuters of the future,” *J. Power Sources*, vol. 186, no. 2, pp. 539–542, 2009.

[34] ——, “Analysis of energy capture by vehicle solar roofs in conjunction with workplace plug-in charging,” *Sol. Energy*, vol. 125, pp. 219–226, 2016.

[35] S. Smart Microgrid Applied Research Team, “Clean Energy Fund Smaller-scale Demonstration Project Integration of Photovoltaic Panels and Li-Ion Storage for Level-3 Electric Vehicle Charge Station BCIT Energy OASIS (Open Access to Sustainable Intermittent Sources),” British Columbia Institute of Technology, Tech. Rep. March, 2015.

[36] F. Fazelpour, M. Vafaeipour, O. Rahbari, and M. A. Rosen, “Intelligent optimization to integrate a plug-in hybrid electric vehicle smart parking lot with renewable energy resources and enhance grid characteristics,” *Energy Convers. Manag.*, vol. 77, pp. 250–261, 2014.

[37] Endesa, “Smartcity Málaga Living Lab: a laboratory to create the city of the future.” [Online]. Available: https://www.endesa.com/en/projects/a201801-living-lab-malaga-city-future.html

[38] R. A. Waraich, M. D. Galus, C. Dobler, M. Balmer, G. Andersson, and K. W. Axhausen, “Plug-in hybrid electric vehicles and smart grids: Investigations based on a microsimulation,” *Transp. Res. Part C Emerg. Technol.*, vol. 28, pp. 74–86, 2013.

[39] Z. Darabi and M. Ferdowsi, “Aggregated impact of plug-in hybrid electric vehicles on electricity demand profile,” *IEEE Trans. Sustain. Energy*, vol. 2, no. 4, pp. 501–508, 2011.

[40] F. A. Amoroso and G. Cappuccino, "Advantages of efficiency-aware smart charging strategies for PEVs," *Energy Convers. Manag.*, vol. 54, no. 1, pp. 1–6, 2012.

[41] M. Moradijoz, M. Parsa Moghaddam, M. R. Haghifam, and E. Alishahi, "A multi-objective optimization problem for allocating parking lots in a distribution network," *Int. J. Electr. Power Energy Syst.*, vol. 46, no. 1, pp. 115–122, 2013.

[42] S. Deilami, A. S. Masoum, P. S. Moses, and M. A. Masoum, "Real-time coordination of plug-in electric vehicle charging in smart grids to minimize power losses and improve voltage profile," *IEEE Trans. Smart Grid*, vol. 2, no. 3, pp. 456–467, 2011.

[43] T. Ma, A. Mohamed, and O. Mohammed, "Optimal charging of plug-in electric vehicles for a car park infrastructure," *Conf. Rec. - IAS Annu. Meet. (IEEE Ind. Appl. Soc.*, vol. 50, no. 4, pp. 2323–2330, 2012.

[44] A. Mohamed, V. Salehi, T. Ma, and O. Mohammed, "Real-time energy management algorithm for plug-in hybrid electric vehicle charging parks involving sustainable energy," *IEEE Trans. Sustain. Energy*, vol. 5, no. 2, pp. 577–586, 2014.

[45] J. Soares, H. Morais, T. Sousa, Z. Vale, and P. Faria, "Day-ahead resource scheduling including demand response for electric vehicles," *IEEE Trans. Smart Grid*, vol. 4, no. 1, pp. 596–605, 2013.

[46] S. Mal, A. Chattopadhyay, A. Yang, and R. Gadh, "Electric vehicle smart charging and vehicle-to-grid operation," *Int. J. Parallel, Emergent Distrib. Syst.*, vol. 28, no. 3, pp. 249–265, 2013.

[47] U. C. Chukwu and S. M. Mahajan, "V2G parking lot with pv rooftop for capacity enhancement of a distribution system," *IEEE Trans. Sustain. Energy*, vol. 5, no. 1, pp. 119–127, 2014.

[48] M. Chandra Mouli, G.R.; Bauer, P., Zeman, "System design for a solar powered electric vehicle charging station for workplaces." vol. 168, pp. 434–443, 2016.

[49] A. Ivanova, J. A. Fernandez, C. Crawford, and N. Djilali, "Coordinated Charging of Electric Vehicles Connected to a Net-Metered PV Parking Lot," in *IEEE PES Innov. Smart Grid Technol.*, Torino, 2017, pp. 1–6.

[50] IBM, “CPLEX User'sManual,” p. 586, 2016. [Online]. Available: https://www.ibm.com/support/knowledgecenter/SSSA5P{_}12.7.0/ilog.odms.studio.help/pdf/usrcplex.pdf

[51] J. a. Duffie, W. a. Beckman, and W. M. Worek, *Solar Engineering of Thermal Processes, 4nd ed.*, 2003, vol. 116.

[52] E. C. Kara, J. S. Macdonald, D. Black, M. Bérges, G. Hug, and S. Kiliccote, “Estimating the benefits of electric vehicle smart charging at non-residential locations: A data-driven approach,” *Appl. Energy*, vol. 155, pp. 515–525, 2015.

[53] P. Nunes, R. Figueiredo, and M. C. Brito, “The use of parking lots to solar-charge electric vehicles,” *Renew. Sustain. Energy Rev.*, vol. 66, pp. 679–693, 2016.

[54] S. Wilcox and W. Marion, “Users manual for TMY3 data sets,” *Renew. Energy*, no. May, p. 51, 2008. [Online]. Available: http://scholar.google.com/scholar?hl=en{&}btnG=Search{&}q=intitle:Users+Manual+for+TMY3+Data+Sets+Users+Manual+for+TMY3+Data+Sets{#}1{%}5Cnhttp://scholar.google.com/scholar?hl=en{&}btnG=Search{&}q=intitle:May.?Users+manual+for+TMY3+data+sets+users+manual+for+TMY3+dat

[55] A. J. Weaver and E. C. Wiebe, “Micro Meteorological Network in Greater Victoria Schools www.victoriaweather.ca,” *C. Bull.*, vol. 34, no. 4, pp. 184–190, 2006.

Appendix A

Model Code

The code used in this thesis is attached below. The general component breakdown is shown in Fig.A.1. The implementation of the model is shown in Fig.A.2.

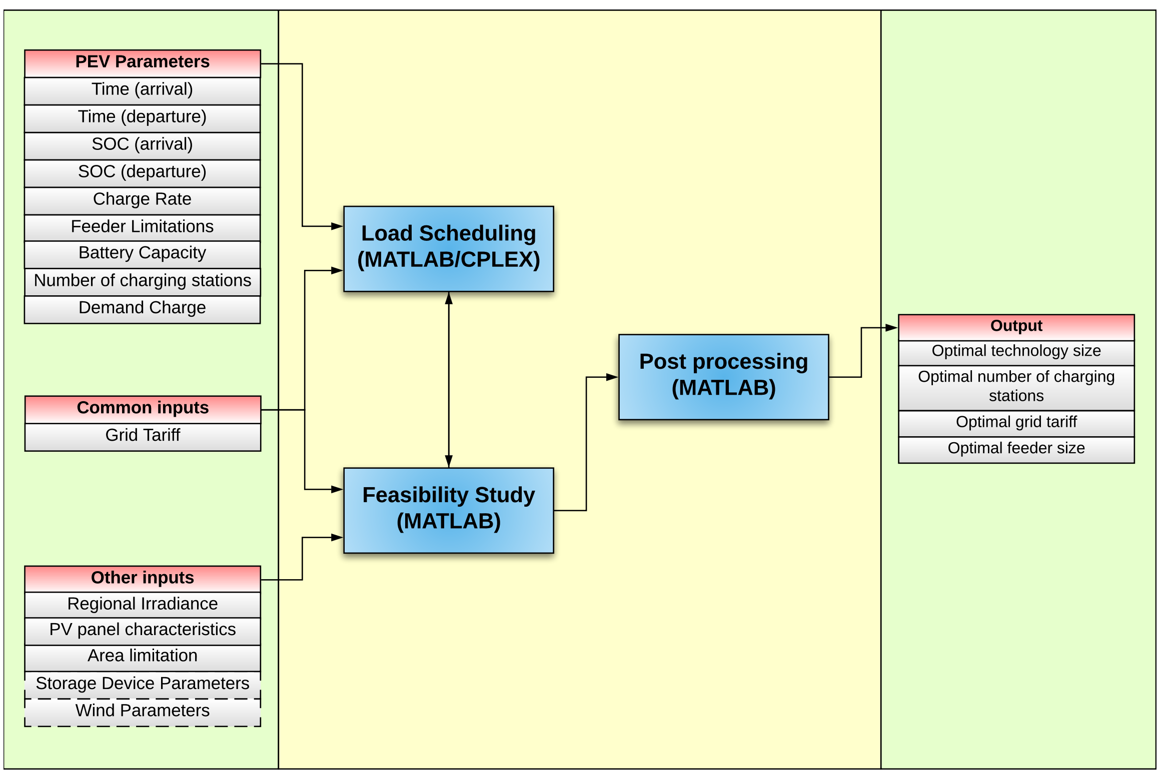

Figure A.1: Model overview.

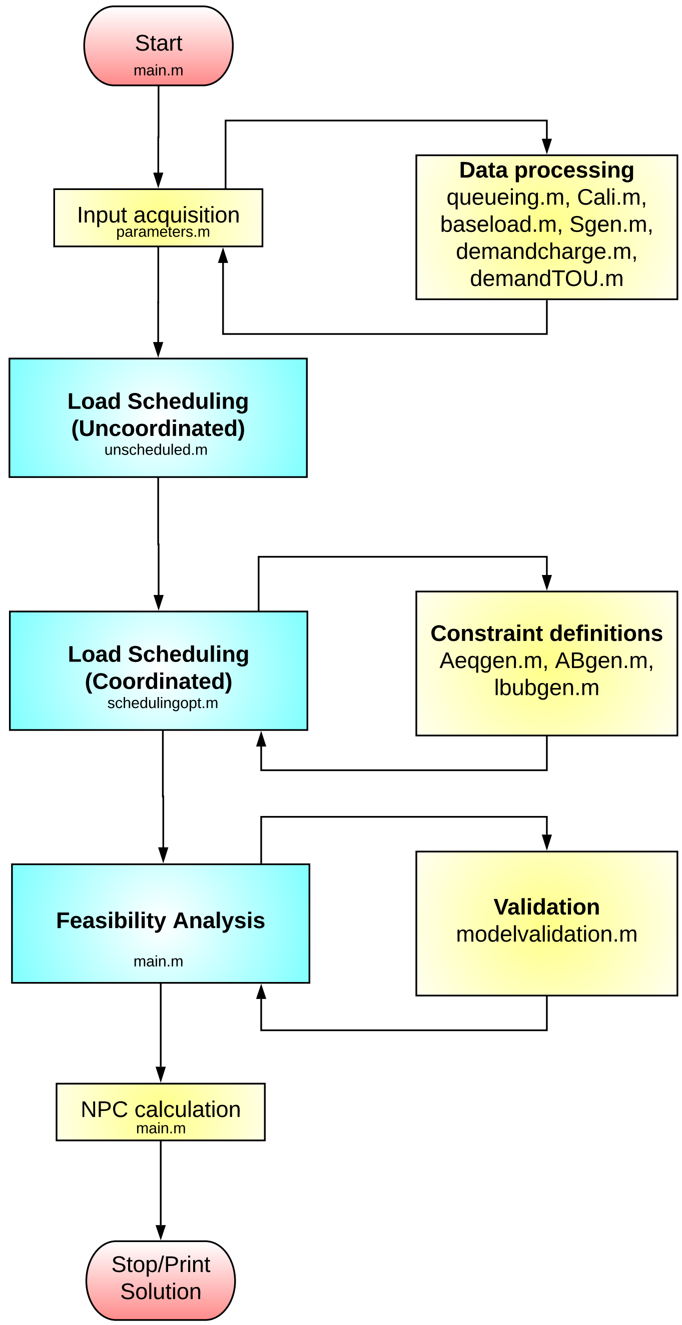

Figure A.2: Flow diagram of the model.

A.1 main.m

This file is the executable file for the model. The notable components are the parameter acquisition, unscheduled model and scheduled model. Once the outputs are gathered from both models the capital investment cost is calculated and discounted to present value here.

```
clc, clear, close all;
 Ppv_vect=[0:5:50];
 Cinv=49000;
%Parameters
tic
[N, N_stations, T, T_dur, Y, S_max, L_max, Energy_rqrd, ...
    P_charger, GHI_cali, GHI_vic, A, PV_eff, P_nom, t_arr_annual, t_dep_annual, ...
    C_ch, C_in_cali, C_in_vic, C_out_cali, C_out_vic,...
    C_d_cali, C_d_base_cali, ...
    C_tax_cali, C_tax_vic,...
    Cf, Cst, Cpv, infl, f, Cost_in_incr, Cost_out_incr, C_d_incr_cali, C_d_incr_vic,...
    D_penalty_med, D_penalty_large, Demand_thresh_med, Demand_thresh_large,...
    delta_thresh_cali, delta_thresh_vic, salvage_cost, Inv_eff]=parameters();
Cpv=[4500:500:6000];
Capex_solar=zeros(length(Cpv),length(Ppv_vect));
Capex_stations=Cst*N_stations;
%Capex_stations=0;
Discount_factor=ones(Y,1);
for year_disc=1:Y
    Discount_factor(year_disc,1)=1/(1+infl)^year_disc;
end
salvage_cost=salvage_cost*Discount_factor(Y,1);
Discount_factor=repmat(Discount_factor,1,length(Ppv_vect));
nom_intr_rate=(infl-f)/(1+f);
```

```
CRF=(nom_intr_rate*(1+nom_intr_rate)^Y)/(((1+nom_intr_rate)^Y)-1);

%% CALIFORNIA
 %Unscheduled model
  [ OP_sum_unsched_cali, Cost_per_charge_unsched_cali, load_only_unsched_cali, Demand_charge_unsched_cali, S_solar_plot, ...
      util_rate_unshed_cali]...
      =unscheduled( T, T_dur, Energy_rqrd, t_arr_annual,...
      P_charger, GHI_cali, A, PV_eff, P_nom, C_in_cali, C_out_cali, C_d_cali, C_d_base_cali, Ppv_vect, 1, Cost_in_incr, Cost_out_incr, C_ch, N_stations, Inv_eff);
 %Scheduled model

  [OP_sum_sched_cali, Cost_per_charge_sched_cali, load_sum_cali, Demand_charge_sched_cali]=...
      scheduling_opt(N, T, T_dur, S_max, L_max, ...
      P_charger, GHI_cali, A, PV_eff, P_nom, t_arr_annual, t_dep_annual, Energy_rqrd,...
      C_in_cali, C_out_cali, C_d_cali, C_d_base_cali, Ppv_vect,1, Cost_in_incr, Cost_out_incr, C_ch, C_d_incr_cali, 0,0, 0, 0, N_stations, Inv_eff);
  if sum(sum(load_only_unsched_cali-load_sum_cali))>5
      fprintf('ERROR: Loads DO NOT MATCH\n');
  end

 %%
 figure(1);
 NPC_unsched_cali=zeros(length(Cpv),length(Ppv_vect));
 NPC_sched_cali=zeros(length(Cpv),length(Ppv_vect));
 OP_sum_unsched_cali_disc=Discount_factor.*repmat(OP_sum_unsched_cali',Y,1);
```

```
OP_sum_sched_cali_disc=Discount_factor.*repmat(
    OP_sum_sched_cali', Y,1);
Demand_charge_unsched_cali_disc=Discount_factor.*repmat(
    Demand_charge_unsched_cali',Y,1);
Demand_charge_sched_cali_disc=Discount_factor.*repmat(
    Demand_charge_sched_cali',Y,1);
Cost_per_charge_unsched_cali=Discount_factor(:,1).*repmat
    (Cost_per_charge_unsched_cali',Y,1);
Cost_per_charge_sched_cali=Discount_factor(:,1).*repmat(
    Cost_per_charge_sched_cali',Y,1);
OP_total_unsched_cali=OP_sum_unsched_cali_disc+
    Demand_charge_unsched_cali_disc-
    Cost_per_charge_unsched_cali;
OP_total_sched_cali=OP_sum_sched_cali_disc+
    Demand_charge_sched_cali_disc-
    Cost_per_charge_sched_cali;
OP_total_sum_unsched_cali=sum(OP_total_unsched_cali);
OP_total_sum_sched_cali=sum(OP_total_sched_cali);

for i=1:length(Cpv)
    Capex_solar=Cpv(i).*Ppv_vect;
    Capex_stations=0; %%% FIX THIS LATER
    %UNSCHEDULED
    Capex_total=Capex_stations+Capex_solar+Cinv;

    NPC_unsched_cali(i,:)=(OP_total_sum_unsched_cali+
        Capex_total);
    %-salvage_cost.*Ppv_vect;
    NPC_sched_cali(i,:)=(OP_total_sum_sched_cali+
        Capex_total);
    %-salvage_cost.*Ppv_vect;
    figure(1)
    plot(Ppv_vect, NPC_sched_cali(i,:),'r');
    hold on
    plot(Ppv_vect, NPC_unsched_cali(i,:),'b');
```

```
    hold on
    legend('Scheduled California', 'Unscheduled
       California')
end

%%
 %%VICTORIA

%Unscheduled model
[ OP_sum_unsched_vic, Cost_per_charge_unsched_vic,
   load_only_unsched_vic,...
    Demand_charge_unsched_vic, util_rate_unsched_vic]...
    =unscheduled( T, T_dur, Energy_rqrd, t_arr_annual,...
    P_charger, GHI_vic, A, PV_eff, P_nom, C_in_vic,
       C_out_vic, C_d_cali,...
    C_d_base_cali, Ppv_vect, 2, Cost_in_incr,
       Cost_out_incr, C_ch, N_stations, Inv_eff);
%Scheduled model
 tic
 [OP_sum_sched_vic, Cost_per_charge_sched_vic,
    load_sum_vic, Demand_charge_sched_vic]=...
     scheduling_opt(N, T, T_dur, S_max, L_max, ...
     P_charger, GHI_vic, A, PV_eff, P_nom, t_arr_annual,
        t_dep_annual, Energy_rqrd,...
     C_in_vic, C_out_vic, C_d_cali, C_d_base_cali,
        Ppv_vect,2, Cost_in_incr, Cost_out_incr,...
     C_ch, C_d_incr_vic,...
     D_penalty_med, D_penalty_large,  Demand_thresh_med,
        Demand_thresh_large,...
     N_stations, Inv_eff);
 toc
 if sum(sum(load_only_unsched_vic-load_sum_vic))>5
     fprintf('ERROR: Loads DO NOT MATCH\n');
 end
C_ch=0.25./(T/24);
```

```
C_ch=0;
Cost_per_charge=0;

figure(2);
NPC_unsched_vic=zeros(length(Cpv),length(Ppv_vect));
%NPC_sched_vic=zeros(length(Cpv),length(Ppv_vect));
OP_sum_unsched_vic_disc=Discount_factor.*repmat(OP_sum_unsched_vic',Y,1);
%OP_sum_sched_vic_disc=Discount_factor.*repmat(OP_sum_sched_vic',Y,1);
Demand_charge_unsched_vic_disc=Discount_factor.*repmat(Demand_charge_unsched_vic',Y,1);
%Demand_charge_sched_vic_disc=Discount_factor.*repmat(Demand_charge_sched_vic',Y,1);
Cost_per_charge_unsched_vic=Discount_factor(:,1).*repmat(Cost_per_charge_unsched_vic',Y,1);
%Cost_per_charge_sched_vic=Discount_factor(:,1).*repmat(Cost_per_charge_sched_vic',Y,1);
OP_total_unsched_vic=OP_sum_unsched_vic_disc+Demand_charge_unsched_vic_disc-Cost_per_charge_unsched_vic;
%OP_total_sched_vic=OP_sum_sched_vic_disc+Demand_charge_sched_vic_disc-Cost_per_charge_sched_vic;
OP_total_sum_unsched_vic=sum(OP_total_unsched_vic);
%OP_total_sum_sched_vic=sum(OP_total_sched_vic);
for i=1:length(Cpv)
    Capex_solar=Cpv(i).*Ppv_vect+Cinv;
    %UNSCHEDULED
    Capex_total=Capex_stations+Capex_solar;
    NPC_unsched_vic(i,:)=(OP_total_sum_unsched_vic+Capex_total);
    NPC_sched_vic(i,:)=(OP_total_sum_sched_vic+Capex_total);

```

```
        NPC_unsched_cali_norm=NPC_unsched_cali./(
            NPC_unsched_cali(1));
        NPC_sched_cali_norm=NPC_sched_cali./(NPC_sched_cali
            (1));
        NPC_unsched_vic_norm=NPC_unsched_vic./(
            NPC_unsched_vic(1));
        NPC_sched_vic_norm=NPC_sched_vic./(NPC_sched_vic(1));


        figure(2)
        plot(Ppv_vect, NPC_sched_vic(i,:),'r');
        hold on
      plot(Ppv_vect, NPC_unsched_vic(i,:), 'b');
      legend('Scheduled Victoria', 'Unscheduled Victoria')
      hold on

end
```

A.2 parameters.m

This function gathers all the required parameters needed to define the particular case study.

```
function [N, N_stations, T, T_dur, Y, S_max, L_max, Energy_rqrd_new, ...
    P_ch_new, I_calc_cali, I_calc_vic, A, PV_eff, P_nom, t_arr_new, t_dep_new, ...
    C_ch, C_in_cali, C_in_vic, C_out_cali, C_out_vic,...
    C_d_cali, C_d_base_cali, ...
    C_tax_cali, C_tax_vic,...
    Cf, Cst, Cpv, infl, f, Cost_in_incr, Cost_out_incr, C_d_incr_cali,C_d_incr_vic,...
    D_penalty_med, D_penalty_large, Demand_thresh_med, Demand_thresh_large,...
    delta_thresh_cali, delta_thresh_vic, Salvage_cost, Inv_eff]=parameters()
N=150; %number of cars waiting to be served (arbitrary number)
T=96; %using 15 minute intervals
T_dur=365;
Y=25; %number of years
infl=0.06; %Discount rate
f=0.02; %inflation
L_max=2000;
% SOLAR POWER SPECS - SUNPOWER X-SERIES
A=1.6; %area of 1 panel (m^2)
P_nom=360./10^3; % (kWp) per panel
PV_eff=0.222; % SUNPOWER X-SERIES
LAT_cali=33.83;
LON_cali=118;
LON_vic=118;
LAT_vic=48.4284;
%For fixed tilt
```

```
TILT_cali=LAT_cali*0.76+3.1; %%% EXPAND TO MULTIPLE TILT
    ADJUSTMENTS
TILT_vic=LAT_vic*0.76+3.1;
S_max=1000000000; %assume that feeder capacity is the same
    bi-directionally
%cap battery - 1xN vector of all car's battery capacities
%already incorporates effiency: break this apart into eff*
    cap_char if needed
%Solar specifications
%fpv=0.85; %derating factor [%]
delta_thresh_cali=zeros(T,T);
delta_thresh_vic=eye(T);
C_in_vic_price=0.1139/(T/24); %starting value - adjusted
    after the energy calc for victoria (tiered rates)
Cost_in_incr=1; % how much higher does Cin have to be for
    an NPC curve
Cost_out_incr=1;
[t_arr, t_dep, P_charger, Energy_rqrd]=Cali_data(N, T_dur)
    ;
Energy_rqrd=Energy_rqrd.*(T/24)-0.00001;
Inv_eff=0.90;
[N_stations, t_arr_new, t_dep_new, Energy_rqrd_new,
    P_ch_new]=...
    queueing(N, T_dur, t_arr, t_dep, Energy_rqrd,
        P_charger);
N_stations
% Post processing of the data
for kk=1:size(P_ch_new,1)
    for ll=1:size(P_ch_new,2)
        if kk==3 && ll==343
            fprintf('here');
        end
        % if charger power is 0 or less and energy is not
            0 - do not
        % charge
```

```
            if P_ch_new(kk,ll)<=0 && Energy_rqrd_new(kk,ll)~=0
                 Energy_rqrd_new(kk,ll)=0;
            end
            %if amount of time available is less than the
                required time
            % to reach full charge
            if (t_dep_new(kk,ll)-t_arr_new(kk,ll))<ceil(
                Energy_rqrd_new(kk,ll)/P_ch_new(kk,ll))
                 Energy_rqrd_new(kk,ll)=P_ch_new(kk,ll)*(
                     t_dep_new(kk,ll)-t_arr_new(kk,ll))-0.001;
            end

            %if charging power was mis-recorded - delete entry
            if P_ch_new(kk,ll)<=0.01 || (ceil(Energy_rqrd_new(
                kk,ll)/P_ch_new(kk,ll)))>50
                 t_arr_new(kk,ll)=0;
                 t_dep_new(kk,ll)=0;
                 P_ch_new(kk,ll)=0;
                 Energy_rqrd_new(kk,ll)=0;
            end
            % if the car needs to charge longer than the
                length of the day
            char_duration=ceil(Energy_rqrd_new(kk,ll)./
                P_ch_new(kk,ll));
            if (t_arr_new(kk,ll)+char_duration)>T
                    char_duration=T-t_arr_new(kk,ll);
                    P_ch_new(kk,ll)=Energy_rqrd_new(kk,ll)./
                        char_duration;
            end
            clear char_duration
      end
end
%if the car arrives in the last time slot of the day
t_dep_new(t_arr_new==T)=0;
Energy_rqrd_new(t_arr_new==T)=0;
```

```
P_ch_new(t_arr_new==T)=0;
t_arr_new(t_arr_new==T)=0;
%Solar generation power profile
day_year=1:365;
[I_cali, I_vic]=Sgen(T, T_dur); %power output from the
    panel
I_cali=reshape(I_cali, 4,96*365/4);
I_cali=sum(I_cali)./4;
I_cali=reshape(I_cali,24,365);
I_vic=reshape(I_vic, 4,96*365/4);
I_vic=sum(I_vic)./4;
I_vic=reshape(I_vic,24,365);
b_azimuth=0;
grnd_ref=0.2;
fpv=0.8;
I_calc_cali=PV_out(LON_cali, LAT_cali, TILT_cali,
    b_azimuth, I_cali, grnd_ref, fpv);
I_calc_vic=PV_out(LON_vic, LAT_vic, TILT_vic, b_azimuth,
    I_vic, grnd_ref, fpv);

%% CALIFORNIA PRICE OF ELECTRICITY
C_in_cali=zeros(T,1);
% %ToU
% %peak 11am-5pm
if T==288
     C_in_cali(132:203)=0.18*(1/(T/24));
    %shoulder
     C_in_cali(85:131)=0.132*(1/(T/24));
     C_in_cali(204:227)=0.132*(1/(T/24));
    %off peak 7pm-7am
     C_in_cali(228:288)=0.087*(1/(T/24));
     C_in_cali(1:84)=0.087*(1/(T/24));
     C_in_cali=repmat(C_in_cali, 1, T_dur);
elseif T==24
     C_in_cali(11:16)=0.132*(1/(T/24));
```

```
    %shoulder
    C_in_cali(7:10)=0.095*(1/(T/24));
    C_in_cali(17:18)=0.095*(1/(T/24));
    %off peak 7pm-7am
    C_in_cali(19:24)=0.065*(1/(T/24));
    C_in_cali(1:6)=0.065*(1/(T/24));
    C_in_cali=repmat(C_in_cali, 1, T_dur);
elseif T==96
    C_in_summer_cali=zeros(T,1);
    C_in_winter_cali=zeros(T,1);
    %summer peak
    C_in_summer_cali(48:71)=0.34020*(1/(T/24)); %12 pm to 6pm
    %summer part-peak
    C_in_summer_cali(34:47)=0.15997*(1/(T/24)); %8:30 am to 12pm
    C_in_summer_cali(72:85)=0.15997*(1/(T/24)); %6pm to 9:30pm
    %summer offpeak
    C_in_summer_cali(86:96)=0.08512*(1/(T/24)); %6pm to 8:30 am
    C_in_summer_cali(1:33)=0.08512*(1/(T/24));
    %winter part-peak
    C_in_winter_cali(34:85)=0.10689*(1/(T/24));
    %winter offpeak
    C_in_winter_cali(86:96)=0.09178*(1/(T/24));
    C_in_winter_cali(1:33)=0.09178*(1/(T/24));
    C_in_A_cali=repmat(C_in_winter_cali, 1, 120);
    C_in_B_cali=repmat(C_in_winter_cali, 1, 61);
    C_in_C_cali=repmat(C_in_summer_cali, 1, 184);
    C_in_cali=[C_in_A_cali, C_in_C_cali, C_in_B_cali];
end

% Demand charges TOU
C_d_base_cali=19.71253;
```

```
%summer peak
C_d_summer_peak_cali=17.57; %12 pm to 6pm
%summer part-peak
C_d_summer_part_cali=0.51;
%winter part-peak
C_d_winter_cali=0.03; %8:30am to 9:30pm
C_d_cali=[C_d_summer_peak_cali, C_d_summer_part_cali,
    C_d_winter_cali];
C_d_A_cali=repmat(C_d_winter_cali,96,120);
C_d_A_cali(1:33,:)=0;
C_d_A_cali(86:96,:)=0;
C_d_B_cali=repmat(C_d_summer_peak_cali,96,61);
C_d_B_cali(34:47,:)=C_d_summer_part_cali;
C_d_B_cali(72:85,:)=C_d_summer_part_cali;
C_d_B_cali(1:33,:)=0;
C_d_B_cali(86:96,:)=0;
C_d_C_cali=repmat(C_d_winter_cali,96,184);
C_d_C_cali(1:33,:)=0;
C_d_C_cali(86:96,:)=0;
C_d_incr_cali=[C_d_A_cali, C_d_B_cali C_d_C_cali];
C_d_incr_vic=10.*ones(T, T_dur);
C_out_cali=C_in_cali; %net metering

C_tax_cali=0;
% VICTORIA PRICE OF ELECTRICITY IS TIERED - RECALCULATED
    IN ENERGYCALC FUNCTIONS
%% VICTORIA PRICE OF ELECTRICITY
C_in_vic=C_in_vic_price.*ones(T,T_dur);
C_out_vic=C_in_vic;
C_rate_rider=0.05;
C_tax_vic=0.12+C_rate_rider;
%% Equipment cost
Cf=50; %feeder cost /W
Cpv=4500;
Cst=2700;
```

```
C_ch=0;
D_penalty_med=4.92;%4.92
D_penalty_large=11.21;
Demand_thresh_med=35;%35
Demand_thresh_large=150;
Salvage_cost=0.33*1000;
end
```

A.3 queueing.m

The queueing function is responsible for ordering the vehicles and determining the optimal number of charging stations required by the parking lot.

```
function [N_st, t_arr_new, t_dep_new, Energy_rqrd_new, P_ch_new]= queueing(N, T_dur, t_arr, t_dep, Energy_rqrd, P_ch)
  %start by assuming that there is one station required for each day
  N_temp=N;
  N_stations=ones(T_dur,1);
  t_arr_new=zeros(size(t_arr));
  t_dep_new=zeros(size(t_dep));
  Energy_rqrd_new=zeros(size(Energy_rqrd));
  P_ch_new=zeros(size(P_ch));
  c_refused_array=ones(100,1);
  for x=1:size(t_arr,1)
      for y=1:size(t_arr,2)
          if t_arr(x,y)~=0 && (t_dep(x,y)-t_arr(x,y))==0
              t_arr(x,y)=0;
              t_dep(x,y)=0;
              Energy_rqrd(x,y)=0;
              P_ch(x,y)=0;
          end
          if (t_dep(x,y)-t_arr(x,y))<(Energy_rqrd(x,y)/P_ch(x,y))
               Energy_rqrd(x,y)=(P_ch(x,y)*(t_dep(x,y)-t_arr(x,y)));
          end
      end
  end
  %sorting in order of arrival
for i=1:T_dur
    fprintf('Queueing day processing: %d \n', i);
```

```
    time_vector=[t_arr(:,i), t_dep(:,i), Energy_rqrd(:,i), P_ch(:,i)];
    N=size(time_vector,1);
    time_vector=sortrows(time_vector, 1);
    t_day_arr=time_vector(:,1);
    t_day_arr(t_day_arr==0)=[];
if sum(t_day_arr)~=0
    t_day_dep=time_vector(:,2);
    t_day_dep(t_day_dep==0)=[];
    Energy_rqrd_day=time_vector(:,3);
    P_ch_day=time_vector(:,4);
    Energy_rqrd_day(t_day_arr==0)=[];
    P_ch_day(t_day_arr==0)=[];
    t_day_arr(t_day_arr==0)=[];
    %arrival time replacement based on charger availability
    count_refused=1;
    %ensures the row is zeroed out
    N=length(t_day_arr);
    while(count_refused~=0)
        count_refused=0; %reset all variables for that day

        t_arr_new(:,i)=zeros(N_temp,1);
        t_dep_new(:,i)=zeros(N_temp,1);
        Energy_rqrd_new(:,i)=zeros(N_temp,1);
        P_ch_new(:,i)=zeros(N_temp,1);
        %matrix with cars currently in the parking lot
        charging_matrix=[t_day_arr(1:N_stations(i)), t_day_dep(1:N_stations(i)),...
                              Energy_rqrd_day((1:N_stations(i))), P_ch_day((1:N_stations(i)))];
        %populate with first vehicles to charge
        %matrix that did not fit into the charging stations
```

```
        queueing_matrix=[t_day_arr(((N_stations(i)+1):N)), t_day_dep(((N_stations(i)+1):N)),...
                         Energy_rqrd_day(((N_stations(i)+1):N)),...
                         P_ch_day(((N_stations(i)+1):N))];
        %constantly updating matrix of chargers
        %check for cars that are already fully charged at arrival
        charging_matrix=sortrows(charging_matrix, 2); % sort according to t_dep
        for j=1:(N-N_stations(i))

            % if the car arrives and there is no spots left
            if (charging_matrix(1,2)>=queueing_matrix(1,1))
                % if the departure time of the first car to leave the full lot
                % is sooner than the departure time of the next queueing car
                if (charging_matrix(1,2)+1)<queueing_matrix(1,2)
                    % record the next queueing car times
                    t_arr_new(j,i)=charging_matrix(1,1);
                    t_dep_new(j,i)=charging_matrix(1,2);
                    Energy_rqrd_new(j,i)=charging_matrix(1,3);
                    P_ch_new(j,i)=charging_matrix(1,4);
                    % replace the first car to leave with the queueing car
```

```
                    % arrival time changed to last car's departure time
                    charging_matrix(1,1)=charging_matrix(1,2)+1;
                    %departure time is from the queueing car
                    charging_matrix(1,2)=queueing_matrix(1,2);
                    charging_matrix(1,3)=queueing_matrix(1,3); %energy update
                    charging_matrix(1,4)=queueing_matrix(1,4); %Pch update
                else
%               fprintf('%d car did not charge (not enough time)\n', i);
                    count_refused=count_refused+1;
                end
            % if there is free spaces in the parking lot
            else
                t_arr_new(j,i)=charging_matrix(1,1);
                t_dep_new(j,i)=charging_matrix(1,2);
                Energy_rqrd_new(j,i)=charging_matrix(1,3);
                P_ch_new(j,i)=charging_matrix(1,4);
                charging_matrix(1,1)=queueing_matrix(1,1);
                charging_matrix(1,2)=queueing_matrix(1,2);
                charging_matrix(1,3)=queueing_matrix(1,3);
                charging_matrix(1,4)=queueing_matrix(1,4);
```

```
                end
            % delete the item from the queue
            queueing_matrix(1,:)=[];
            % sort the matrix of chargers again depending on the departure time
            charging_matrix=sortrows(charging_matrix, 2);
        end
        t_arr_new((N-N_stations(i)+1):N,i)=charging_matrix(:,1); % add the cars charging first
        t_dep_new((N-N_stations(i)+1):N,i)=charging_matrix(:,2);
        Energy_rqrd_new((N-N_stations(i)+1):N,i)=charging_matrix(:,3);
        P_ch_new((N-N_stations(i)+1):N,i)=charging_matrix(:,4);
    %    fprintf('%d cars did not fit into the parking lot.\n', count_refused);
         N_stations(i)=N_stations(i)+1;
         clear charging_matrix;
    end
end
count_refused=0;
N_stations(i)=N_stations(i)-1;
 %      fprintf('%d cars did not fit into the parking lot.\n', count_refused);
end
%%FINAL QUEUE WITH MINIMUM NUMBER OF CHARGING STATIONS
%N_st=max(N_stations); %max amount of stations needed to serve of all customers
N_st=round(mean(N_stations)); %max amount of stations needed to serve of all customers
%recalculate the times of arrival and departure with the final station
%number
```

```
t_arr_new=zeros(size(t_arr));
t_dep_new=zeros(size(t_dep));
%SOC_arr_new=zeros(size(SOC_arr));
Energy_rqrd_new=zeros(size(Energy_rqrd));
P_ch_new=zeros(size(P_ch));
if (N_st>=N)
    t_arr_new=t_arr;
    t_dep_new=t_dep;
    Energy_rqrd_new=Energy_rqrd;
    P_ch_new=P_ch;
else
    for i=1:T_dur
        %populate with first vehicles to charge
        if sum(t_arr(:,i))~=0
            t_arr_temp=t_arr(:,i);
            t_dep_temp=t_dep(:,i);
            Energy_rqrd_temp=Energy_rqrd(:,i);
            P_ch_temp=P_ch(:,i);
            t_dep_temp(t_arr_temp==0)=[];
            Energy_rqrd_temp(t_arr_temp==0)=[];
            P_ch_temp(t_arr_temp==0)=[];
            t_arr_temp(t_arr_temp==0)=[];
            if N_st>=length(t_arr_temp)
                t_arr_new(1:length(t_arr_temp),i)=t_arr_temp;
                t_dep_new(1:length(t_dep_temp),i)=t_dep_temp;
                Energy_rqrd_new(1:length(Energy_rqrd_temp),i)=Energy_rqrd_temp;
                P_ch_new(1:length(P_ch_temp),i)=P_ch_temp;
            else
        charging_matrix=[t_arr_temp(1:N_st), t_dep_temp(1:N_st),...
                                Energy_rqrd_temp(1:N_st), P_ch_temp(1:N_st)]; %first
```

```
100 cars to arrive sorted according to t_arr
        queueing_matrix=[t_arr_temp(((N_st+1):length(t_arr_temp))),...
            t_dep_temp(((N_st+1):length(t_arr_temp))),...
            Energy_rqrd_temp(((N_st+1):length(t_arr_temp))),...
            P_ch_temp(((N_st+1):length(t_arr_temp)))];
        %constantly updating matrix of chargers
        charging_matrix=sortrows(charging_matrix, 2); % sort according to t_dep
        for j=1:(length(t_arr_temp)-N_st)
                if (charging_matrix(1,2)>=queueing_matrix(1,1))
                    if (charging_matrix(1,2)+1)<queueing_matrix(1,2)
                        % record the next queueing car times
                        t_arr_new(j,i)=charging_matrix(1,1);
                        t_dep_new(j,i)=charging_matrix(1,2);
                        Energy_rqrd_new(j,i)=charging_matrix(1,3);
                        P_ch_new(j,i)=charging_matrix(1,4);
                        % replace the first car to leave with the queueing car
                        % arrival time changed to last car's departure time
                        charging_matrix(1,1)=charging_matrix(1,2)+1;
                        %departure time is from the queueing car
```

```
                        charging_matrix(1,2)=
                            queueing_matrix(1,2);
                        charging_matrix(1,3)=
                            queueing_matrix(1,3);
                        charging_matrix(1,4)=
                            queueing_matrix(1,4);
                    else
                        count_refused=count_refused+1;
                    end
                else
                    t_arr_new(j,i)=charging_matrix(1,1);
                    t_dep_new(j,i)=charging_matrix(1,2);
                    Energy_rqrd_new(j,i)=charging_matrix
                        (1,3);
                    P_ch_new(j,i)=charging_matrix(1,4);
                    charging_matrix(1,1)=queueing_matrix
                        (1,1);
                    charging_matrix(1,2)=queueing_matrix
                        (1,2);
                    charging_matrix(1,3)=queueing_matrix
                        (1,3);
                    charging_matrix(1,4)=queueing_matrix
                        (1,4);
                end
            % delete the item from the queue
            queueing_matrix(1,:)=[];
            % sort the matrix of chargers again depending
                on the departure time
            charging_matrix=sortrows(charging_matrix, 2);
        end
            t_arr_new((N-N_st+1):N,i)=charging_matrix(:,1)
                ; % add the cars charging first
            t_dep_new((N-N_st+1):N,i)=charging_matrix(:,2)
                ;
```

```
                Energy_rqrd_new((N-N_st+1):N,i)=
                    charging_matrix(:,3);
                P_ch_new((N-N_st+1):N,i)=charging_matrix(:,4);
                end
            end
            clear t_arr_temp t_dep_temp Energy_rqrd_temp
                P_ch_temp;
        end
end

end
```

A.4 Sgen.m

This function is responsible for post processing the solar irradiation data.

```
function [S_gen_cali, S_gen_vic]=Sgen(Time_Incr,T_dur)
%% CALIFORNIA
filename='38.84_-117.9_psm_satellite_60_tmy.csv';
% Year, Month, Day, Hour, Min, Dew Point, DHI (W/m2), DNI (W/m2), Col 9 - GHI (W/m2), Pressure (mbar),
% Temperature (C), Wind Direction, Wind Speed
T=csvread(filename, 3,0);
S_gen_hour=zeros(24,T_dur);
month=T(:,2);
day=T(:,3);
hour=T(:,4);
GHI=T(:,9);
m= [31, 59, 90, 120, 151, 181, 212, 243, 273, 304, 334, 365];
month(month==1)=zeros(length(month(month==1)),1);
for mnth=1:11
    month(month==(mnth+1))=m(mnth)*ones(length(month(month==(mnth+1))),1);
end
day_year=month+day; % day of the year 1:365

% ASSUMING THE DATA IS AT AN HOUR FREQUENCY
S_gen_hour(:,1)=GHI(1:24,1);
for i=2:365
    S_gen_hour(:,i)=GHI(((i-1)*24+1):(i*24),1);
end
S_gen_hour=reshape((S_gen_hour./(Time_Incr/24)),T_dur*24,1);
S_gen_hour=(repmat(S_gen_hour,1,Time_Incr/24))';
S_gen_cali_nodaylight=reshape(S_gen_hour,Time_Incr,T_dur);
S_gen_cali_daylight=circshift(S_gen_cali_nodaylight(:,70:308),4); %daylight savings portion
```

```
S_gen_cali=[S_gen_cali_nodaylight(:,1:69),
    S_gen_cali_daylight, S_gen_cali_nodaylight(:,309:365)
    ]./1000;   % CONVERSION TO KW/m^2
clear filename T S_gen_hour month day hour GHI m mnth
    day_year i
%% VICTORIA
solar_vic=dlmread('Sgen_Vic.txt');
solar_vic=reshape(solar_vic, 288*T_dur,1);
solar_vic=sum(reshape(solar_vic, 3,288*T_dur/3));
solar_vic=reshape(solar_vic,Time_Incr,T_dur)./3;
solar_vic_daylight=circshift(solar_vic(:,70:308),4);
S_gen_vic=[solar_vic(:,1:69), solar_vic_daylight,
    solar_vic(:,309:365)];
end
```

A.5 unscheduled.m

The function outputs the demand profile for uncoordinated charging.

```
function [OP_final, Cost_per_charge, load_only, Demand_charge_total, S_solar_plot, util_rate]...
    =unscheduled( T, T_dur, Energy_rqrd, t_arr_annual,...
     P_charger, I_calc, A, PV_eff, P_nom, C_in, C_out, C_d, C_d_base, Ppv_vect, loc, Cost_in_incr, Cost_out_incr, C_ch, N_st, Inv_eff,...
     C_d_base_vic,C_in_vic_new, C_d_vic)
Load_annual=zeros(T,T_dur);
OP_annual=zeros(T,T_dur);
Snet_day=zeros(T_dur,length(Ppv_vect));
OP_final=zeros(length(Ppv_vect),1);
S_solar_plot=zeros(96,length(Ppv_vect));
%Demand_charge=zeros(length(m),T_dur/365);
Demand_charge_total=zeros(length(Ppv_vect),1);
Cost_per_charge=zeros(length(Ppv_vect),1);
Feeder_size=zeros(length(Ppv_vect),1);
Load_monthly=zeros(12,T_dur/365);
P_charger(P_charger==0)=0.001;
E_test=zeros(96,365);
util_rate=zeros(T,T_dur);
car_util=zeros(T,1);
car_util_temp=zeros(T,1);
%Demand curve
%load_only=sum(Energy_rqrd);
for ii=1:T_dur %go through every day
    if ii==240
        fprintf('here\n');
    end
    t_arr=t_arr_annual(:,ii);
    E_day=Energy_rqrd(:,ii);
    E_day(t_arr==0)=[];
    E_day(t_arr==T)=[];
```

```
    P_ch=P_charger(:,ii);
    P_ch(t_arr==0)=[];
    P_ch(t_arr==T)=[];
    t_arr(t_arr==0)=[];
    t_arr(t_arr==T)=[];
    Load_per_car=zeros(T,length(t_arr));
    for x=1:length(t_arr) % go through N cars
        char_duration=ceil(E_day(x,1)./P_ch(x,1));
        Load_per_car(t_arr(x):(t_arr(x)+char_duration-1),x
            )=...
                P_ch(x,1)*ones(length(t_arr(x):(t_arr(x)+
                    char_duration-1)),1);
        car_util_temp(t_arr(x):(t_arr(x)+char_duration-1)
            ,1)=ones(length(t_arr(x):(t_arr(x)+
            char_duration-1)),1);
        car_util=car_util+car_util_temp;
        car_util_temp=zeros(T,1);
    end
    util_rate(:,ii)=car_util/N_st;
    fprintf('Day %d\n', ii);
    Load_annual(:,ii)=sum(Load_per_car,2);
    E_test(1:length(E_day),ii)=E_day;
    clear Load_per_car char_duration P_ch t_arr
    car_util=zeros(T,1);
end
[base_load_day, base_load_year]=base_load(1);
load_only=sum(Load_annual);
clear I_calc
if loc==1
    file_temp=readtable('model_valid_output40.txt');
    scale_factor=40;
end
if loc==2
    file_temp=readtable('homer_vic_solar.txt'); %victoria
    scale_factor=5;
```

```
end
I_calc=file_temp.kW_4;
I_calc=I_calc';
I_calc=repmat(I_calc,4,1);
I_calc=reshape(I_calc,96,365)./scale_factor;
for p=1:length(Ppv_vect)
    Ppv=Ppv_vect(p);
    S_gen=Ppv_vect(p).*I_calc;
    S_net=Load_annual-S_gen+base_load_year;
    S_net(S_net>0)=S_net(S_net>0)./(Inv_eff);
    S_net(S_net<0)=S_net(S_net<0).*(Inv_eff);
    Feeder_size(p,1)=max(max(S_net));
    S_solar_plot(:,p)=S_net(:,172);
    Snet_day(:,p)=sum(S_net);
    Snet_neg_annual=S_net;
    Snet_neg_annual(Snet_neg_annual<0)=0;  %Take only the load that's from the grid for demand charge calculations
    if(loc==2) % if victoria
        clear C_in C_d C_d_base
        % Demand charges calculated - tiered usage
        if (max(max(Snet_neg_annual))<35) %small general service rate
            C_d_base=0.3312; % basic charge per day
            C_in=(1/(T/24)).*0.1139.*ones(T,T_dur);
            C_d=zeros(1,3);
            fprintf('Small Business Classification with %d kWp PV\n', Ppv);
        elseif (max(max(Snet_neg_annual))<135 && max(max(Snet_neg_annual))>=35) % medium general service rate
            C_d_base=C_d_base_vic;
            C_in=C_in_vic_new.*ones(T,T_dur);
            C_d=C_d_vic;
```

```
                fprintf('Medium Business Classification with %d kWp PV\n', Ppv);
            else % large general service rate
                C_d_base=0.2429;
                C_in=(1/(T/24)).*0.055.*ones(T,T_dur);
                C_d=11.21.*ones(1,3);
                fprintf('Large Business Classification with %d kWp PV\n', Ppv);
            end
            [Demand_charge]=demand_charge(Snet_neg_annual, C_d, C_d_base);
            Demand_charge_total(p)=(Demand_charge);
            C_out=C_in;
        else
            [Demand_charge]=demand_charge(Snet_neg_annual, C_d, C_d_base);
            Demand_charge_total(p)=(Demand_charge);

        end
        Cost_per_charge(p)=C_ch*sum(sum(Load_annual));
        OP_annual(S_net>0)=Cost_in_incr*C_in(S_net>0).*(S_net(S_net>0));
        OP_annual(S_net<0)=Cost_out_incr*C_out(S_net<0).*(S_net(S_net<0));
        OP_annual_sum=sum(OP_annual);
        OP_final(p)=sum(OP_annual_sum);
        clear Load_monthly Demand_charge S_gen OP_annual S_net peak_load
        OP_annual=zeros(T,T_dur);

end
end
```

A.6 schedulingopt.m

This function is responsible for calculating the demand profile for coordinated charging.

```
function [OP_sum, Cost_per_charge, load_sum, Demand_charge_total]=...
    scheduling_opt(N, T, T_dur, S_max, L_max, ...
    P_charger, I_calc, Area_per_panel, PV_eff, P_nom, t_arr, t_dep, Energy_rqrd,...
    C_in, C_out, C_d, C_d_base, Ppv_vect, loc, Cost_in_incr, Cost_out_incr,...
    C_ch, C_d_incr, D_penalty_med, D_penalty_large, Demand_thresh_med, Demand_thresh_large, N_st, Inv_eff,...
    C_d_base_vic,C_in_vic_new, C_d_vic)
%options=cplexoptimset('Display', 'on', 'Algorithm', 'auto', 'MaxNodes',4000000000000,'TolXInteger', 1e-3);
    options=[];
m= [31, 59, 90, 120, 151, 181, 212, 243, 273, 304, 334, 365];
Demand_charge_total=zeros(length(Ppv_vect),1);
%Output_annual=zeros((3*T+N*T+2*T+2),T_dur);
Output_annual=zeros(3*T,T_dur);
OP_annual_base_price=zeros(T_dur,1);
OP_sum=zeros(length(Ppv_vect),1);
Feeder_size=zeros(length(Ppv_vect),1);
Cost_per_charge=zeros(length(Ppv_vect),1);
if loc==1
    C_d_summer_cali=zeros(T,1);
    C_d_winter_cali=zeros(T,1);
    C_d_summer_cali(48:71)=10*ones(24,1); %12 pm to 6pm
    %summer part-peak
    C_d_summer_cali(34:47)=5*ones(14,1); %8:30 am to 12pm
    C_d_summer_cali(72:85)=5*ones(14,1); %6pm to 9:30pm
    %summer offpeak
```

```
    C_d_summer_cali(86:96)=zeros(11,1); %6pm to 8:30 am
    C_d_summer_cali(1:33)=zeros(33,1);
    %winter part-peak
    C_d_winter_cali(34:85)=C_d(3)*ones(52,1);
    %winter offpeak
    C_d_winter_cali(86:96)=zeros(11,1);
    C_d_winter_cali(1:33)=zeros(33,1);
    C_d_A_cali=repmat(C_d_winter_cali, 1, 120);
    C_d_B_cali=repmat(C_d_winter_cali, 1, 61);
    C_d_C_cali=repmat(C_d_summer_cali, 1, 184);
    C_d_cali=[C_d_A_cali, C_d_C_cali, C_d_B_cali];
    C_in_demand=Cost_in_incr.*(C_in+C_d_base+C_d_cali);
end
if loc==2
    C_in_demand=Cost_in_incr.*(C_in+C_d_base);
end
util_rate=zeros(T,T_dur);
%% TEMP
clear I_calc
if loc==1
    file_temp=readtable('model_valid_output40.txt'); %
        california
    scale_factor=40;
end
if loc==2
    file_temp=readtable('homer_vic_solar.txt'); %victoria
    scale_factor=5;
end
I_calc=file_temp.kW_4;
I_calc=I_calc';
I_calc=repmat(I_calc,4,1);
I_calc=reshape(I_calc,96,365)./scale_factor;
for ii=1:length(Ppv_vect)
    Ppv=Ppv_vect(ii);
    S_gen=Ppv.*I_calc;
```

```
    clear C_out_new
    C_out_new=C_out;
    C_out_new(S_gen==0)=0;
    Count_flag=0;
    %parfor i=1:T_dur
    if ii==1
        S_net_max=L_max.*ones(1,T_dur);
    end
    for i=1:T_dur
            t_arr_day=t_arr(:,i);
            t_dep_day=t_dep(:,i);
            Energy_rqrd_day=Energy_rqrd(:,i);
            P_ch_day=P_charger(:,i);
            t_arr_day(t_arr_day==0)=[];
            t_dep_day(t_dep_day==0)=[];
            Energy_rqrd_day(Energy_rqrd_day==0)=[];
            P_ch_day(P_ch_day==0)=[];
            N=length(t_arr_day);
            ctype=[ 67*ones(1,(3*T)), 66*ones(1,(2*T+N*T))
                , 67*ones(1,(2*T)) ]; %sets first 1+4T to
                continuous and states to Binary in ASCII
            ctype=char(ctype);
            f=[(C_in_demand(:,i)'), -Cost_out_incr*
                C_out_new(:,i)', zeros(1, ((T+N*T))), zeros
                (1,2*T),...
                 D_penalty_med.*ones(1,T), zeros(1,T)];
            [A, b]=AB_gen(N, T, P_ch_day, S_net_max(i),
                S_max, Energy_rqrd_day);
            [A_eq, b_eq]=AB_eq_gen(N, T, P_ch_day, S_gen
                (:,i),i,Demand_thresh_med,
                Demand_thresh_large, loc);
            [lb, ub]=lb_ub_gen(N, T, S_max, S_net_max(i),
                 t_arr_day, t_dep_day ,i,Ppv,loc);
            [x,fval,exitflag,output]=cplexmilp(f,A,b,A_eq,
                b_eq,[],[],[],lb,ub,ctype,[],options);
```

```
            fprintf('Solved with exitflag %d \n', exitflag);
            if (exitflag==5)
                Count_flag=Count_flag+1;
                fprintf('Solution with numerical issues on Day %d \n', i);
            end
            if (exitflag==-2)
                fprintf('Integer infeasible on Day %d \n', i);
            end
            Output_annual(:,i)=x(1:3*T);
            OP_annual_base_price(i)=fval;
            states_annual_day=x((1+3*T):(3*T+N*T),:);
            states_annual_day=reshape(states_annual_day,T,N); %96xN
            util_rate(:,i)=sum(states_annual_day,2)./N_st;
            clear states_annual_day
    end
        %% PARAMETER OUTPUT
        Snet_neg_annual=Output_annual(1:T,:);
        Snet_max=max(Snet_neg_annual);
        Snet_neg_annual=Snet_neg_annual./(Inv_eff);
        Snet_pos_annual=Output_annual((T+1):2*T,:);
        Snet_pos_annual=Snet_pos_annual.*(Inv_eff);
        Load_annual=Output_annual((2*T+1):(3*T),:);
        load_sum=sum(Load_annual);
        if(loc==2) % if victoria
            clear C_d C_d_base
            % Demand charges calculated - tiered usage
            if (max(max(Snet_neg_annual))<35) %small general service rate
                C_d_base=0.3312; % basic charge per day
                C_in_vic=(1/(T/24)).*0.1139;
                C_d=zeros(T,T_dur);
```

```
            elseif (max(max(Snet_neg_annual))<135 && max(
                max(Snet_neg_annual))>=35) % medium general
                  service rate
                C_d_base=C_d_base_vic;
                C_in_vic=C_in_vic_new;
                C_d=C_d_vic;
            else % large general service rate
                C_d_base=0.2429;
                C_in_vic=(1/(T/24)).*0.055;
                C_d=11.21.*ones(T,T_dur);
            end
            C_out_vic=C_in_vic;
            [Demand_charge, month_max]=demand_charge(
                Snet_neg_annual, C_d, C_d_base);
            Demand_charge_total(ii)=sum(Demand_charge);
            OP_sum(ii)=sum(sum(Cost_in_incr*C_in_vic.*
                Snet_neg_annual))-sum(sum(Cost_out_incr*
                C_out_vic.*Snet_pos_annual));
        else
            [Demand_charge, month_max]=demand_charge(
                Snet_neg_annual, C_d, C_d_base);
            Demand_charge_total(ii)=sum(Demand_charge);
            OP_sum(ii)=sum(sum(Cost_in_incr*C_in.*
                Snet_neg_annual))-sum(sum(Cost_out_incr*
                C_out_new.*Snet_pos_annual));
        end
        clear Load_monthly Demand_charge S_gen S_net
            peak_load
    Cost_per_charge(ii)=C_ch.*sum(sum(Load_annual));
end
end
```

A.7 ABeqgen.m

This function is embedded into the coordinated charging algorithm for constraint definition.

```
function [A_eq, b_eq]=AB_eq_gen(N, T,P_charger, S_gen, day
    ,Demand_thresh_med, Demand_thresh_large, loc)
P_ch=zeros(T,T*N);
P_ch(:,1:T)=P_charger(1)*eye(T);
for i=2:length(P_charger)
    P_ch(:,((i-1)*T+1):(i*T))=P_charger(i)*eye(T);
end
if loc==1
    demand_delta_A=[];
    demand_delta_b=[];
elseif loc==2
    demand_delta_A=[eye(T),zeros(T,2*T), zeros(T, (N*T)),
        zeros(T,T), zeros(T,T), -eye(T), eye(T,T)];
    demand_delta_b=[Demand_thresh_med.*ones(T,1)+base_load
        (1)];
end
A_eq=[-1*eye(T),       eye(T),   eye(T), zeros(T, (N*T)),
    zeros(T,4*T);...
      zeros(T,2*T),              -1*eye(T),         P_ch,
        zeros(T,4*T);demand_delta_A];
b_eq=[ S_gen-base_load(day); zeros(T,1); demand_delta_b];
end
```

A.8 ABgen.m

This function is embedded into the coordinated charging algorithm for constraint definition.

```
function [A, b]= AB_gen(N, T, P_charger, L_max, S_max, Energy_rqrd)
%cap_battery=cap_battery*ones(T,1);
% creates a TxN repeated vector of battery capacities for vector_diag
% allows for different battery capacities
A=[ zeros(N,3*T), vector_diag(N,T,P_charger), zeros(N,4*T);...
    zeros(T,T),eye(T), zeros(T, (T+N*T)), -S_max.*eye(T), zeros(T,3*T);...
    eye(T),zeros(T,2*T), zeros(T, (N*T)), zeros(T,T), -L_max.*eye(T),zeros(T,2*T);...
    zeros(T,3*T), zeros(T, (N*T)), eye(T), eye(T), zeros(T,2*T)];
b=[-Energy_rqrd; zeros(2*T,1) ;ones(T,1)];
end
```

A.9 lbubgen.m

This function is embedded into the coordinated charging algorithm for constraint definition.

```
function [lb, ub] = lb_ub_gen(N, T, S_max, L_max, t_arr, t_dep, day, Ppv, loc)
state_lim=zeros(T,N);
cars_skipped=0;
if loc==1
    ub_delta=zeros(2*T,1);
elseif loc==2
    ub_delta=[L_max*ones(T,1); Inf(T,1)];
end
for i=1:N
    if t_arr(i)==0
        state_lim(:,i)=zeros(T,1);
    else
         state_lim(:,i)=[zeros(t_arr(i)-1,1); ones((t_dep(i)-t_arr(i)),1); zeros(T-t_dep(i)+1,1)];
    end
end
state_lim=reshape(state_lim, N*T,1);
%inf - no limit on the load
% T+1 T - for all the load; 1 for the first decision variable 'w'
lb=[ zeros(T,1); zeros(T,1); zeros(T,1); zeros((N*T),1); zeros(2*T, 1); zeros(2*T,1)];
ub=[ L_max.*ones(T,1); S_max.*ones(T,1); Inf(T,1); state_lim; ones(2*T,1); ...
    ub_delta];
fprintf('%d skipped cars ', cars_skipped)
fprintf('on day %d ', day)
fprintf('with %d kW capacity \n', Ppv)
  end
```

A.10 vectordiag.m

This function is embedded into ABgen.m to generate a diagonal matrix of horizontal vectors.

```
function [out_mat]=vector_diag(N, T, P_charger)
mat=zeros(N,N*T);
mat(:,1:T)=ones(N, T);
X=[0:T:(N*T-1)]';
r = rem(X,N*T);
c = [mat,mat];
% creates a diagonal matrix of horizontal array of ones
out_mat_ones = c(bsxfun(@plus,bsxfun(@plus,N*T - r,0:(N*T-1))*N,(1:N)'));
out_mat_ratio=diag(-P_charger);
out_mat=out_mat_ratio*out_mat_ones;
end
```

A.11 baseload.m

This function is responsible for the defining the base load.

```
function [base_load_day base_load_year]=base_load(D)
    file_data=csvread('
       RefBldgFullServiceRestaurantNew2004_7_1_5_0_3B_USA_CA_LOS_ANGEL
       .csv',2,1);
    total_kW=zeros(8760,1);
    total_kW(1:8759,1)=file_data(:,1)+file_data(:,2)+
       file_data(:,3)...
        +file_data(:,4)+file_data(:,5)+file_data(:,6)...
        +file_data(:,7)+file_data(:,8)+file_data(:,9);
    total_kW(8760,1)=total_kW(8759,1);
    total_kW=total_kW';
    total_kW=repmat(total_kW,4,1)./4;
    total_kW=reshape(total_kW, 35040,1);
    base_load_year=reshape(total_kW, 96,365);
    base_load_year=0.*base_load_year;
    base_load_day=base_load_year(:,D);
end
```

A.12 Calidata.m

This function is responsible for post-processing the ChargePoint data.

```
function [t_arr, t_dep, P_ch, Energy_rqrd]= Cali_data(N,
    T_dur)
m= [31, 59, 90, 120, 151, 181, 212, 243, 273, 304, 334,
    365];
incrm=15;
t_arr=zeros(N,T_dur);
t_dep=zeros(N,T_dur);
P_ch=zeros(N,T_dur);
Energy_rqrd=zeros(N,T_dur);
    T=readtable('EV_total.dat');
     T.Properties.VariableNames = {'EVSE_ID' 'PORT_TYPE' '
        DRIVER_ID' ...
        'EVENT_ID' 'TIME_ZONE' 'PEAK_POWER' 'AVERAGE_POWER
           ' 'ENERGY' 'EVSE_ZIP' 'sublap'...
        'INTERVAL_start_datetime' 'INTERVAL_stop_datetime'
           };
     %T=readtable(EV_files(ii).name);
     % INPUT ALL PARAMETERS
     EVSE_id=T.EVSE_ID;
     DRIVER_id=T.DRIVER_ID;
     DRIVER_id=cellfun(@str2num,DRIVER_id);
     EVENT_id=T.EVENT_ID;
     EVENT_id=cellfun(@str2num,EVENT_id);
     %TIME_zone=T.INTERVAL_TIME_ZONE;
     PEAK_PWR=T.PEAK_POWER;
     %PEAK_PWR=cellfun(@str2num,PEAK_PWR);
     AVG_PWR=T.AVERAGE_POWER;
     ENERGY_RQRD=T.ENERGY;
     time_arr=T.INTERVAL_start_datetime;
     time_dep=T.INTERVAL_stop_datetime;
     % PULL OUT ONLY TIME OF ARRIVAL AND DEPARTURE
     t_arr_temp=cell(length(EVSE_id),1);
```

```
    t_dep_temp=cell(length(EVSE_id),1);
    energy_consumed=cell(length(EVENT_id),1);
    power_peak=cell(length(EVENT_id),1);
    power_avg=cell(length(EVENT_id),1);

    t_arr_temp(1,1)=time_arr(1,1);
    power_peak(1,1)=PEAK_PWR(1,1);
    power_avg(1,1)=AVG_PWR(1,1);
    %supresses all the values that are in between start
       and stop time
    for i=1:(length(EVENT_id)-1)
        if EVENT_id(i,1)~=EVENT_id(i+1,1) && cellfun(@
           str2num, ENERGY_RQRD(i,1))>cellfun(@str2num,
           ENERGY_RQRD(i+1,1))
            %last values of the period
            t_dep_temp(i,1)=time_dep(i,1);
            energy_consumed(i,1)=ENERGY_RQRD(i,1);
            %first values of the period
            t_arr_temp(i+1,1)=time_arr(i+1,1);
            if cellfun(@str2num, PEAK_PWR(i+1,1))<1
                power_peak(i+1,1)=PEAK_PWR(i+2,1);
                power_avg(i+1,1)=AVG_PWR(i+2,1);
            else
                power_peak(i+1,1)=PEAK_PWR(i+1,1);
                power_avg(i+1,1)=AVG_PWR(i+1,1);
            end
        end
    end
    % record the last values into the table
    t_dep_temp(length(EVENT_id),1)=time_dep(length(
       EVENT_id),1);
    energy_consumed(length(EVENT_id),1)=ENERGY_RQRD(length
       (EVENT_id),1);
    % deleting all the empty cells
    time_arr=t_arr_temp(~cellfun('isempty',t_arr_temp));
```

```
    time_dep=t_dep_temp(~cellfun('isempty',t_dep_temp));
    energy_consumed=energy_consumed(~cellfun('isempty',
        energy_consumed));
    energy_consumed=cellfun(@str2num, energy_consumed);
    power_peak=power_peak(~cellfun('isempty',power_peak));
    power_peak=cellfun(@str2num, power_peak);
    power_avg=power_avg(~cellfun('isempty',power_avg));
    time_arr=datevec(time_arr, 'yyyy-mm-dd HH:MM:SS');
    time_dep=datevec(time_dep, 'yyyy-mm-dd HH:MM:SS');
    t_min_arr=ceil((time_arr(:,5)+60.*time_arr(:,4))./
        incrm);
    t_min_dep=ceil((time_dep(:,5)+60.*time_dep(:,4))./
        incrm);
    clear AVG_PWR ENERGY_RQRD PEAK_PWR t_arr_temp
        t_dep_temp
    month_arr=time_arr(:,2);
    %first month starts at 0
    month_arr(month_arr==1)=zeros(length(month_arr(
        month_arr==1)),1);
    month_dep=time_dep(:,2);
    month_dep(month_dep==1)=zeros(length(month_dep(
        month_dep==1)),1);
    %Multi-day parkers - FIX THIS

    for mnth=1:11
        month_arr(month_arr==(mnth+1))=m(mnth)*ones(length
            (month_arr(month_arr==(mnth+1))),1);
        month_dep(month_dep==(mnth+1))=m(mnth)*ones(length
            (month_dep(month_dep==(mnth+1))),1);
    end
    day_arr=month_arr+time_arr(:,3);
    day_dep=month_dep+time_dep(:,3);
    day_diff=day_dep-day_arr;
    t_min_dep(day_diff>0)=96;
    day_dep(day_diff>0)=day_arr(day_diff>0);
```

```

    %erroneous entries - day of arrival is after day of departure
    t_min_arr(day_diff<0)=[];
    t_min_dep(day_diff<0)=[];
    day_arr(day_diff<0)=[];
    day_dep(day_diff<0)=[];
    day_diff(day_diff<0)=[];
    energy_consumed(day_diff<0)=[];
    month_arr(day_diff<0)=[];
    month_dep(day_diff<0)=[];
    power_peak(day_diff<0)=[];

    %time of departure before time of arrival
    day_arr((t_min_arr-t_min_dep)>0)=[];
    day_dep((t_min_arr-t_min_dep)>0)=[];
    day_diff((t_min_arr-t_min_dep)>0)=[];
    energy_consumed((t_min_arr-t_min_dep)>0)=[];
    month_arr((t_min_arr-t_min_dep)>0)=[];
    month_dep((t_min_arr-t_min_dep)>0)=[];
    power_peak((t_min_arr-t_min_dep)>0)=[];
    t_min_arr((t_min_arr-t_min_dep)>0)=NaN;
    t_min_dep(isnan(t_min_arr))=[];
    t_min_arr(isnan(t_min_arr))=[];

    for day_iter=1:365
        t_arr(1:length(day_arr(day_arr==day_iter)),day_iter)=t_min_arr(day_arr==day_iter);
        t_dep(1:length(day_dep(day_dep==day_iter)),day_iter)=t_min_dep(day_dep==day_iter);
        if size(t_dep,1)>N
            fprintf('Error');
        end
        P_ch(1:length(day_arr(day_arr==day_iter)),day_iter)=power_peak(day_arr==day_iter);
```

```
            Energy_rqrd(1:length(day_arr(day_arr==day_iter)),
                day_iter)=energy_consumed(day_arr==day_iter);
      end
end
```

A.13 demandcharge.m

This function is responsible for calculating the monthly demand charge.

```
function [Demand_charge, month_max]=demand_charge(Snet,
    C_d, C_d_base)
m= [31, 59, 90, 120, 151, 181, 212, 243, 273, 304, 334,
    365];
% C_d_summer_cali(48:71)=17.57; %12 pm to 6pm
% %summer part-peak
% C_d_summer_cali(34:47)=0.51; %8:30 am to 12pm
% C_d_summer_cali(72:85)=0.51; %6pm to 9:30pm
% %winter part-peak
% C_d_winter_cali(34:85)=0.03; %8:30am to 9:30pm
C_summer_peak=C_d(1,1)+C_d_base;
C_summer_part=C_d(1,2)+C_d_base;
C_winter_peak=C_d(1,3)+C_d_base;
C_winter_offpeak=C_d_base;
C_summer_offpeak=C_d_base;
month_max=zeros(1,12);

demand_summer_peak=C_summer_peak.*[max(max(Snet(48:71,m(4)
    +1:m(5)))), ...
     max(max(Snet(48:71,m(5)+1:m(6)))),...
     max(max(Snet(48:71,m(6)+1:m(7)))),...
     max(max(Snet(48:71,m(7)+1:m(8)))),...
     max(max(Snet(48:71,m(8)+1:m(9)))),...
     max(max(Snet(48:71,m(9)+1:m(10))))];
demand_summer_part=C_summer_part.*[max(max(Snet
    ([34:47,72:85],m(4)+1:m(5)))), ...
     max(max(Snet([34:47,72:85],m(5)+1:m(6)))),...
     max(max(Snet([34:47,72:85],m(6)+1:m(7)))),...
     max(max(Snet([34:47,72:85],m(7)+1:m(8)))),...
     max(max(Snet([34:47,72:85],m(8)+1:m(9)))),...
     max(max(Snet([34:47,72:85],m(9)+1:m(10))))];
```

```
demand_winter_peak=C_winter_peak.*[max(max(Snet(34:85,1:m(1)))), ...
    max(max(Snet(34:85,m(1)+1:m(2)))),...
    max(max(Snet(34:85,m(2)+1:m(3)))),...
    max(max(Snet(34:85,m(3)+1:m(4)))),...
    max(max(Snet(34:85,m(10)+1:m(11)))),...
    max(max(Snet(34:85,m(11)+1:m(12))))];

demand_winter_offpeak=C_winter_offpeak.*[max(max(Snet([1:33, 86:96],1:m(1)))), ...
    max(max(Snet([1:34, 86:96],m(1)+1:m(2)))),...
    max(max(Snet([1:34, 86:96],m(2)+1:m(3)))),...
    max(max(Snet([1:34, 86:96],m(3)+1:m(4)))),...
    max(max(Snet([1:34, 86:96],m(10)+1:m(11)))),...
    max(max(Snet([1:34, 86:96],m(11)+1:m(12))))];

demand_summer_offpeak=C_summer_offpeak.*[max(max(Snet([1:33, 86:96],m(4)+1:m(5)))), ...
    max(max(Snet([1:33, 86:96],m(5)+1:m(6)))),...
    max(max(Snet([1:33, 86:96],m(6)+1:m(7)))),...
    max(max(Snet([1:33, 86:96],m(7)+1:m(8)))),...
    max(max(Snet([1:33, 86:96],m(8)+1:m(9)))),...
    max(max(Snet([1:33, 86:96],m(9)+1:m(10))))];

month_max(1,5:10)=[max(max(Snet(:,m(4)+1:m(5)))), ...
    max(max(Snet(:,m(5)+1:m(6)))),...
    max(max(Snet(:,m(6)+1:m(7)))),...
    max(max(Snet(:,m(7)+1:m(8)))),...
    max(max(Snet(:,m(8)+1:m(9)))),...
    max(max(Snet(:,m(9)+1:m(10))))];
month_max(1,[1:4, 11:12])=[max(max(Snet(:,1:m(1)))), ...
    max(max(Snet(:,m(1)+1:m(2)))),...
    max(max(Snet(:,m(2)+1:m(3)))),...
    max(max(Snet(:,m(3)+1:m(4)))),...
    max(max(Snet(:,m(10)+1:m(11)))),...
```

```
    max(max(Snet(:,m(11)+1:m(12))))];
Demand_charge=sum(demand_summer_peak)+sum(
    demand_summer_part)+sum(demand_winter_peak)...
    +sum(demand_summer_offpeak)+sum(demand_winter_offpeak)
        ;
end
```

A.14 demandTOU.m

This function is embedded into demandcharge.m for calculating the TOU demand.

```
function [month_x, month_y] = demand_TOU(season, month_x,
    month_y)
if (season==1) %winter = 1
            temp_x=zeros(length(month_x),1);
            temp_y=zeros(length(month_y),1);
            temp_x(month_x>33)=month_x(month_x>33);
            temp_y(month_x>33)=month_y(month_x>33);
            temp_x(month_x>85)=[];
            temp_y(month_x>85)=[];
            temp_x(temp_x==0)=[];
            temp_y(temp_y==0)=[];
            if (length(temp_x)>1)
                clear month_x month_y;
                month_x=temp_x(1,1);
                month_y=temp_y(1,1);
            elseif (isempty(temp_x))
                month_x(2:length(month_x))=[];
                month_y(2:length(month_y))=[];
            else
                month_x=temp_x;
                month_y=temp_y;
            end
            clear temp_x temp_y;
end
if (season==2) %summer = 2
            temp_x_peak=zeros(length(month_x),1);
            temp_y_peak=zeros(length(month_y),1);
            temp_x_part=zeros(length(month_x),1);
            temp_y_part=zeros(length(month_y),1);
            temp_x_part(month_x>33)=month_x(month_x>33);
            temp_y_part(month_x>33)=month_y(month_x>33);
            temp_x_part(month_x>85)=[];
```

```
            temp_y_part(month_x>85)=[];
            temp_x_part(temp_x_part==0)=[];
            temp_y_part(temp_y_part==0)=[];
            temp_x_peak(temp_x_part>47)=temp_x_part(
               temp_x_part>47);
            temp_y_peak(temp_x_part>47)=temp_y_part(
               temp_x_part>47);
            if temp_x_peak>71
                temp_y_peak=[];
                temp_x_peak=[];
            else
                temp_y_part(temp_x_part>47)=[];
                temp_x_part(temp_x_part>47)=[];
                temp_x_peak(temp_x_part>71)=[];
                temp_y_peak(temp_x_part>71)=[];
                temp_x_peak(temp_x_peak==0)=[];
                temp_y_peak(temp_y_peak==0)=[];
            end
            if (length(temp_x_peak)>1)
                clear month_x month_y;
                month_x=temp_x_peak(1,1);
                month_y=temp_y_peak(1,1);
            elseif (length(temp_x_part)>1)
                clear month_x month_y;
                month_x=temp_x_part(1,1);
                month_y=temp_y_part(1,1);
            elseif (isempty(temp_x_peak))
                month_x(2:length(month_x))=[];
                month_y(2:length(month_y))=[];
            else
                month_x=temp_x;
                month_y=temp_y;
            end
            clear temp_x_peak temp_y_peak temp_x_part
               temp_y_part;
```

```
end
end
```

A.15 modelvalidation.m

```
clc;
clear all
close all

N=50;
%RANDOM NUMBER GENERATOR
%random number generator hault
%s_rand = RandStream('mt19937ar','Seed',0);
%RandStream.setGlobalStream(s_rand);
t_arr=round(24+(80-24).*rand(N,1));
t_ch=round(0+(16-0).*rand(N,1));
hist(t_arr, 50);
hist(t_ch,50)
t_dep=t_arr+t_ch;
t_dep(t_dep>24*12)=24*4;

%battery caps 10.4, 19.2, 4
%CAP=
P_ch=6.6;
```